1. Introduction

In the desalination process of the multi-stage flash distillation process(MSF plants), the materials used for these plants, in particular those used for heat transfer tubes of the large-sized heat exchanger must be able to withstand seawater at high temperature because it cools and condenses water vapor that is produced by the distillation of sea water. Also, in the construction of the MSF sea water desalination plant, the large part of the construction costs, as much as 30%-55%, is taken up by the cost of these tube bundles of the heat exchangers.

Due to this, many kinds of former anti-corrosive materials used in the MSF sea water desalination plants have undergone comparison and evaluation results focusing upon the heat transfer tubes through laboratory tests, field tests and actual plant tests. Gradually, as the results of these tests have been made public and have accumulated, the evaluation results of anti-corrosive materials has been consolidated.

The materials used for heat exchangers in the main MSF sea water desalination plants in the world, which were put into service recently are shown in the separate table. As shown in this table, high grade materials such as cupronickel and titanium are often used. In Japan, aluminum brass is also being used, as it has been shown to possess the same anti-corrosive properties as that of 90/10 cupronickel. The use of these high grade materials should mean that there are no problems with general corrosion, but even with these materials, there are still incidents of corrosion that stand out. More importantly, there are different types of corrosion, for example local corrosion such as pitting corrosion and galvanic corrosion that attacks the tube sheets of the heat transfer tubes and they cause greater damage than that caused by general corrosion in some sense.

On the other hand, due to the magnitude in the size of the costs and the importance of the function of the heat transfer tubes mentioned before, in reality, research and development into existing materials in order to improve the quality and to lower the costs, and those into new materials are on-going projects.

On the basis of these conditions, we shall try to evaluate the use of anti-corrosive materials in the MSF sea water desalination plant and try to determine the reasons and conditions focusing on materials for use in the heat transfer tubes. Also, it is necessary to evaluate anti-corrosive materials now under development and their possibilities and based on this research try to find a future course and to determine a practical solution to deal with present technology for the prevention of corrosion, local corrosion such as galvanic corrosion mentioned above in particular.

Consequently, this research will investigate up-to-date information already published and, with these results, examine and propose subjects for which the SWCC should conduct the necessary research and development project.

4.1.2

Structure Materials of each Heat Exchengers for Major Seawater Desalination Plants (Distillation Process) in the Middle East Regions

Name of Country		Saudi-Arabia				Kwait
Name of Plants		AJ-I	AJ-II	MY	MT-I	KW-II, -III
Capacity(m^3/D *5) × Number of Plants		22,900×6	28,400×10 23,500	22,000×5	26,760×10 22,300	32,731×10 27,276
Scaling Prevention Methods		Chemicals Dosing	Chemicals Dosing	pH Control *6)	Chemicals Dosing	Chemicals Dosing
Max. Temparature *5)		90.56	112.8 90.1	121.0	104.7 90.0	110.0 90.0
Heat Rejection Section	Heat Transfer Tube	Ti (B338-Gr2)	Ti (TTH 35)	Ti (B338-Gr2)	66/30 Cu-Ni (Cu 108)	66/30 Cu-Ni (CN 108)
	Tube Plate	Al Bronze (C6161 P-0)	Ni-Al Bronze (C63000)	Ni-Al Bronze (C6301 P)	Al Bronze (C61400)	Naval Brass (C46400)
	Water Box	Al Bronze (C6161 P-0)	Ni-Al Bronze *2) (C65800)	90/10 Cu-Ni *1) (C7060 P)	90/10 Cu-Ni *1) (C70500)	Epoxy Coating
Heat Recovary Section	Heat Transfer Tube	Ti (B338-Gr2)	90/10 Cu-Ni (C70600)	66/30 Cu-Ni 90/10 Cu-Ni	90/10 Cu-Ni (C70600)	66/30 Cu-Ni Al Brass *4)
	Tube Plate	Al Bronze (C6161 P-0)	90/10 Cu-Ni *1) (C70600)	90/10 Cu-Ni *1) (C70600)	90/10 Cu-Ni (C70600)	Naval Brass (C46400)
	Water Box	Al Bronze (C6161 P-0)	90/10 Cu-Ni *1) (C70600)	90/10 Cu-Ni *1) (C70600)	90/10 Cu-Ni *1) (C70600)	90/10 Cu-Ni *1) Epoxy Coating
Brine Heater	Heat Transfer Tube	Ti (B338-Gr2)	66/30 Cu-Ni (CN 108)	66/30 Cu-Ni (CN 108)	66/30 Cu-Ni (CN 108)	66/30 Cu-Ni (CN 108)
	Tube Plate	Al Bronze (C6161 P-0)	70/30 Cu-Ni *1) (C7150 P)	90/10 Cu-Ni *1) (C7060 P)	70/30 Cu-Ni (C7150 P)	Naval Brass (C4621 P)
	Water Box	Al Bronze (C6161 P-0)	90/10 Cu-Ni *1) (C7060 P)	90/10 Cu-Ni *1) (C7060 P)	90/10 Cu-Ni *1) (C7060 P)	90/10 Cu-Ni *1) (C7060 P)

Notes *1) : Clad
*2) : Casting
*3) : ( )indicatas the symbols established by JIS, ASTM and BS.
*4) : (C68700)
*5) : Each Capacity Correspond to maximum temperature presented next column.
*6) : Have been changed to additives now on.

2. Methods

At present, the most widely recognized data bases are JOIS, in Japan and DIALOG, in the USA and these will be used as the main source of information.

Consequently, we aim to obtain references in line with the above-mentioned objective by various key words and by combining these from amongst an expanding information system(JOIS has approx. 7,000,000 items and DIALOG has more than 10,000,000 items) which have been stored in these data bases. At the same time, valuable data can be found in various PR data which have been published by various material manufacturers, and if uncovered, will also be given attention to.

3. Results

3.1 Metals and Alloys for MSF Plants

The data related to corrosion resistance in this report involves literature retrieved primarily by JICST for 15 years from 1976 to date, but after careful selection, literature for about 10 years from 1981 to date accounts a majority (73%) of the data.

In this report, basic descriptions such as the characteristics of various corrosion phenomena and basic properties of various materials are limited, but these are adequately addressed by textbooks and handbooks. As a recent general introduction to these various characteristics in seawater, an excellent review by F. P. Ijesseling should be mentioned. The title is concerned with the corrosion testing which follows but the latter half provides concise information on the captioned items: "F.P. Ijesseling: General Guideline for Corrosion Testing of materials for Marine Application, Br. Corros. J., 24, No.1(1989), 55-78"

(This report was intended as a collection of as many specific data as possible and therefore places primary stress on charts. These charts are copies from the original texts, however, given the lack of space in this paper, in addition to the small symbols used for specifying materials in the original charts, they are presented without any modification. Consequently, they not only lack consistency but also are difficult to read. To overcome this disadvantage, a list of these unclear material symbols and their explanations is prepared and attached at the end. However, material symbols and experimental material No. special to companies which are not stated in the texts are left unidentified, but this will not constitute an obstacle in understanding this paper.)

3.1.1 Types, Chemical Compositions, and Costs of Metallic Materials

The types, chemical compositions and costs of metallic materials are shown in Table 3.1.1- 3.1.14.

3.1.2 Physical Properties of Metallic Materials

The physical properties of metallic materials are shown in Table 3.1.15- 3.1.18.

3.1.3 Mechanical Properties of Metallic Materials

The mechanical properties of metallic materials are shown in Table 3.1.19- 3.1.25.

3.1.4 Corrosion Resistance of Metallic Materials to Seawater and Brine

(1) Copper Alloys

a) Corrosion Resistance of Various Copper Alloys to Seawater

In this section, data were collected to compare the general corrosion resistance of various copper alloys to seawater. Figure 3.1.1 shows the results for as many as 11 types of copper

Chemical Compositions (Heat Transfer Tube Materials and Structural Materials)

1.Heat Transfer Tube Materials

(1)Copper Alloy Tubes (Table 3.1.1)

JIS Code	Grade	Chemical Composition								
		Cu	Al	As	Ni	Fe	Pb	Zn	Others	Remarks
C6872T	Al-Brass	76.0-79.0	1.8-2.5	0.02-0.06	-	≦0.05	≦0.05	Balance	-	
C7060T	90/10Cupro-Nickel	—	—	—	9.0-11.0	1.0-1.8	≦0.05	≦0.50	Mn 0.20-1.0	Cu+Ni+Fe+Mn≧99.5
C7150T	70/30Cupro-Nickel	—	—	—	29.0-33.0	0.4.-1.0	≦0.05	≦0.50	Mn 0.20-1.0	Cu+Ni+Fe+Mn≧99.5
*C7164T	Yorkoron	—	—	—	29.0-32.0	1.7-2.3	≦0.05	≦0.50	Mn 1.5-2.5	Cu+Ni+Fe+Mn≧99.5 *equivalent to Yorkoron.

(2)Titanium Tubes (Table 3.1.2)

JIS Code	Grade	H	O	N	Fe	Pd	Others	Remarks
JIS Class 1	Pure Titanium	≦0.015	≦0.20	≦0.05	≦0.25	-	Ti	
JIS Class 12	Ti-0.15Pd	≦0.015	≦0.20	≦0.05	≦0.25	0.12-0.25	Ti	

(3)Stainless Steel Tubes (Table 3.1.3)

JIS code	Grade	C	Si	Mn	P	S	Ni	Cr	Mo	Cu	N	Others	Remarks
SUS304	19Cr-9Ni	≦0.08	≦0.75	≦2.00	≦0.040	≦0.030	8.00-10.00	18.00-20.00	-	-	-	-	
SUS304L	LC 19Cr-11Ni	≦0.030	≦0.75	≦2.00	≦0.040	≦0.030	9.00-13.00	18.00-20.00	-	-	-	-	
SUS316	17Cr-12Ni-2.5Mo	≦0.08	≦0.75	≦2.00	≦0.040	≦0.030	11.0-14.0	16.0-18.00	2.00-3.00	-	-	-	
SUS316L	LC 17Cr-14Ni-2.5Mo	≦0.030	≦0.75	≦2.00	≦0.040	≦0.030	12.0-16.0	16.0-18.00	2.00-3.00	-	-	-	
SUS317	19Cr-13Ni-3.5Mo	≦0.080	≦0.75	≦2.00	≦0.040	≦0.030	11.0-15.0	18.0-20.0	3.00-4.00	-	-	-	
SUS329YM	25Cr-7Ni-3.5Mo-0.5Cu-0.16N	≦0.030	≦0.50	≦1.50	≦0.030	≦0.010	6.5-7.5	23.5-25.5	3.00-4.00	0.40-0.60	0.14-0.18	-	
*KES825M1	AVESTA 254SMO	≦0.050	≦1.00	3.00-4.00	≦0.035	≦0.010	22.0-24.0	20.0-21.0	5.00-6.00	1.00-2.00	0.15-0.25	-	

*Kobe Steel Ltd'Code, equivalent to AVESTA 254SMO.

4)Aluminum Alloy Tubes (Table 3.1.4)

JIS Code	Grade	Si	Fe	Cu	Mn	Mg	Cr	Zn	Ti	Others		Al	Remarks
										Each	Total		
A3004		≦0.30	≦0.7	≦0.25	1.0～1.5	0.8～1.3	–	≦0.25	–	≦0.05	≦0.15	Balance	
A5052		≦0.25	≦0.40	≦0.10	≦0.10	2.2～2.8	0.15～0.35	≦0.10	–	≦0.05	≦0.15	Balance	
A6061		0.40～0.8	≦0.7	0.15～0.40	≦0.15	0.8～1.2	0.04～0.35	≦0.25	≦0.15	≦0.05	≦0.15	Balance	
A6063		0.20～0.6	≦0.35	≦0.10	≦0.10	0.45～0.9	≦0.10	≦0.10	≦0.10	≦0.05	≦0.15	Balance	

2 . Structural Materials

(1)Copper Alloy Plates (Table 3.1.5)

JIS Code	Grade	Cu	Pb	Fe	Sn	Zn	Al	Mn	P	Others	Remarks
C6140P-F	Aluminum Bronze	88.0-92.5	≦0.01	1.5-3.5	-	≦0.20	6.0-8.0	≦1.0	≦0.015	-	Cu+Pb+Fe+Zn+Mn+Al+P ≧99.5
C4621P-F	Naval Brass	61.0-64.0	≦0.20	≦0.10	0.7-1.5	Balance	-	-	-	-	

(2)Nickel Alloy and Nickel-Chromium-Iron Alloy Plates (Table 3.1.6)

JIS Code	Grade	C	Mn	Fe	Cr	Mo	Cu	Si	Ni	Others	Remarks
*M-M	Monel 400	≦0.3	≦2.0	≦2.5	-	-	Balance	≦0.5	63.0-70.0	S≦0.024	
	Hastelloy C-276	-	-	**5.0	**16	**16	-	-	Balance	-	
***MA-20Nb	Carpenter20Nb3	≦0.07	-	Balance	**20.0	**2.5	**3.5	-	**35.0	Cb+Ta=C×8 ~1.0	

* Mitsubishi Materials Corp.'s code, equivalent to Monel 400 .
**mean value.
*** Mitsubishi Materials Corp.'s code, equivalent to Carpenter20Nb3 .

(3)Others (Table 3.1.7)

JIS Code	Grade	C	Si	Mn	Ni	Cu	Cr	P	S	Fe	Remarks
SM 400A	Rolled Steel Sheet	≦0.23	-	≧2.5xC	-	-	-	≦0.035	≦0.035	Balannce	
* FCA-NiCr20 2	NiresistII(Iron Casting)	≦0.30	1.0-2.5	0.8-1.5	18.0-22.0	≦0.50	1.75-2.50	-	-	Balannce	*Eqivalent to NiresistII

Prices
(Heat Transfer Tube Materials and Structural Materials)

- The followings are domestic prices in Japan in January, 1992. 125 Japanese yen is converted to 1US$.
- Prices change by supply-demand relations or by volume of order. So, the following prices are only examples concerning the materials.

1. Heat Transfer Tube Materials

(1) Copper Alloy Tubes (Table 3.1.8)

JIS Code	Grade	Price (US$/M.T)	Remarks
C6872T	Al-Brass	5,920	
C7060T	90/10Cupro-Nickel	8,160	
C7150T	70/30Cupro-Nickel	10,960	
*C7164T	Yorkoron	11,200	

*equivalent to Yorkoron.

(2) Titanium Tubes (Table 3.1.9)

JIS Code	Grade	Price (US$/M.T)	Remarks
JIS Class 1	Pure Titanium	33,280	
JIS Class 12	Ti-0.15Pd	67,000	

(3)Stainless Steel Tubes (Table 3.1.10)

JIS Code	Grade	Price (US$/M.T)	Remarks
SUS304	19Cr-9Ni	10,080	
SUS304L	LC 19Cr-11Ni	10,560	
SUS316	17Cr-12Ni-2.5Mo	11,360	
SUS316L	LC 17Cr-14Ni-2.5Mo	12,080	
SUS317	19Cr-13Ni-3.5Mo	13,120	
SUS329YM	25Cr-7Ni-3.5Mo-0.5Cu-0.16N	11,200	

(4)Aluminum Alloy Tubes (Table 3.1.11)

JIS Code	Grade	Price (US$/M.T)	Remarks
A3004		6,640	
A5052		6,840	
A6061		6,880	
A6063		6,640	

2 . Structural Materials

(1)Copper Alloy Plates (Table 3.1.12)

JIS code	Grade	Price (US$/M.T)	Remarks
C6140P-F	Aluminum Bronze	9,600	
C4621P-F	Naval Brass	6,200	

(2)Nickel Alloy and Nickel-Chromium-Iron Alloy Plates (Table 3.1.13)

JIS code	Grade	Price (US$/M.T)	Remarks
*M-M	Monel 400	20,000	* Mitsubishi Materials Corp.'s code , equivalent to Monel 400
	Hastelloy C-276	34,400	
*MA-20Nb	Carpenter20Nb3	14,800	* Mitsubishi Materials Corp.'s code , equivalent to Carpenter20Nb3 .

(3)Others (Table 3.1.14)

JIS code	Grade	Price (US$/M.T)	Remarks
SM 400A	Rolled Steel Sheet	680	
* FCA-NiCr20 2	NiresistII(Iron Casting)	3,680 —10,120 (Casing) (Rotor)	

Physical Properties (Heat Transfer Tube Materials)

(1)Copper Alloy Tubes (Table 3.1.15)

JIS Code	Grade	Density (g/ cm³, Room-temp.)	Thermal expansion coefficient x10⁻⁶(cm/cm/·c) (20 -300·c)	Heat conductivity (W/m··c) Room-temp.	Specific heat (J/kg/·c) Room-temp.	Remarks
C6872T	Al-Brass	8.4	18.5	100	380	
C7060T	90/10Cupro-Nickel	8.9	17.1	46	380	
C7150T	70/30Cupro-Nickel	8.9	16.2	29	380	
*C7164T	Yorkoron	**	**	**	**	*Equivalent to Yorkoron. **Equivalent to C7150T.

(2)Titanium Tubes (Table 3.1.16)

JIS Code	Grade	Density (g/ cm³, Room-temp.)	Thermal expansion coefficient x10⁻⁶(cm/cm/·c) (0 -100·c)	Heat conductivity (W/m··c) Room-temp.	Specific heat (J/kg/·c) Room-temp.
JIS Class 1	Pure Titanium	4.51	8.4	17	540
JIS Class 12	Ti-0.15Pd	4.51	8.4	17	540

(3)Stainless Steel Tubes (Table 3.1.17)

JIS Code	Grade	Density (g/ cm^3, Room-temp.)	Thermal expansion coefficient $\frac{x10^{-6}(cm/cm/\cdot C)}{100\cdot C}$	Heat conductivity $\frac{(W/m\cdot\cdot c)}{100\cdot C}$	Specific heat $\frac{(J/kg/\cdot c)}{Room\text{-}temp.}$	Remarks
SUS304	19Cr-9Ni	7.9	17.3	16.3	500	
SUS304L	LC 19Cr-11Ni	7.9	17.3	16.3	500	
SUS316	17Cr-12Ni-2.5Mo	8.0	16.0	16.3	500	
SUS316L	LC 17Cr-14Ni-2.5Mo	8.0	16.0	16.3	500	
SUS317	19Cr-13Ni-3.5Mo	8.0	16.0	16.3	500	
SUS329YM	25Cr-7Ni-3.5 Mo-0.5Cu-0.16N	7.8	13.1	15.5	490	
*KES825M1	AVESTA254SMO	8.1	15.3	13.8	-	*Kobe Steel Ltd'Code, equivalent to AVESTA 254SMO.

(4)Aluminum Alloy Tubes (Table 3.1.18)

JIS Code	Grade	Density (g/ cm^3, Room-temp.)	Thermal expansion coefficient $\frac{x10^{-6}(cm/cm/\cdot C)}{20\cdot C\text{-}100\cdot C}$	Heat conductivity $\frac{(W/m\cdot\cdot c)}{Room\text{-}temp.}$	Specific heat $\frac{(J/kg/\cdot c)}{Room\text{-}temp.}$
A3004- H34		(2.72)	23.2	162	893
A5052- H34		(2.68)	23.8	137	900
A6061-T4		(2.70)	23.6	154	896
A6063-T5		(2.69)	23.4	209	900

Mechanical Properties (Heat Transfer Tube Materials and Structural Materials)

1.Heat Transfer Tube Materials

(1)Copper Alloy Tubes (Table 3.1.19)

JIS Code	Grade	Yield strength (N/mm^2)	Tensile strength (N/mm^2)	Elongation (%)	Hardness (HRB)	Remarks
C6872T	Al-Brass	177-226	392-460	55-70	85-110	
C7060T	90/10Cupro-Nickel	118-196	314-373	40-55	70-90	
C7150T	70/30Cupro-Nickel	147-216	392-471	40-55	90-110	
*C7164T	Yorkoron	147-216	411-490	40-55	95-110	*Equivalent to Yorkoron.

(2)Titanium Tubes (Table 3.1.20)

JIS Code	Grade	Yield strength (N/mm^2)	Tensile strength (N/mm^2)	Elongation (%)	Hardness (HRB)
JIS Class 1	Pure Titanium	216-441	340-510	≧23	-
JIS Class 12	Ti-0.15Pd	216-441	340-510	≧23	-

(3)Stainless Steel Tubes (Table 3.1.21)

JIS Code	Grade	Yield strength (N/mm^2)	Tensile strength (N/mm^2)	Elongation (%)	Hardness (HRB)	Remarks
SUS304	19Cr-9Ni	235-335	530-640	55-65	75-85	
SUS304L	LC 19Cr-11Ni	205-305	500-600	52-62	71-81	
SUS316	17Cr-12Ni-2.5Mo	235-335	540-640	55-65	75-85	
SUS316L	LC 17Cr-14Ni-2.5Mo	205-305	500-600	53-63	70-80	
SUS317	19Cr-13Ni-3.5Mo	255-355	550-650	52-62	76-87	
SUS329YM	25Cr-7Ni-3.5Mo-0.5Cu-0.16N	590-675	780-860	27-35	20-24	
*KES825M1	AVESTA254SMO	325-420	690-820	40-55	-	*Kobe Steel Ltd'Code, equivalent to AVESTA 254SMO.

(4)Aluminam Alloy Tubes (Table 3.1.22)

JIS Code	Grade	Yield strength (N/mm^2)	Tensile strength (N/mm^2)	Elongation (%)	Hardness (HRB)
A3004P-H34		≧175	265-225	≧3	63
A5052TD-H34		≧175	≧235	≧12	68
A6061TD-T4		≧110	≧205	≧16	65
A6063-T5		≧145	≧185	≧12	60

2. Structural Materials

(1)Copper Alloy Plates (Table 3.1.23)

JIS Code	Grade	Yield strength (N/mm^2)	Tensile strength (N/mm^2)	Elongation (%)	Hardness (HRB)
C6140P-F	Aluminum Bronze	≧485	≧205	≧35	-
C4621P-F	Naval Brass	-	≧343	≧20	-

(2)Nickel Alloy and Nickel-Chromium-Iron Alloy Plates (Table 3.1.24)

JIS Code	Grade	Yield strength (N/mm^2)	Tensile strength (N/mm^2)	Elongation (%)	Hardness (HRB)	Remarks
* M-N	Monel 400	≧193	≧482	≧35	-	* Mitsubishi Materials Corp.'s code, equivalent to Monel400.
	Hastelloy C-276	*353	*795	*61	*90	*mean value.
*MA-20Nb	Carpenter20Nb3	≧207	≧517	≧30	-	* Mitsubishi Materials Corp.'s code, equivalent to Carpenter20Nb3.

(3)Others (Table 3.1.25)

JIS Code	Grade	Yield strength (N/mm^2)	Tensile strength (N/mm^2)	Elongation (%)	Hardness (HRB)	Remarks
SM 400A	Rolled Steel Sheet	≧245	400-510	≧18	-	
*FCA-NiCr20 2	NiresistII (Iron Casting)	-	167-206	2-3	120 - 215	*equivalent to NiresistII.

[Remarks]

- The values of above tables on chemical compositions, physical properties, and mechanical properties were quoted mainly from JIS code. In some cases, they were quoted from AGNES's Dictionary of Metallurgy(1982), Metals Handbook(Japan Institute of Metals, 19-86.), Kobe Steel Ltd.'s catalogs and Mitsubishi Materials Corp.'s catalogs.
- The market prices were heard from Kobe Steel Ltd., Nisshin Steel Co. Ltd. and Mitsubishi Materials Corp. at the end of Jannuary this year.

alloys which were exposed to seawater up to 800 days. The corrosion rates of almost all alloys tend to decrease with time and converge to a given value as the protective surface film grows. Under this test condition, the alloy which exhibited the best corrosion resistance was a Cu–Ni alloy. Figure 3.1.2 shows the experimental results of effects of temperature under the presence of 200 ppb oxygen. Figure 3.1.3 shows the time–course of corrosion resistance of C70600 exposed to flowing seawater, which was measured for over 14 years. Figure 3.1.4 shows the effects of oxygen concentration, dissolved in seawater.

Figure 3.1.5 compares the effects of flow rates at three stages of oxygen concentration from 5 to 100 ppb, indicating that below 5 ppb of oxygen concentration, Cu–Ni series and Al–brass approach the same level. Figure 3.1.6 shows the results of jet impingement tests conducted on various Cu–Ni alloys, while Fig. 3.1.7 indicates the possibility of damage due to impingement for the flow rates of seawater.

Comparing the two test results, 70/30 Cu–Ni material is not always the best. Tables 3.1.26 and 3.1.27 show the maximum and minimum flow rates (to prevent sedimentation of slime) for several types of copper alloy tubes (partly pipes). When this type of performance is compared, superiority of the Cu/Ni is evident. Table 3.1.28 shows the guidelines to peripheral velocity when several types of copper alloys are used for pump propellers.

b) Corrosion Behavior in MSF Plants

It is difficult to directly determine the corrosion rates of MSF plant components and in general, it is a common practice to place specimens in specified sections and monitor corrosion rates or measure weight losses when operation is stopped. However, in the case of heat transfer tubes, the failure rates (percentage of plugged tube) are determined and compared. Table 3.1.29 shows an example of failure rates for heat transfer tubes at the heat rejection and recovery sections, while Table 3.1.30 compares the effects of the acid process and additive process on corrosion in terms of failure rates for heat transfer tubes at the recovery section. Table 3.1.31 shows the corrosion rates determined by specimens for each stage and brine pH. The effect of pH varies greatly according to the stage and shows no regularity. The case exhibiting the lowest corrosion rates is Al–brass at stage 15, 16, and 25 and at pH 7.2 and 7.5. Figure 3.1.8 shows the results of the monitoring of copper alloys for heat transfer tubes at the recovery section up to 30 months, and 706, 613, and 715 alloys exhibit a decreasing tendency of corrosion rates. Figure 3.1.9 shows the monitoring results up to 30 months in the brine heater, in which oxygen concentration was held to 0 ppb and corrosion rates lowered remarkably from those at the recovery section. Figure 3.1.10 shows the results when the salinity of brine was varied, but the effects have not yet been identified. Figure 3.1.11 plots corrosion rates of 90/10 Cu–Ni and Al–brass in MSF plants collected from 11 data sources on log–log graph paper, but no significant difference between the two alloys is clearly recognized. Figure 3.1.12 shows test results of 70/30 Cu–Ni and

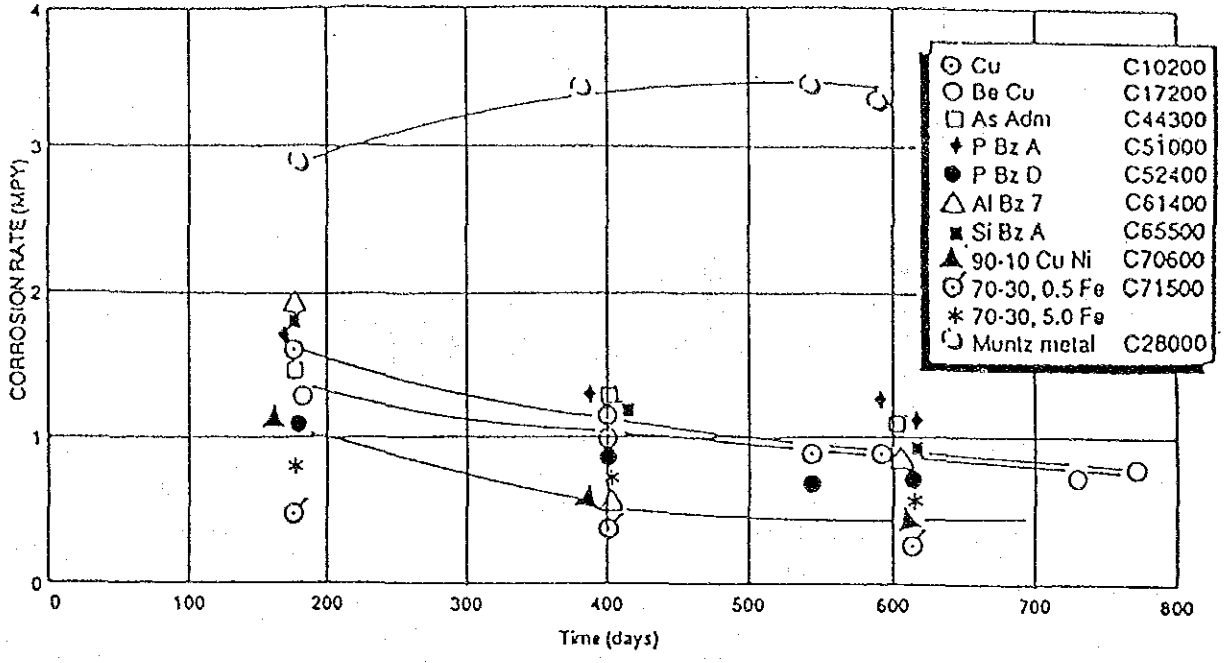

Fig.3.1.1 FIGURE 3—Corrosion rates for copper alloys for up to 800-day seawater exposures.[1]

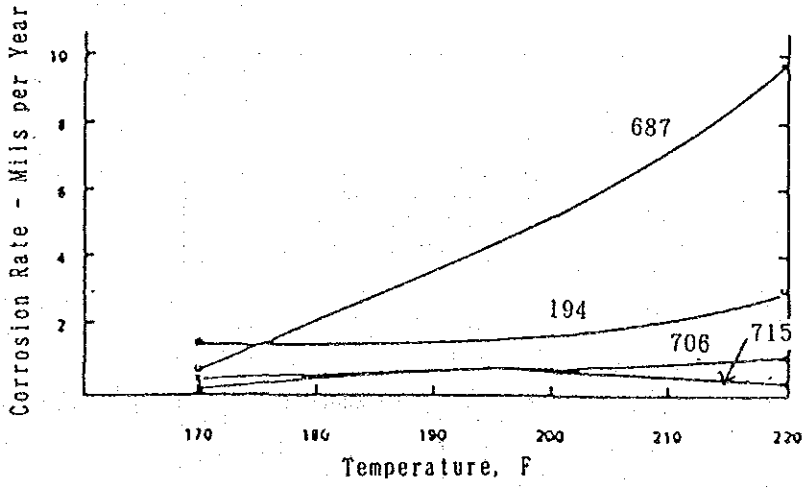

Fig.3.1.2 Effect of temperature after 90 days exposure to 200 ppb (µg/l) oxygen.[2]

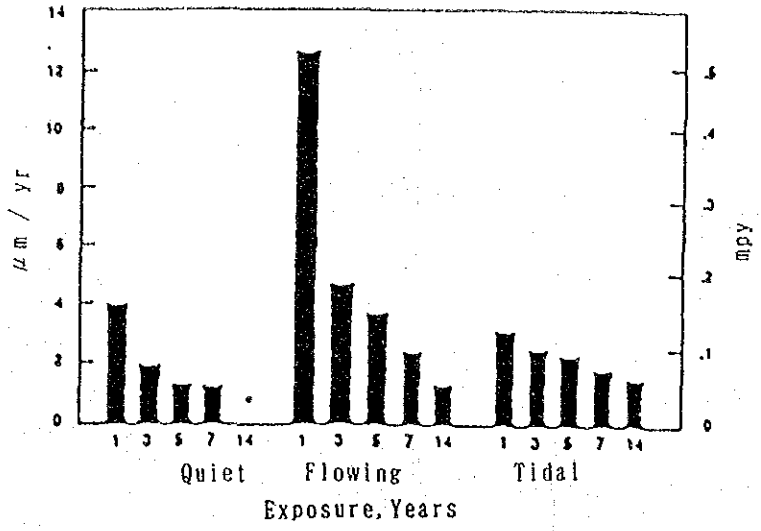

Fig.3.1.3 Corrosion rates for Alloy C70600 for long-term seawater exposures. [1]

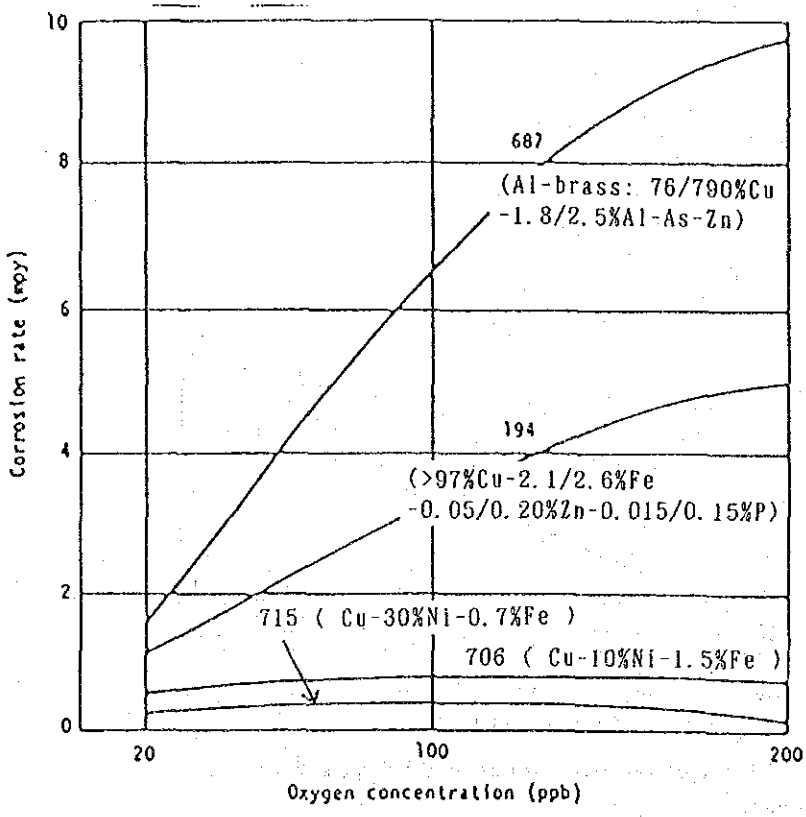

Fig.3.1.4 Effect of oxygen concentration on the corrosion of four copper alloys (CDA numbers shown) in the CDA side unit for 90 days at 220 F (TDS = 35,000 ppm). [3]

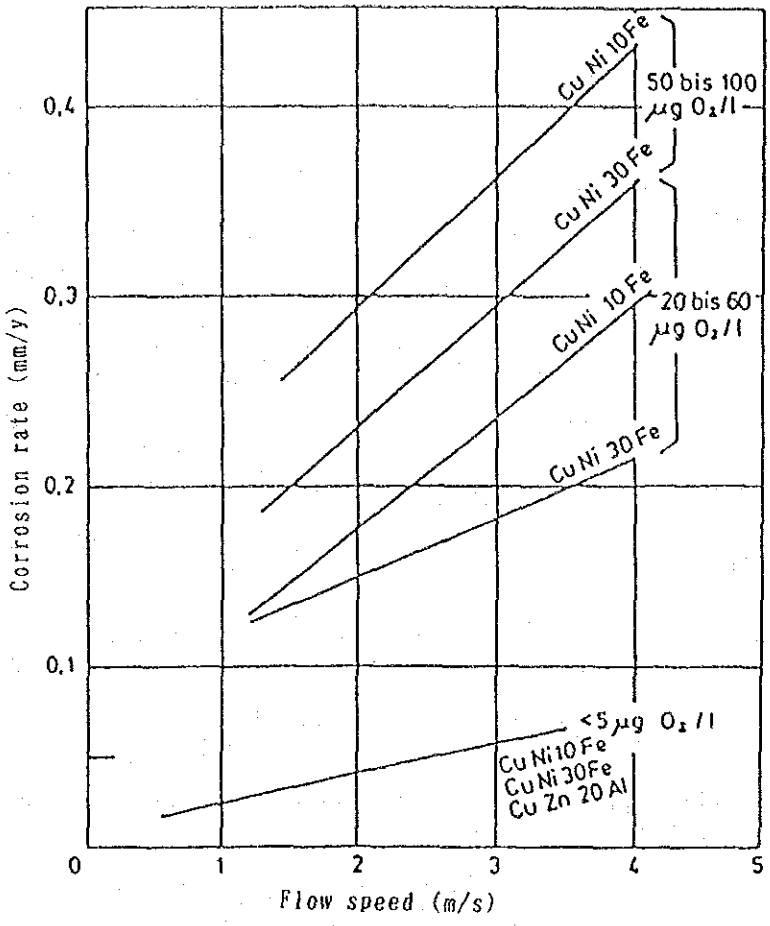

Fig.3.1.5 Influence of Oxygen content and fluid flow speed about several Cu alloys. Temperature is 108℃ ; Test endurance is more than 14 days. pH is 7; CO_2 content < 3 mg/l (n.H.Westphal)[4]

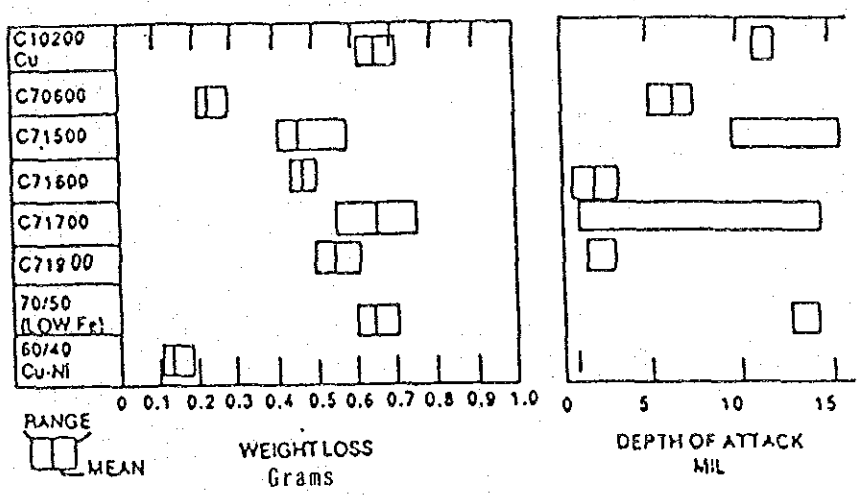

Fig.3.1.6 Weight loss and depth of attack on copper alloys in BNRMRA jet impingement tests.[1]

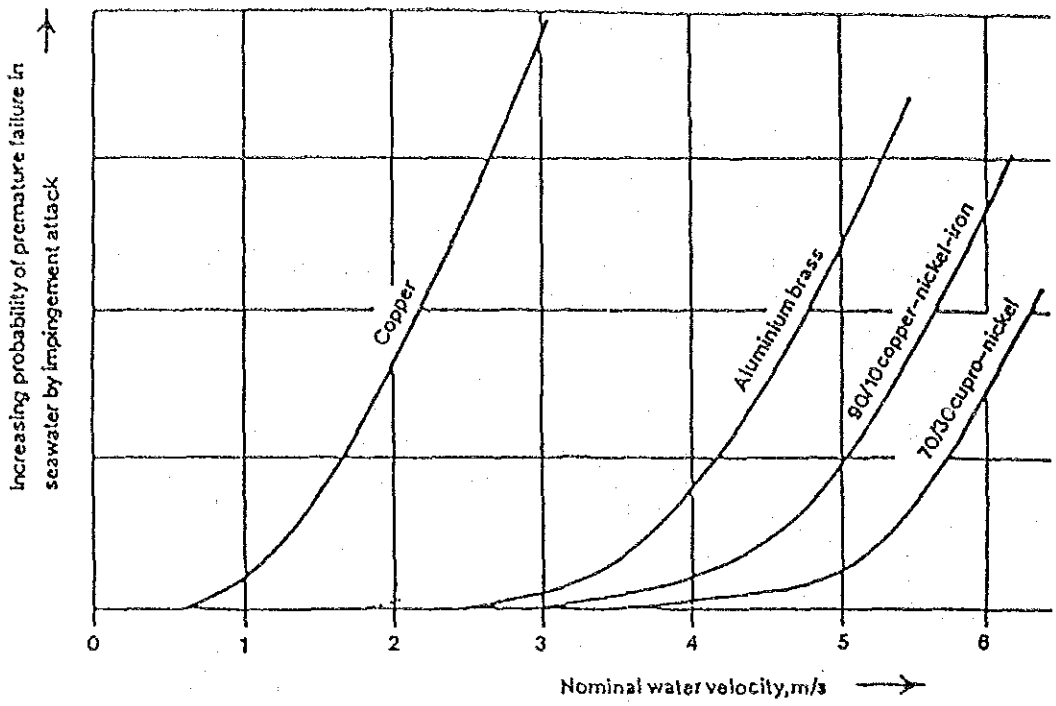

Fig.3.1.7 Velosity limitations for copper alloys in seawater.[5]

Table 3.1.26

Accepted Maximum Tubular Design Velocities for Some Copper Alloys[5]

Alloy	Maximum Design Velocity (m/s)
C12200	0.6
C44300	1.2
C68700	2.4
C70600	3.6
C71500	4.6
C72200	>9.0
Minimum velocity to prevent sediment deposition and under deposit corrosion	1.0
Normal design velocity	2.0

Table 3.1.27 Velocity guidelines for copper alloys in seawater[1]

Condensors and heat exchangers Maximum velocity-any tube, any alloy, 3 fps(0.9 m/s)				
	Maximum velocity- fps, average CA68700	CA70600	CA71500	CA72200
Once through	6.5(2.0)	7.5(2.3)	9.5(2.9)	10(3.1)
Two pass	5.5(1.7)	6.5(2.0)	8 (2.4)	10(3.1)
	Piping Nominal velocity- fps(m/s)		CA70600	CA71500
3-in.(76-mm)diameter and smaller			5(1.5)	6(1.8)
4-to 8-in.(101-to 203-mm) diameter with short radius bands			6.5(2.0)	7.5(2.3)
4-in.(101-mm) and larger with long radius bands and 8in.(203mm)			11(3.35)	12(3.7)

Table 3.1.28 Velocity guidelines for copper alloys in pumps and propellers—seawater[1]

Peripheral velocity—fps (m/s)	Copper alloys
30 (9.1)	C83600 C87600
35 (10.7)	C90300 C92200
50 (15.2)	C95200 C86500
775 (22.9)	C95500 C95700 C95800

Table 3.1.29 Failure Rates of Tubing in Rejection & Recovery [6]

	failure rates * in rejection	tube costs
Al Brass	6.8	least expensive
90/10 CuNi	2.3	↓
70/30 CuNi	1.6	↓
66/30/2/2 CuNiFeMn	0.05	most exjpensive
	failure rates in recovery	
Al Brass	1.07	
90/10 CuNi	0.38	
70/30 CuNi	0	
66/30/2/2 CuNiFeMn	0.02	

*Defined as % of tubes plugged and in retubed bundles

Table 3.1.30 Failure Rates with Acid and Additive Anti-scalants. Heat Recovery Section.[6]

	ACID	ADDITIVE
Al Brass	9.0	0.02
90\10 CuNi	0.36	0.60
70\30 CuNi	0	0

Table 3.1.31 CORROSION RATE OF CUPRONICKEL 90:10 AND ALUMINUM-BRASS PROBES.

MICROMETERS PER YEAR: (μm/y)

	STAGE	pH=6.5	pH=7.2	pH=7.5
Cupronickel 90:10	1	140	255	270
	2	150	260	200
	30	210	185	180
Aluminum Brass	15	140	60	25
	16	160	55	85
	25	80	75	50
	26	20	150	40

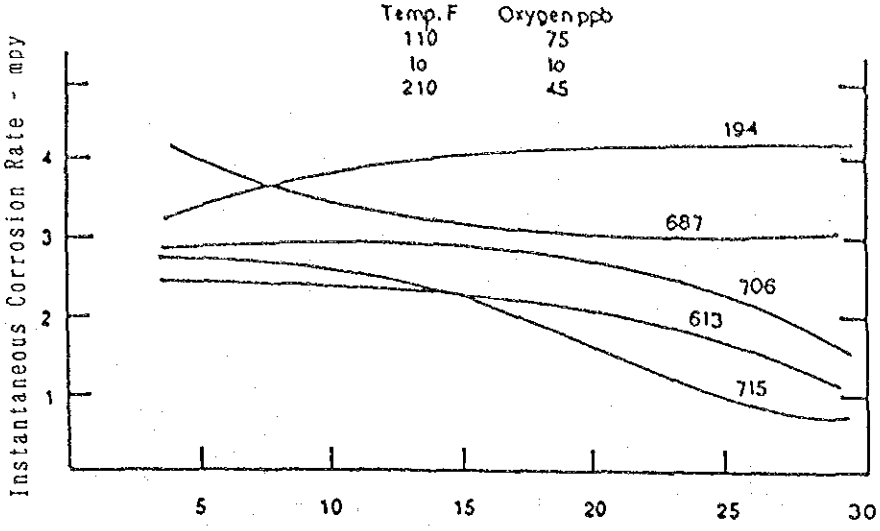

Fig.3.1.8 Variation in corrosion rate for copper alloys from 5 to 30 months in the heat recovery section of an experimental desalination plant. [1]

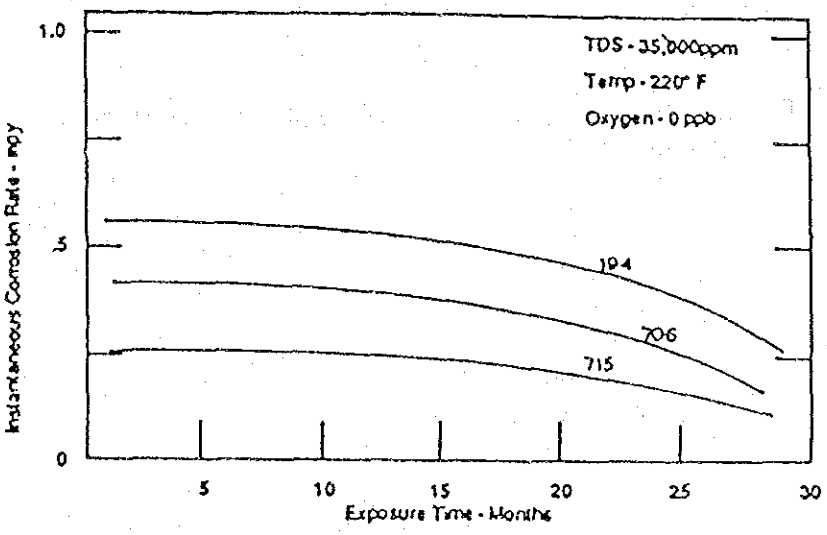

Fig.3.1.9 Variation in corrosion rate for copper alloys from 5 to 30 months in the brine heater section of an experimental desalination plant. [1]

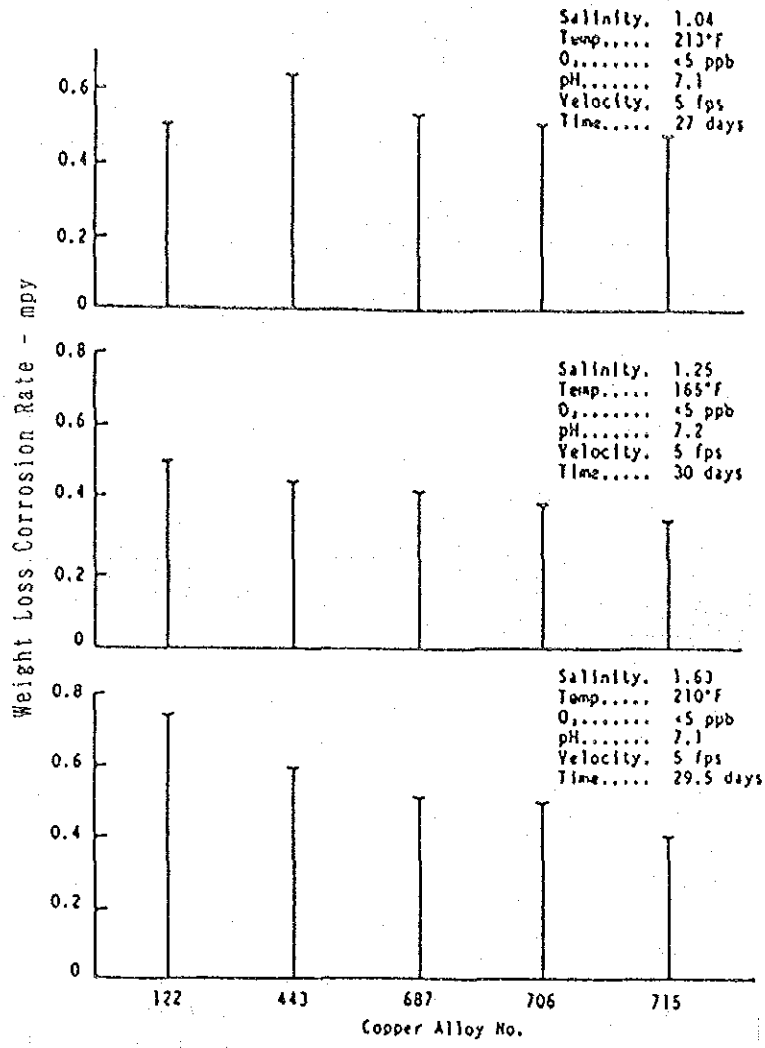

Fig.3.1.10 Effect of brine concentration on copper alloy corrosion rate. [8]

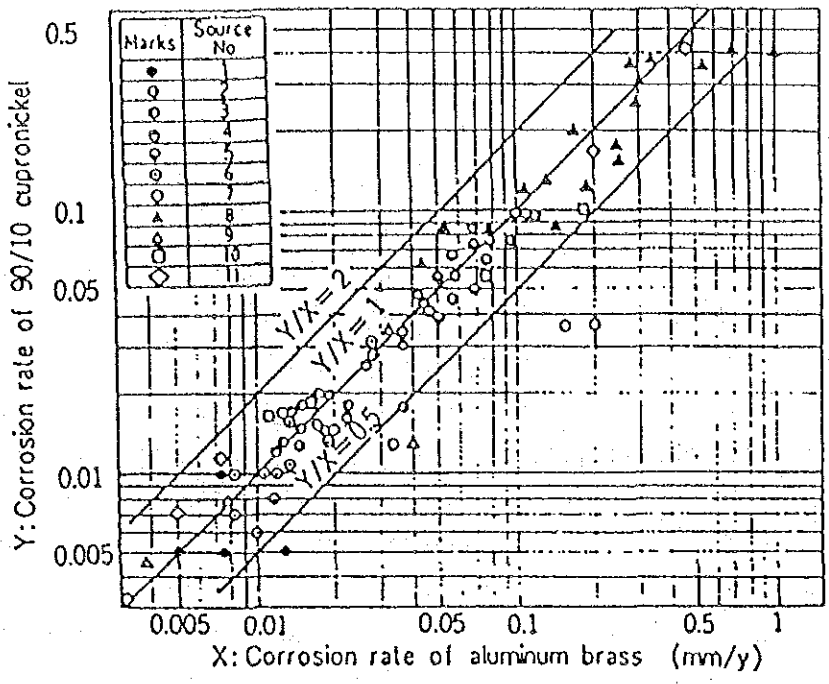

Fig.3.1.11 Comparison of corrosion rate of aluminum brass with that of 90/10 cupronickel in deaerated brine, based on the data obtained from 11 sources.[9]

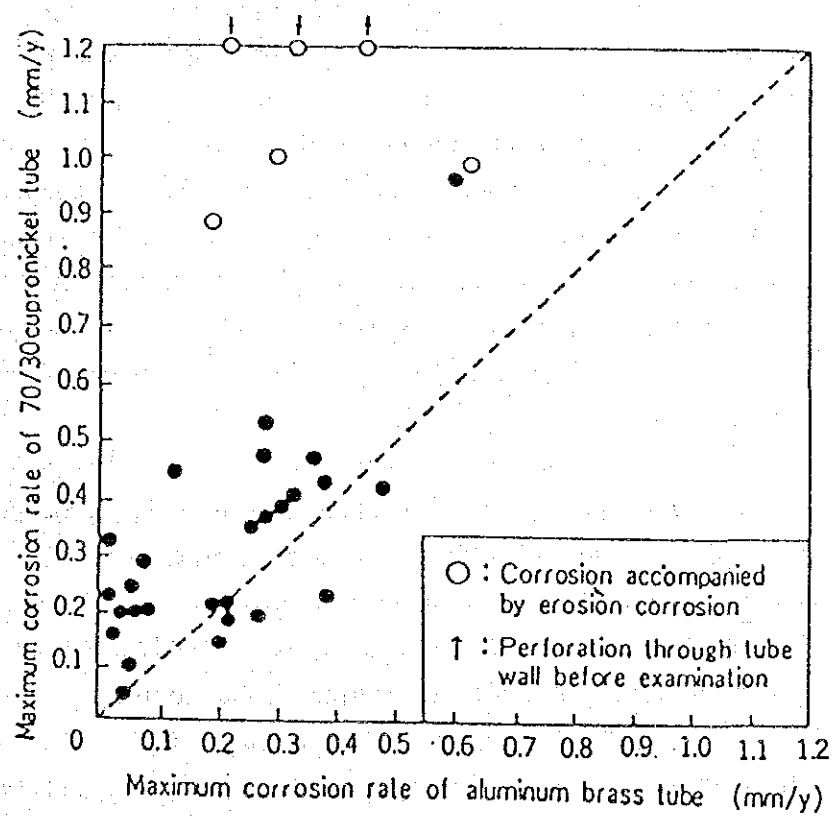

Fig.3.1.12 Comparison of corrosion rate of aluminum brass tubes with that of 70/30 cupronickel tubes, used in polluted sea water containing hydrogen sulfide, in service.[9]

Al-brass in H_2S polluted seawater, in which 70/30 Cu-Ni exhibits considerable corrosion.

In an MSF plant of 180,000 ton/day (by the acid process) which was constructed in Hong Kong by a Japanese manufacturer, Al-brass was adopted to heat transfer tubes. Since its commencement of operation in 1955, overhaul was carried out after 10,000 hours and inspection results[10] on the heat transfer tubes were reported. With respect to the inner side of heat transfer tubes, slight corrosion was found in the inlet path of the brine heater and at both ends of the outlet of the evaporator, and for the tube outside surface, minor corrosion in the form of spots was recognized at the venting section for noncondensable gas.

It was concluded that Al-brass heat transfer tubes in this plant exhibited satisfactory behavior even during high-temperature operation (as high as 121.1°C), but that this was achieved by use of the proper maintenance system.

c) Corrosion by Polluted Seawater

Syrett[11] has found that sulfide in seawater is not so harmful to copper alloys unless dissolved oxygen coexists. For example, under the condition of zero oxygen and at a flow rate below 5 m/s, corrosion rates are held low even if sulfide increases to 55 g/m^3. Figure 3.1.13 shows the electrochemical effects of sulfide and oxygen on copper-nickel alloy, indicating that the absence of oxygen results in comparatively slight corrosion caused by sulfide only. That is, the straight line CD is an anodic polarization curve of Cu which dissolves as Cu^+, and if the cathodic reaction consists of the reaction of hydrogen evolution (straight line IJ), the intersection (1) between the two lines shows the corrosion current i_1. If a considerable amount of oxygen exists, the cathodic reaction curve becomes, for example, GH, and the intersection (2) corresponds to the corrosion current i_4. Table 3.1.32 shows the effects of sulfide-polluted seawater on corrosion at the inlet end of heat transfer tubes, and the increase in corrosion due to pollution reaches 5 to 16 times.

Table 3.1.33 shows the corrosion of tubesheets with and without cathodic protection by a combination of copper alloy tubes (partly Ti tube) and tubesheets in sulfide-polluted seawater. The cathodic protection is considerably effective in the polluted seawater. Figure 3.1.12, previously mentioned, also shows the results of a corrosion test in the polluted seawater containing hydrogen sulfide, and 70/30 Cu-Ni and Al-brass are considerably subjected to corrosion. In Japan, for copper-based alloy heat transfer tubes to be applied to this type of environment, AP bronze (Cu-8Sn-1Al-Si) has been developed and extensively put into practical use. It has been clarified that copper alloys exposed to sulfide-polluted seawater form typical black sulfide film, but that subsequent exposure to clean seawater replaces it with normal oxide film.[11] However, in the stage of transition, considerably high corrosion rates last for some time. It is said that no

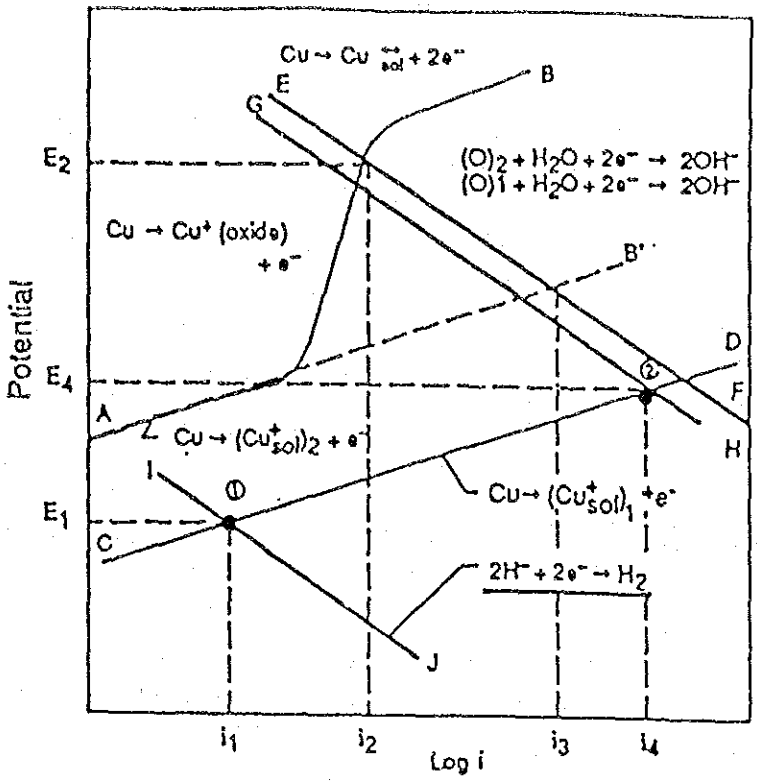

Fig.3.1.13 Influence of sulfide and oxygen on the corrosion current in a copper-nickel alloy exposed to flowing seawater. [11]

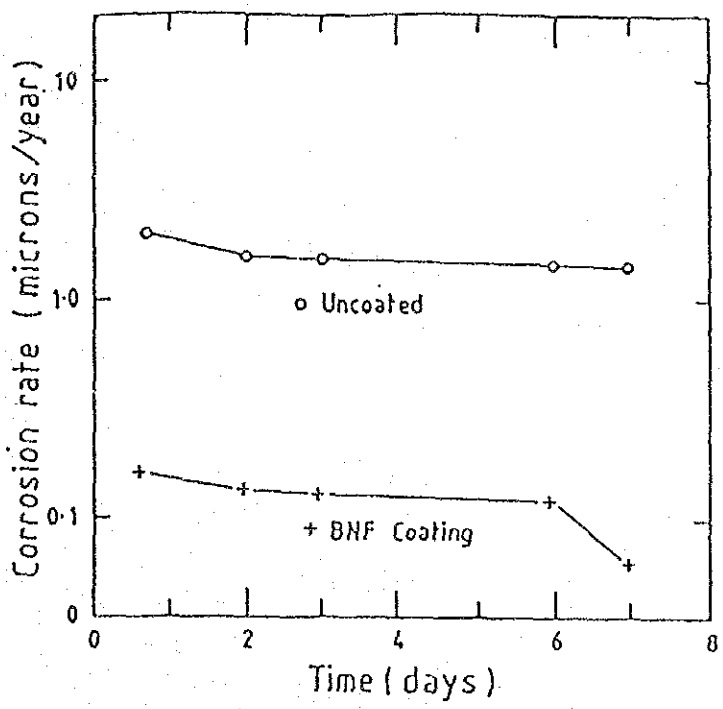

Fig.3.1.14 Corrosion rate versus time for 90/10 copper nickel after one week in polluted seawater, followed by clean flowing seawater. [13]

Table 3.1.32 CORROSION RATES (mm/y) DETERMINED BY WEIGHT LOSS MEASUREMENTS ON INLET ENDS OF TUBES[12]

Tube	Unpolluted	Sulfide-Polluted
Cold Water Conditions		
Aluminum Brass	0.030	0.498
90-10 Cu-Ni	0.030	0.460
70-30 Cu-Ni	0.063	0.333
Warm Water Conditions		
Aluminum Brass	0.046	0.220
90-10 Cu-Ni	0.036	0.025
70-30 Cu-Ni	0.022	0.182

Table 3.1.33 TUBESHEET CORROSION RATES (mm/y) WITH AND WITHOUT CATHODIC PROTECTION IN SULFIDE-POLLUTED SEAWATER[12]

Tubesheet/Tube	No C.P.	Low Level C.P.	Intermediate Level C.P.	High Level C.P.
Cold Water Conditions				
Aluminum Bronze/Titanium	1.56	0.172	0.083	0.023
Muntz/Titanium	6.07	0.622	0.159	0.191
Muntz/Aluminum Brass	2.41	0.386	0.161	0.135
Muntz/90-10 Cu-Ni	2.92	0.391	0.133	0.107
Muntz/70-30 Cu-Ni	3.33	0.437	0.201	0.199
Warm Water Conditions				
Aluminum Bronze/Titanium	0.927	0.076	0.010	0.010
Muntz/Titanium	7.34	0.113	0.041	0.027
Muntz/Aluminum Brass	5.44	0.131	0.030	0.021
Muntz/90-10 Cu-Ni	1.88	0.399	0.025	0.023
Muntz/70-30 Cu-Ni	5.41	0.287	.028	.018

more than 9 days are required for the normal oxide film to be changed into sulfide film by polluted seawater. Table 3.1.34 shows the results of an experiment simulating the gas venting zone, which constitutes problems when ammonia polluted seawater is handled, and clearly indicates the high capability of 70/30 Cu-Ni under this environment. BNF has developed a protective coating technique which is applied to copper-based heat transfer tubes to be exposed to seawater for the first time.[13] This treatment provides a film naturally formed on the copper alloy surface in clean seawater and an inorganic film with similar composition and corrosion resistance to the copper-based heat transfer tubes, achieving low cost and providing practical resistance to pollutants. Figure 3.1.14 shows the results when this treatment was applied to 90/10 Cu-Ni tubes, and further longer tests are being carried out on actual equipment at various places.

Table 3.1.34 Corrosion in 500ppm/1400ppm NH_3/NH_4CO_3 Solution

Alloy	Corrosion Rate(mm/year)
Al Brass	0.13
90/10 CuNi	0.10
70/30 CuNi	0.08

d) Chlorine Dosing Conditions

Chlorine dosing conditions for copper alloys differ considerably among researchers. For example, R. Frances at BNF[13] set the following chlorine dosing conditions by experiments using the jet flow rate of 9 m/s. Al-brass: only intermittent chlorine dosing is possible. 1 ppm of Cl_2 is dosed for 2 hours every 12 hours. In general, in copper alloys, the pit depth by impingement increases as the chlorine dosing rate increases, and in particular, for Al-brass the tendency increases when iron coexist. 90/10 Cu-Ni: continuous chlorine dosing is possible if the concentration of Cl_2 is up to 0.3 ppm, and intermittent dosing is allowed if it is up to 0.5 ppm. 70/30 Cu-Ni: intermittent chlorine dosing is possible if its concentration is up to 2 ppm and is dosed for 2 hours every 12 hours. 60/30/2/2 Cu-Ni-Fe-Mn: resistance to impingement is great and both continuous and intermittent dosing are possible if its concentration is up to 2 ppm.

As an actual accident, there was a case in which Al-brass tubes were attacked considerably rapidly by simultaneous additions of ferrous sulfate and chlorine. This corresponds to the above-mentioned results of Frances. With respect to chlorine dosing to Yorkoron, the following

different conclusions have been drawn by Gusmano et al[14].

(1) Yorkoron should not be used under conditions which result in a high corrosion potential (free Cl_2>0.6 ppm, or conditions which promote microbe activity on the metal surface without chlorine dosing).

(2) Consequently, chlorine dosing is absolutely essential and the free Cl_2 content must be maintained to less than 0.5 ppm. The desalting plant shall not be operated without chlorine dosing even for a few days.

(3) The condition of free Cl_2 <0.5 ppm can be accurately controlled by measuring the redox potential.

(4) In a desalting plant using Yorkoron, simultaneous monitoring of the corrosion potential and redox potential (also corrosion rates, if possible) plays an important role in preventing corrosion failures.

In addition to these, another experiment on 70/30 Cu–Ni pipes shows that condition of free Cl_2<0.5 ppm is required as shown in Fig. 3.1.15. According to this figure, a flow rate of

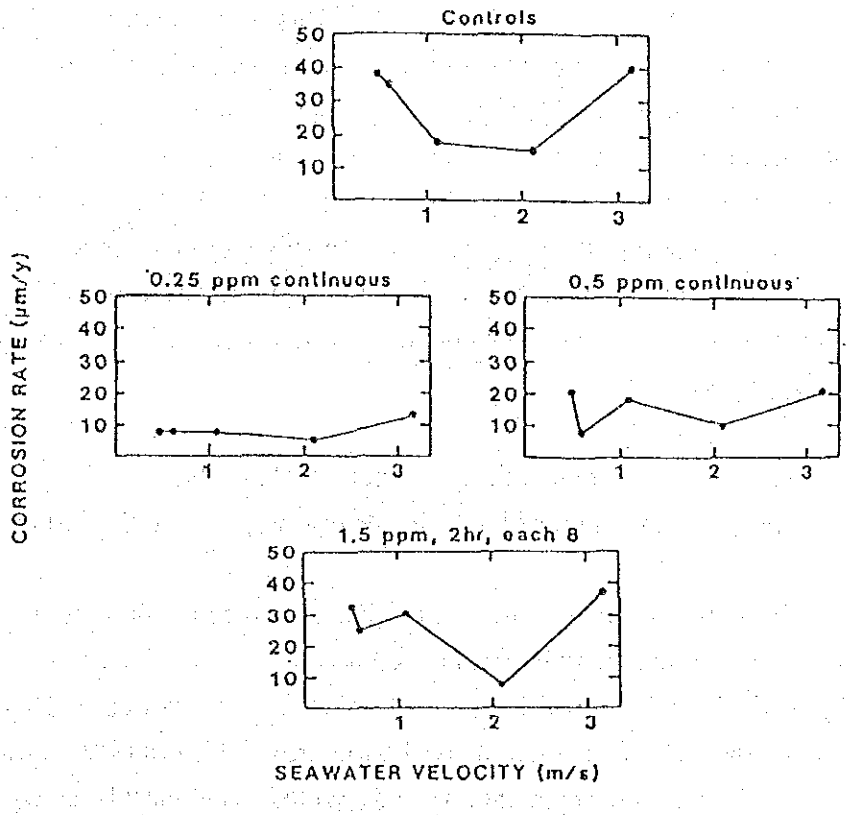

Fig.3.1.15 Effects of velocity and chlorination on corrosion of 70/30 Cu–Ni piping in seawater service(187 days test at average seawater temperature of 24°C) [5]

1–2 m/s is desirable. It is interesting to note that the condition of quiescent seawater without chlorine dosing is particularly dangerous.

e) Hydrotalcite and Erosion Corrosion of Al–brass

It was Castle, Peplow et al.[15] that identified hydrotalcite $Mg_6Al_2(CO_3)(OH)_{16}$ for the first time as the white corrosion product on Al–brass heat transfer tubes in seawater service, and reported the fact that it is difficult for the iron compound film necessary for corrosion protection to adhere to this film. However, Yamamoto et al.[16] was the first to report on the relationship between hydrotalcite in Al–brass tubes and erosion corrosion. They found leakage in Al–brass tubes due to erosion corrosion 10 months after the inauguration of condensers in a power plant and identified hydrotalcite from the white film adhering to the inner surface of these tubes. In this condenser, clean seawater was used and ferrous salt and chlorine were injected. However, there was a substantial distance from the ferrous salt injection point to the condenser. As a result of jet tests on the hydrotalcite adhering surface of Al–brass tubes, violent erosion corrosion occurred to the film which had been damaged previously. The potential difference between the Al–brass substrate and this film is 100–40 mV, forming the anode on the substrate. Hydrotalcite is believed to be an initial corrosion product of Al–brass in seawater, and tends to be generated unless effective corrosion protection is provided at the initial stage of water introduction. The normal iron compound film on copper alloy has self–healing capabilities and can recover its original state naturally even when flaws occur due to impingement of a solid body, but iron compound on hydrotalcite film has minimal protective capabilities and erosion corrosion rapidly takes place once the film is damaged. From the above results, for Al–brass tubes in seawater service, it is necessary to clarify the conditions of hydrotalcite and draft the required countermeasures; Minamoto et al.[17] have drawn the following conclusions from a wide range of investigations and experiments.

(1) Chlorine dosing to the seawater promote the generation of white film.
(2) The simultaneous injection of iron ions and chlorine dosing promote the forming of white film.
(3) When Mn–rich film is formed in advance on the inner surface of the tube, white film is formed by chlorine dosing irrespective of the presence of iron ion injection.
(4) If dense iron hydroxide film is formed in advance, white film does not form. Therefore, as a measure to prevent white film formation, dense iron hydroxide film must be formed on the inner surface of the tube from the beginning. For this purpose, care must be taken concerning the following:

<1> Chlorine dosing should be stopped during ferrous ion injection.

<2> Ferrous ion injection should be conducted as close as possible to a condenser.
<3> Ferrous ion solution must be freshly prepared each day and obsolete solution must be discarded.

f) Corrosion Attack Attributable to Stress

This section discusses stress corrosion cracking (SCC) and corrosion fatigue, but in MSF plants, this type of damage is comparatively rare. When stress is applied to brass containing a large amount of Zn, Zn brass is subjected to ammonia SCC under the presence of air, steam, and traces of ammonia. This kind of environment may appear in stored seawater (the decay of organisms gives rise to ammonia), and the leakage of air into the plant during plant shutdown must be minimized. Table 3.1.35 arranges corrosion resistances of copper alloys to ammonia SCC from low to high. Al-bronze such as 606 and 614 provides a corrosion resistance one digit higher, and Cu-Ni alloys and pure copper exhibit virtual immunity against SCC. There was a case in which Al-brass tubes in the condenser of a desalting plant and Cu-Ni tubes of feed- water heaters showed inter granular SCC. Figure 3.1.16 shows experimental results of the effects of steam temperature and stress on the SCC of these copper alloys.

The critical stress lowers as temperature rises. Figure 3.1.17 shows experimental results of the effects of ammonia on the SCC of Al-brass in high-temperature water.

Susceptibility to SCC increases as temperature rises and the amount of ammonia increases. In addition, in the section about 3 cm from an inlet of heat transfer tubes (Al-brass) at the heat recovery section of MSF plant at Abudabi, SCC in the circumferential direction was generated (Fig. 3.1.18). It has been asserted that the cause was attributed to the stress generated during expanding and to some corrosive media. This was later prevented by cathodic corrosion protection using a sacrificial iron anode installed to the water chamber.

Strength to corrosion fatigue is generally expressed as the maximum cyclic stress with the mean stress of zero under which the specimen is not ruptured at 10^8cycles. Table 3.1.36 compares the corrosion fatigue strength of various copper alloys.

(2) Titanium and Titanium Alloys

Among titanium-based materials, pure titanium is used primarily for MSF plants and Ti-0.15Pd is used for places where crevice corrosion is particularly liable to occur. Pure titanium (hereinafter called "titanium") has stable corrosion resistance, achieved by passivity against normal temperature seawater (Fig. 3.1.19), and provides particularly outstanding pitting resistance (Fig. 3.1.20, R504: titanium G2; R5 64: Ti-6Al-4V), high resistance to high flow rate and sand erosion (Tables 3.1.37 and Fig.3.1.21), and excellent corrosion resistance in polluted seawater (Table 3.1.38). In this way, titanium exhibits excellent corrosion resistance in environment containing chloride ions, but has problems of susceptibility to crevice corrosion in high

Table 3.1.35 Ammoniacal stress corrosion resistance of brasses, aluminum bronzes, and copper-nickel alloys—Thompson[1]

Alloy	Time to 50% relaxation (h)
C44300	0.30
C2800	0.35
C46500	0.50
C26000	0.51
C68700	0.60
C60600	4.08
C61400	5.94
C70600	234
C14200 PDO copper	312
C71500	2000

Table 3.1.36 Corrosion fatigue strength of propeller alloys in seawater—Metals Properties Council—Prager [1]

Cast alloy	Corrosion fatigue strength[1] (psi)	(MPa)
C86500 ABS Type 2	9000 + 20%	62 + 20%
C95500 ABS Type 4	14,000 + 20%	96 + 20%
C95700 ABS Type 5	12,000 + 20%	83 + 20%

[1]These corrosion fatigue strengths were measured at 10^8 cycles

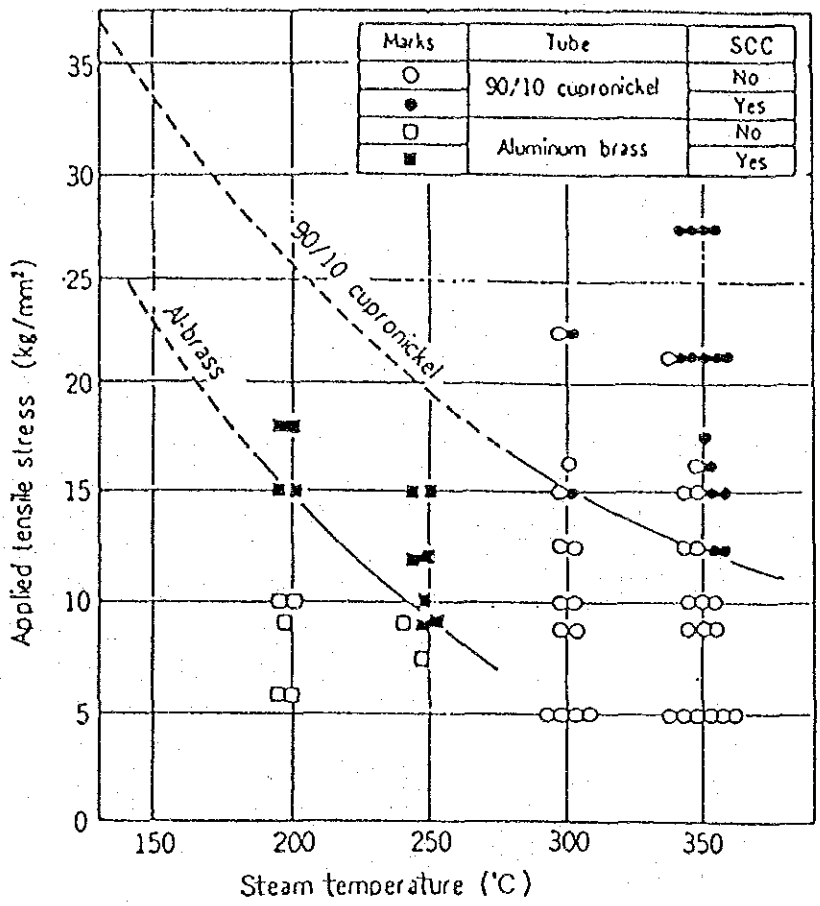

Fig.3.1.16 Effect of applied tensile stress and steam temperature on stress corrosion cracking of aluminum brass, as compared with 90/10 cupronickel. [9]

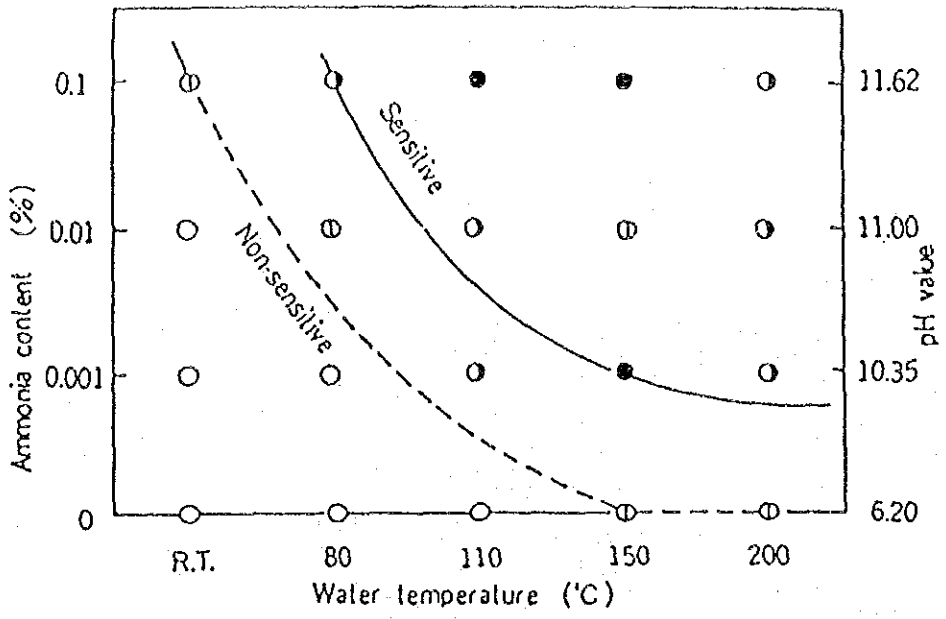

Fig.3.1.17 Effect of an ammonia content on stress corrosion cracking of aluminum brass tube in water at elevated temperature.[9]
Hoop stress : 25.0 kg/mm², Test duration : 300 h.

Marks	○	◐	◑	●
Depth of SCC (μ)	<20	20~50	50~200	>200

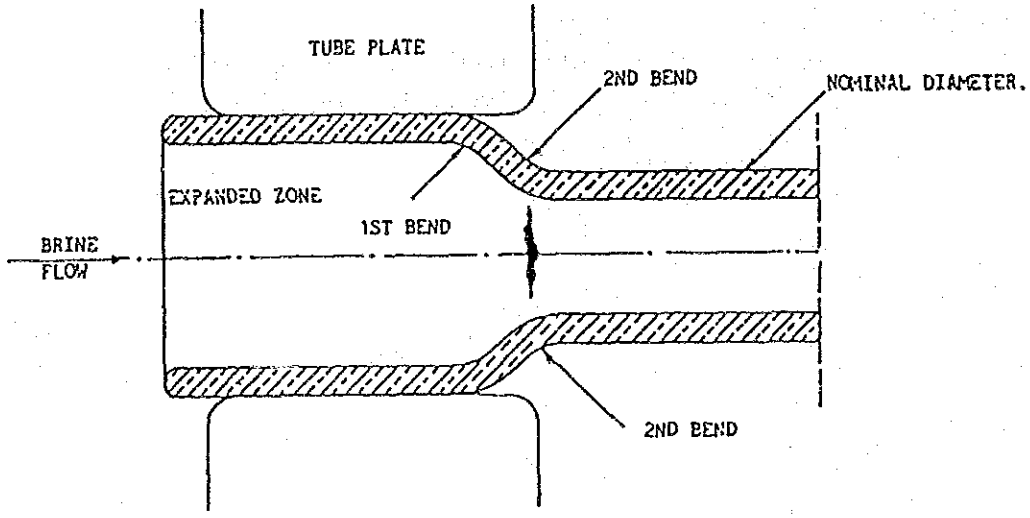

Fig.3.1.18 Schematic presentation of failure in an Al-brass tube. Drawing not to scale.[18]

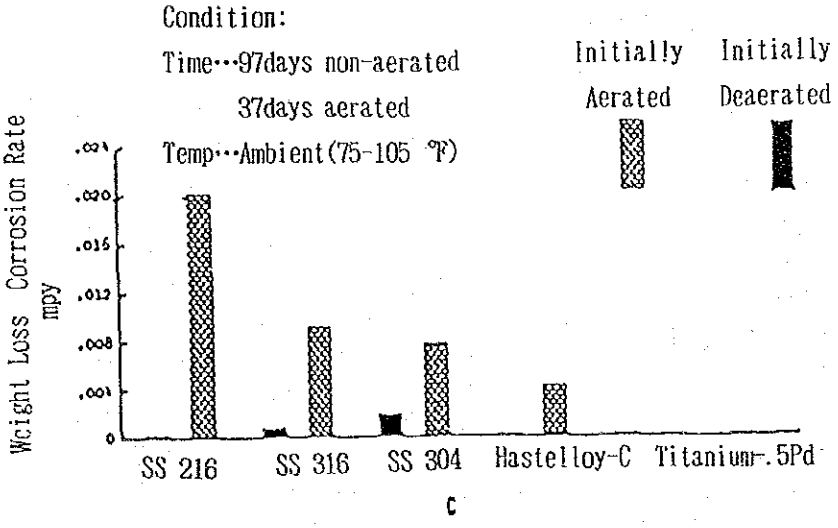

Fig.3.1.19 Corrosion rate comparisons in initially aerated and nonaerated quiescent sea water. [8]

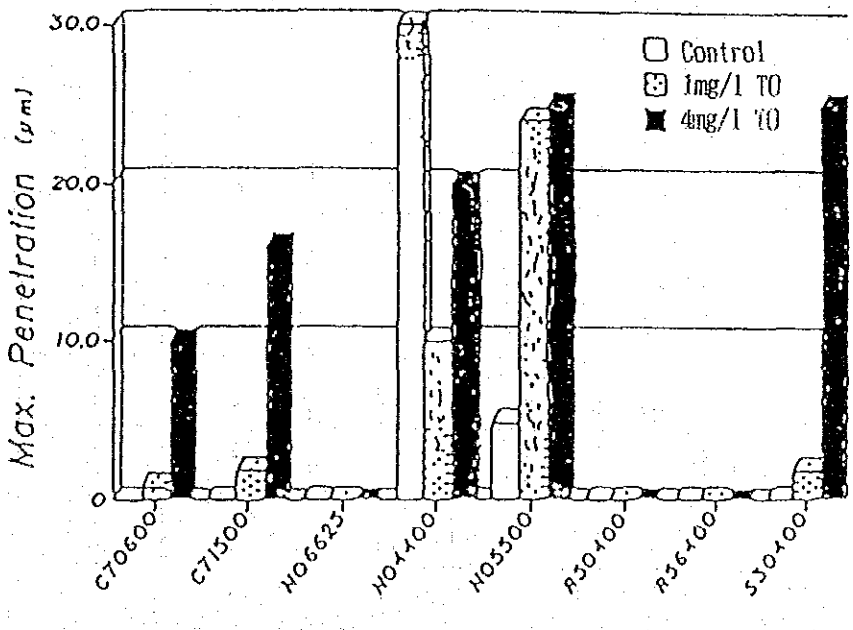

Fig.3.1.20 Maximum Corrosion Depth [19]

Table 3.1.37 Design flow rate [20]

Material	Design velocity that should not be exceeded (ft/sec)
Copper	3[a]
Silicon bronze	3[a]
Admiralty brass	5[a]
Aluminum brass	8[a]
90–10 copper nickel	10[a]
70–30 copper nickel	12[a]
Monel alloy 400	No maximum velocity limit[b]
Type 316 stainless steel	No maximum velocity limit[b]
Incoloy 825 and Carpenter 20 cb	No maximum velocity limit[b]
Inconel 625 and Hastelloy C	No velocity limits
Titanium	No velocity limits

[a] In deaerated brines encountered in the heat recovery heat exchangers in desalination plants the critical velocities can be increased from 1 to 2 ft/sec.

[b] Minimum velocity 5 ft/sec.

Table 3.1.38 Comparison of corrosion resistance of various condenser tube materials [20]

Material		Water quality	Resistance to:				
			General corrosion	Pitting		Stress corrosion cracking	Drop impingement corrosion
				Running water	Stagnant water		
Admiralty brass	Fresh Water	clean	2	1	2	1	3
		dirty	2	4	4	4	
Stainless steel		clean	1	2	2	1	1
		dirty	1	4	4	3*	
Aluminum brass	Sea Water	clean	2	1	3	1	2
		dirty	2	4	4	4	
Cupro-nickel Cu Ni 90/10		clean	2	1	2	1	3
		dirty	2	4	4	4	
Cupro-nickel Cu Ni 70/30		clean	1	1	2	1	2
		dirty	2	4	4	4	
Titanium		clean	1	1	1	1	2
		dirty	1	2	2	1	

Definition of clean: COR** < 4 ppm; O2 > 4 ppm; NH3 < 1 ppm; S^{-1} < 0.020 ppm
Definition of dirty: COR > 4 ppm; O2 < 4 ppm; NH3 > 1 ppm, S^{-1} > 0.020 ppm
*At higher Cl contents
**COR = Chemical Oxygen Requirement
1 = excellent 2 = good 3 = average 4 = poor

temperature seawater and brine (for example, at the crevice formed when titanium tube is expanded into titanium tubesheet), hydrogen absorption under saline water environment at high temperature, hydride formation depending on the amount of hydrogen, as well as the problem of embrittlement. In seawater, the corrosion potential of titanium is relatively noble, but it comes in contact with less noble metal such as copper alloys, these alloys become anodic and copper alloys are subjected to galvanic corrosion.

a) Crevice Corrosion of Titanium and Titanium Alloys

In the generation and growth of crevice corrosion of metal in saline water, the decrease of pH in the saline water in the crevice plays an important role. Figure 3.1.22 shows experimental results on titanium in 6% NaCl solution at 95°C. For the critical conditions under which titanium generates crevice corrosion, a wide variety of data are available, but this section introduces data with different crevice conditions. Figure 3.1.23 is a test in which a titanium tube is expanded into a titanium tubesheet, and shows critical conditions at 60°C, irrespective of the NaCl concentration (conventional critical line is located on the high-temperature side), which represent the conditions closer to those in actual plants. Figure 3.1.24 shows the results of testing Ti-0.15 Pd tubes under the same conditions as in the previous figure. No crevice corrosion was generated up to 125°C and the critical line was not determined. Figures 3.1.25 and 3.1.26 show electrochemical tests under the crevice condition with many plastic washers bolted to a titanium plate. First, crevice corrosion was allowed to generate on the specimen and the potential ER.CREV which repassivates the specimen, and then the critical concentration CR.CREV and the critical temperature TR.CREV of repassivation were determined and plotted. The former plots the relationship between ER and NaCl % and the latter plots that between temperature and NaCl% , at which ER and CR, as well as TR were measured, and determines the critical lines (shown in double line) which summarize these results. These critical lines vary considerably according to the experimental method used, but for practical applications, a critical line on the safety side should be selected with the actual crevice type taken into account. Figure 3.1.27 compares critical lines of crevice corrosion occurrence by two crevice types, Ti/Ti and Ti/ sealant/Ti, using titanium specimens. The specimen type containing sealant exhibited severer results. Figure 3.1.28 shows critical lines for crevice corrosion of titanium and Gr12 titanium (Ti-0.8Ni-0.3Mo), and Figure 3.1.29 shows those of titanium and Gr7 titanium (Ti-0.15Pd). Figure 3.1.30 shows critical lines with varying pH and temperature of the saturated sodium chloride solution for the above three titanium-based materials, indicating excellent resistance to crevice corrosion for Gr7 and Gr12. This is attributed to Pd in Gr7 and Ni in Gr12, which facilitate passivation by lowering the hydrogen overvoltage of each alloy. In particular, Ti-0.15Pd excels

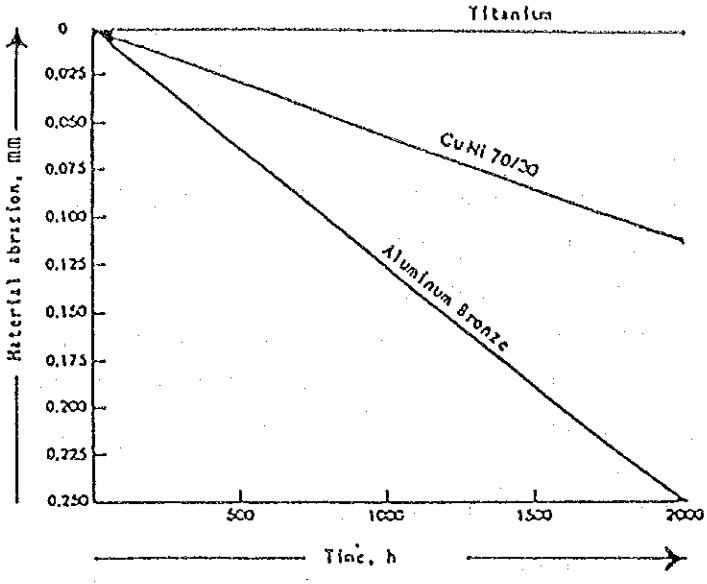

Fig.3.1.21 Material abresion by fine sand in seawater. Velocity 1.8 m/sec.[20]

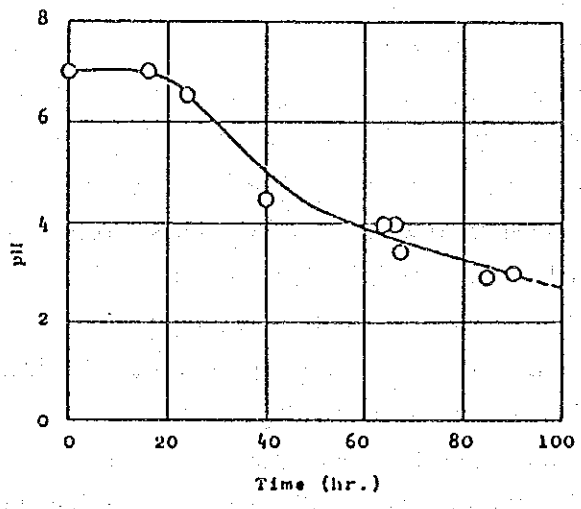

Fig.3.1.22 Variation of pH of the crevice solution [21]

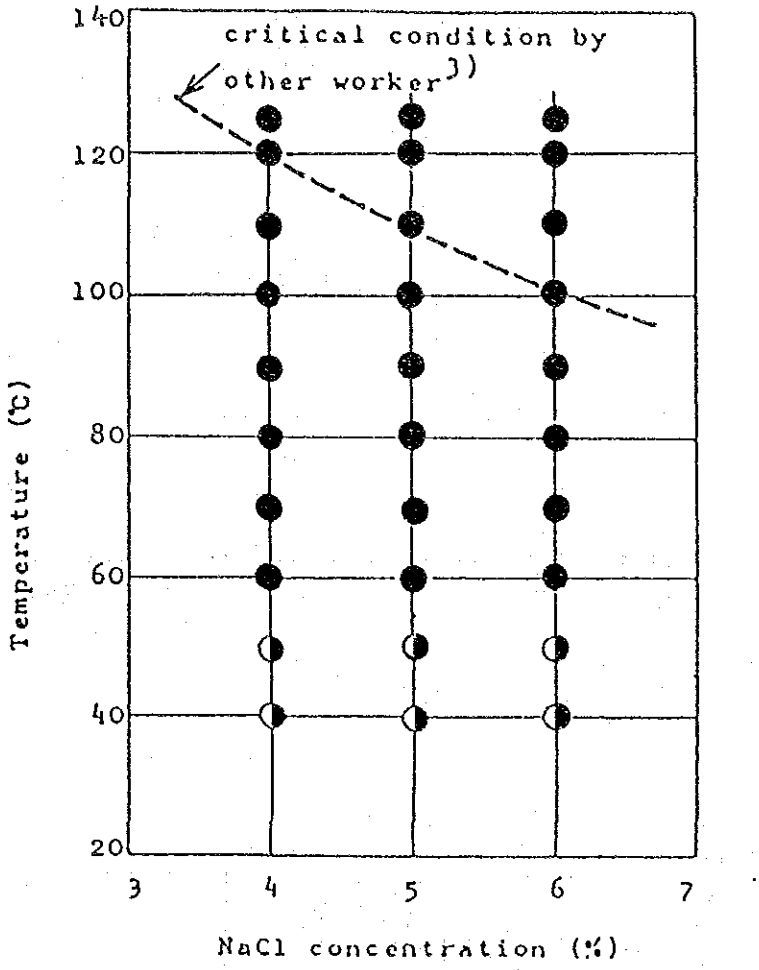

Fig. 3.1.23 Effects of NaCl concentration and temperature on the crevice corrosion of c.p. Ti tube [21]

◑ ; tarnished, ◉ : suffering crevice corrosion

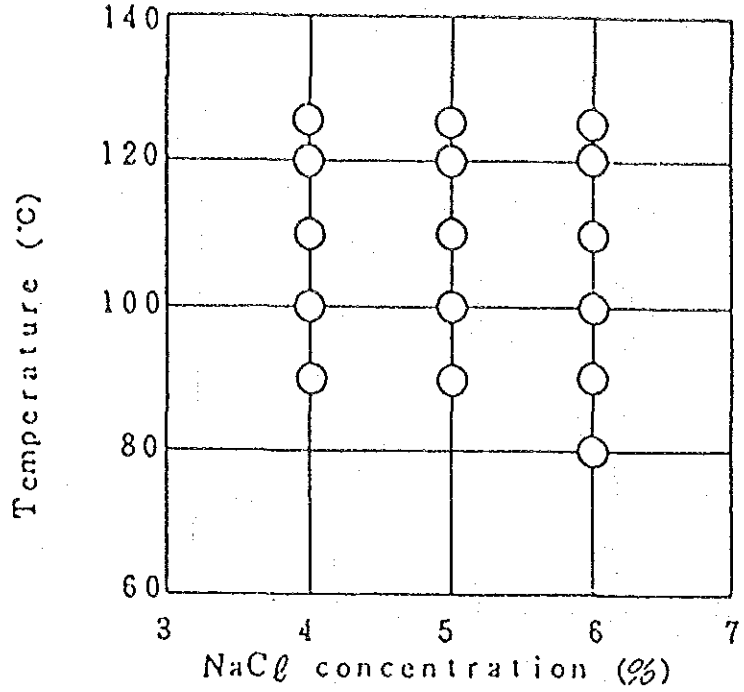

Fig.3.1.24 Effects of NaCl concentration and temperature on the crevice corrosion of Ti-0.15Pd alloy tube.[21]

○: free from corrosion

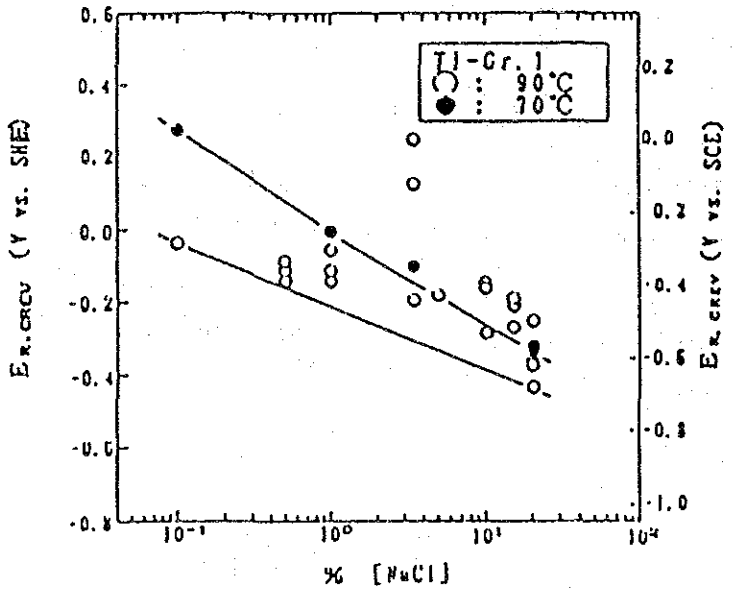

Fig.3.1.25 [NaCl] concentration dependency and temperature dependency of $E_{R,CREV}$ of Ti-Gr.1 in the chloride environment[22]

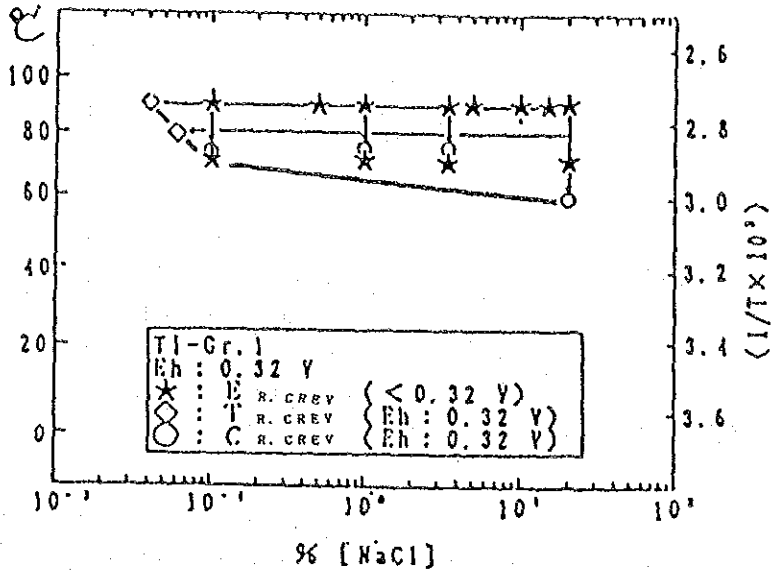

Fig.3.1.26 Applicable range of Ti-Gr.1 in the chloride environment [22]

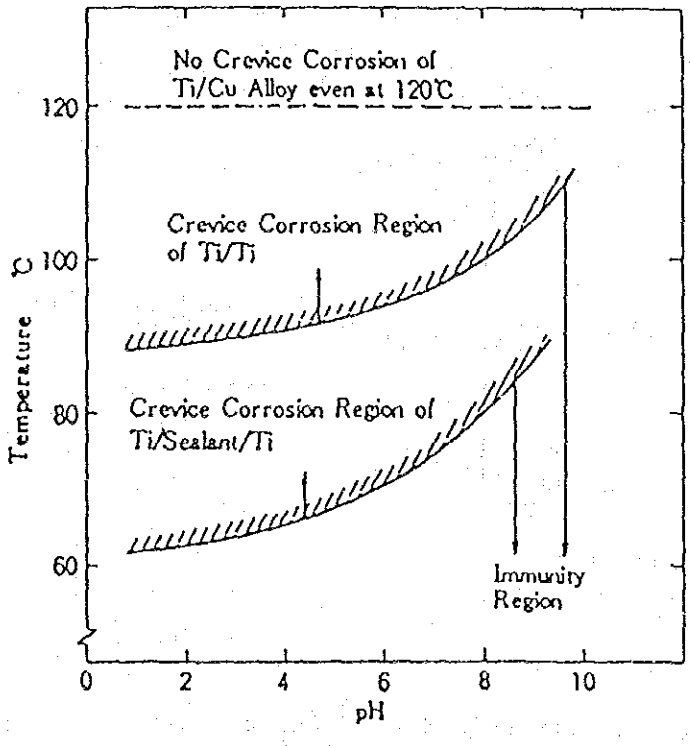

Fig.3.1.27 Critical conditions for crevice corrosion occurrence in commercially pure titanium in deaerated 6% NaCl solution [23]

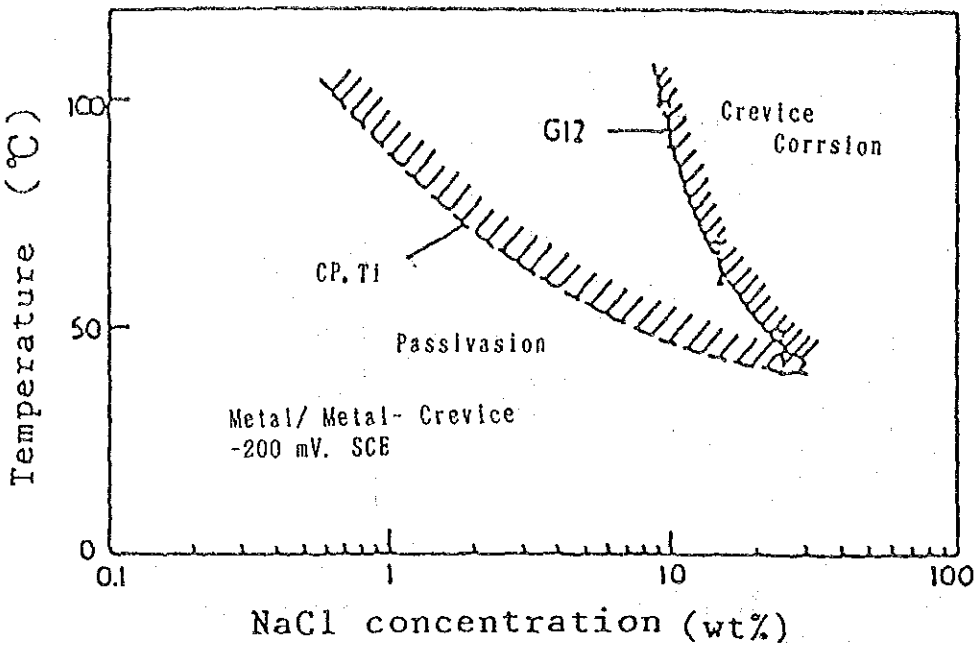

Fig.3.1.28 Crevice corrosion map of titanium Grade 12 concerning temperature and NaCl concentration [20]

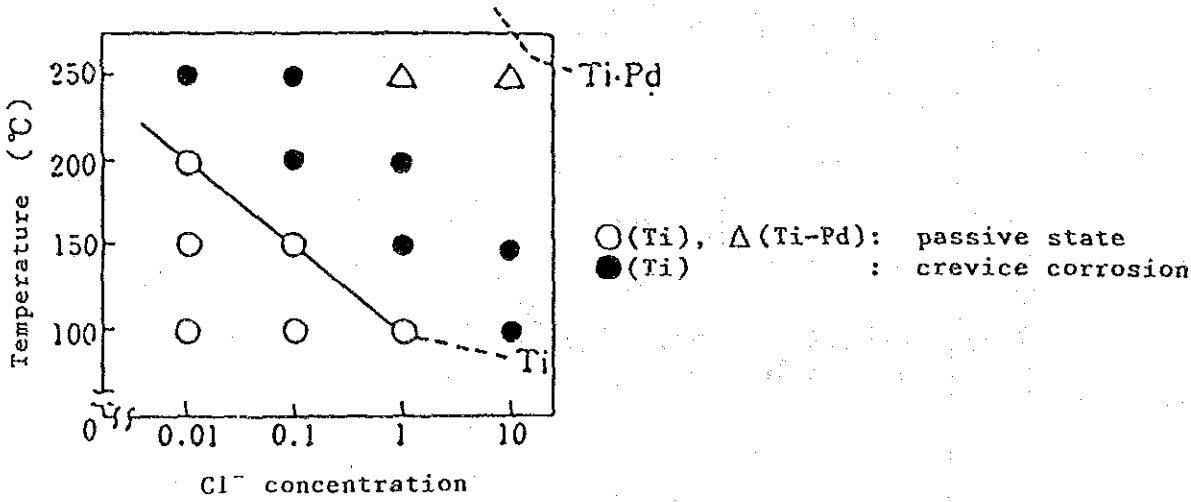

Fig.3.1.29 Critical temperature and Cl^- concentration which cause crevice corrosion in Titanium and Ti-0.15 Pd alloy (titanium/titanium crevice, pH7, NaCl solution, 240-h immersed) [24]

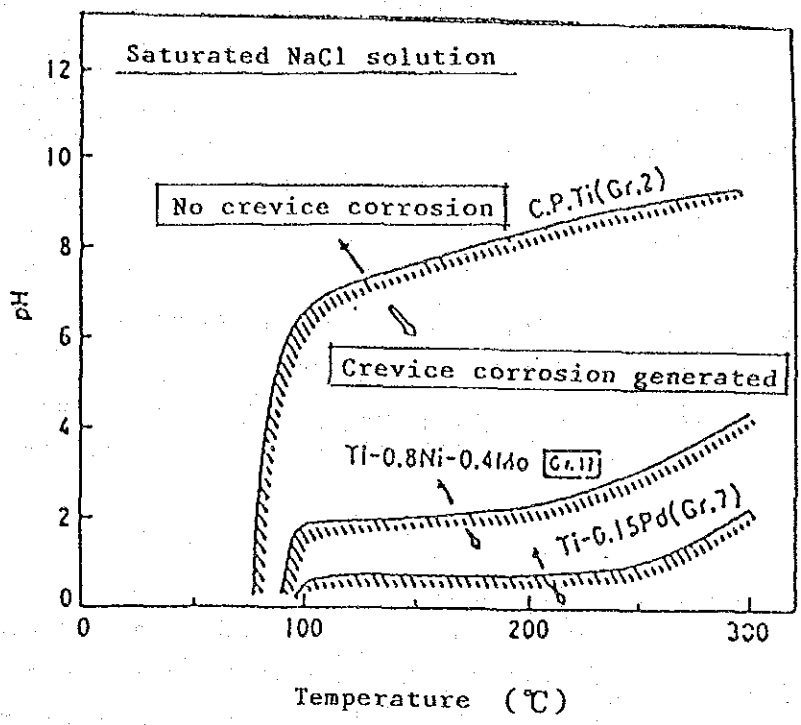

Fig.3.1.30 Critical conditions which cause crevice corrosion in various titanium materials [25]

in resistance to crevice corrosion and provides high reliability. To prevent crevice corrosion, various surface treatments for titanium have been developed. Figure 3.1.31 represents the result of investigations on the presence of crevice corrosion occurrence in titanium according to the time of air oxidation, and the effectiveness is exhibited at 400°C for over 10 minutes (lower than 700°C). Another method is to coat Pd compound. In this method, $PdCl_2$ and $TiCl_3$ are coated on the titanium surface and PdO/TiO_2 film is formed by thermal decomposition. Figure 3.1.32 compares the polarization curves of untreated titanium and coated titanium in the 10 % H_2SO4 solution, indicating that hydrogen overvoltage of Pd- coated titanium is extremely low (easy to passivate). The lower limit potential of crevice corrosion growth for titanium is believed to be about-0.4V, and holding the potential less noble than this by cathodic protection (however, holding it over about -0.6V for prevention of hydrogen embrittlement) can prevent crevice corrosion.

b) Hydrogen Absorption and Galvanic Corrosion of Titanium

Figure 3.1.33 shows hydrogen absorption rates of thin-walled titanium tubes used in the test plant of a seawater desalting project by MITI, indicating the large absorption rates at the high-temperature section only. As to the causes of these hydrogen absorption phenomena of titanium tubes, a wide variety of research has been carried out in Japan and several hypotheses have been offered, but an accurate mechanism has not yet been clearly elucidated. For example, some researchers advocate that atomic hydrogen evolves from the decomposition of iron rust on the titanium surface and that this is absorbed by the titanium. In relation to this, experiments were performed in a solution containing $Fe(OH)_2$. In this case, as seen in Fig. 3.1.34, as-manufactured tubes absorb more hydrogen as the temperature rises, but tubes from which contaminant or iron rust has been removed by pickling absorb less hydrogen. Figure 3.1.35 shows the change of hydrogen absorption rates with time for titanium and Ti-0.15P d. As predicted, after 3000 hours, Ti-0.15Pd (low hydrogen overvoltage) absorbed hydrogen several times that of titanium. Figure 3.1.36 shows the hydrogen absorption rates when titanium is coupled with various types of metal, indicating that titanium reached the potential for hydrogen evolution when coupled with the least noble mild steel. Table 3.1.39 shows the hydrogen absorption rates and presence of hydride when titanium is immersed and cathodic-polarized to -750 mV and -1000 mV. With the hydrogen absorption rate of 25 ppm as a boundary, the formation of dangerous hydride was not recognized be low this boundary.

Figure 3.1.37 shows the mean corrosion rates and maximum penetration depth (pit depth) of copper alloys in an immersion test carried out on galvanic couples between titanium and various copper alloys in artificial seawater. The decrease of mean corrosion rate at 100 may be attributed to de-aeration by heating. In this way, copper alloys are subjected to galvanic corrosion when coupled with titanium, requiring proper cathodic protection.

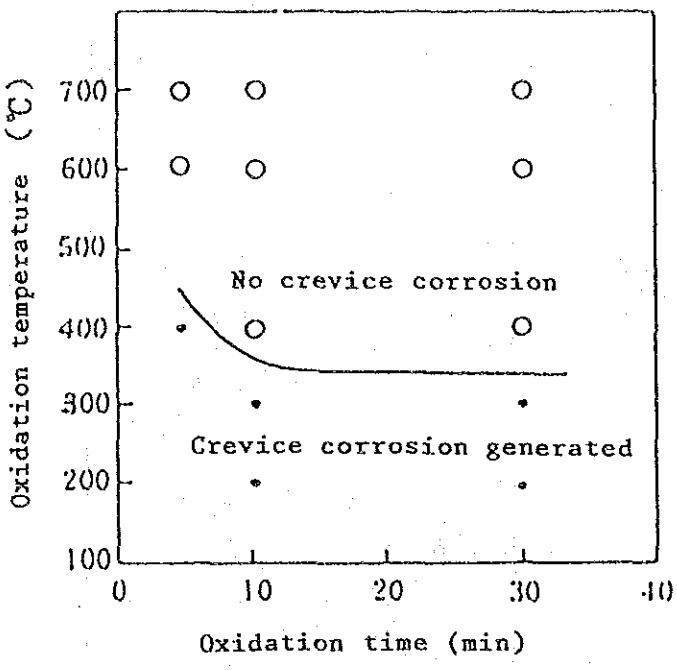

Fig.3.1.31 Effects of atmospheric oxidation on generation of titanium crevice corrosion (boiling 6%NaCl solution) [24]

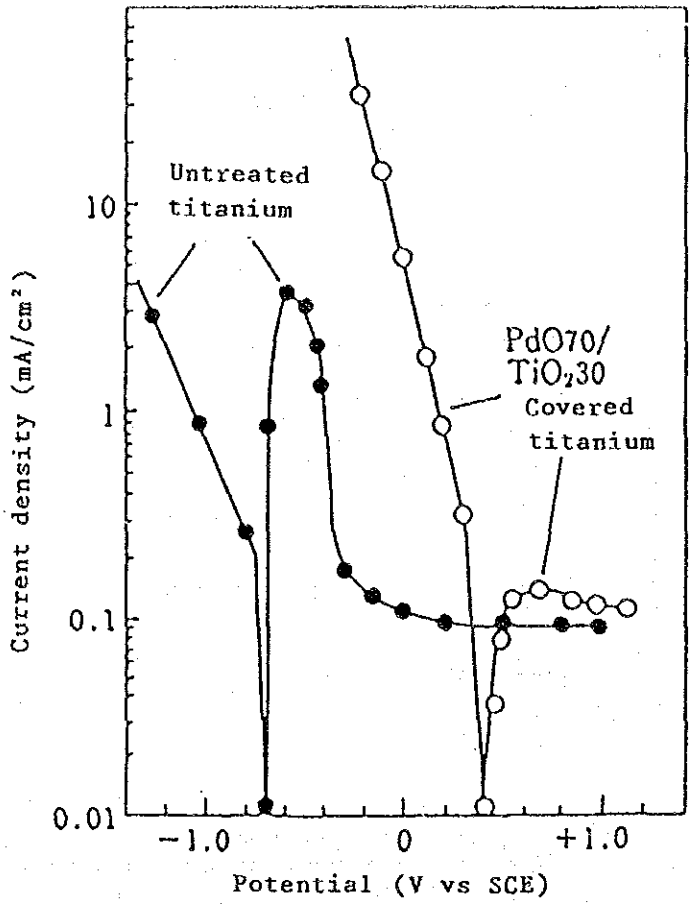

Fig.3.1.32 Polarization curve of PdO70/TiO₂30-Ti and untreated titanium in 70℃, 10% H_2SO_4 solution[24]
(Oxidation condition: 500 ℃ x 30 min)

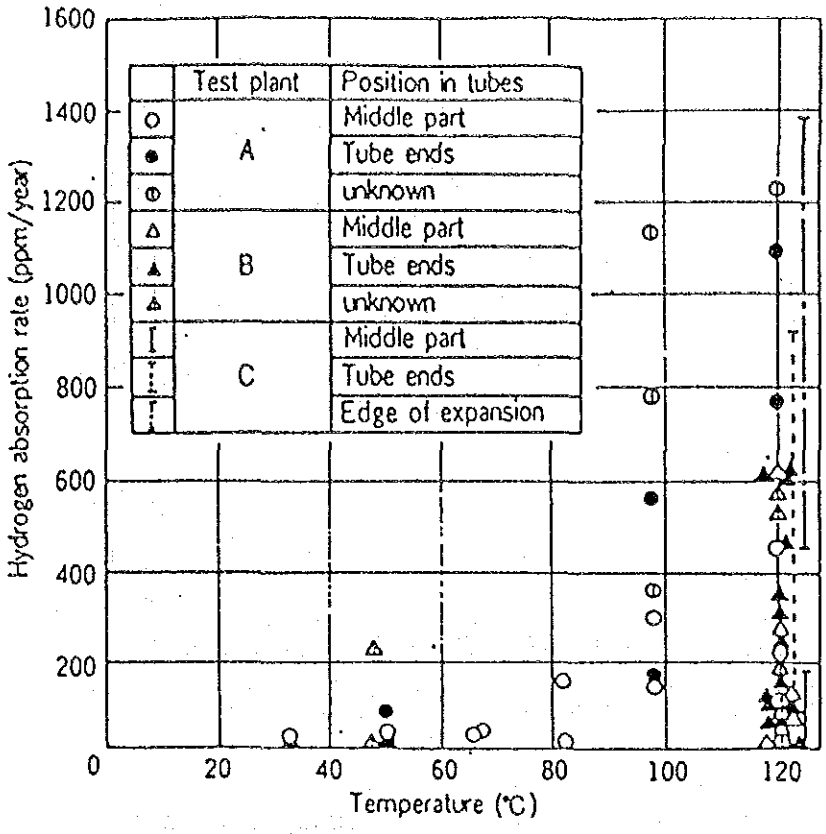

Fig.3.1.33 Relationship between hydrogen absorption rate and temperature in MITI's test plants. [26]

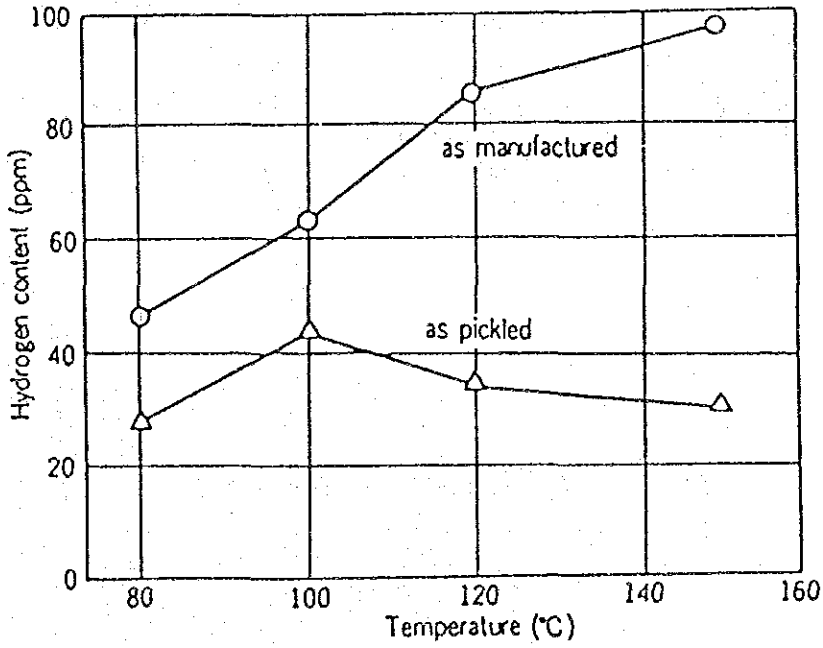

Fig.3.1.34 Effect of temperature on the hydrogen absorption of c.p. titanium tube without coupling (1M $Fe(OH)_3$, 3,000hr). [26]

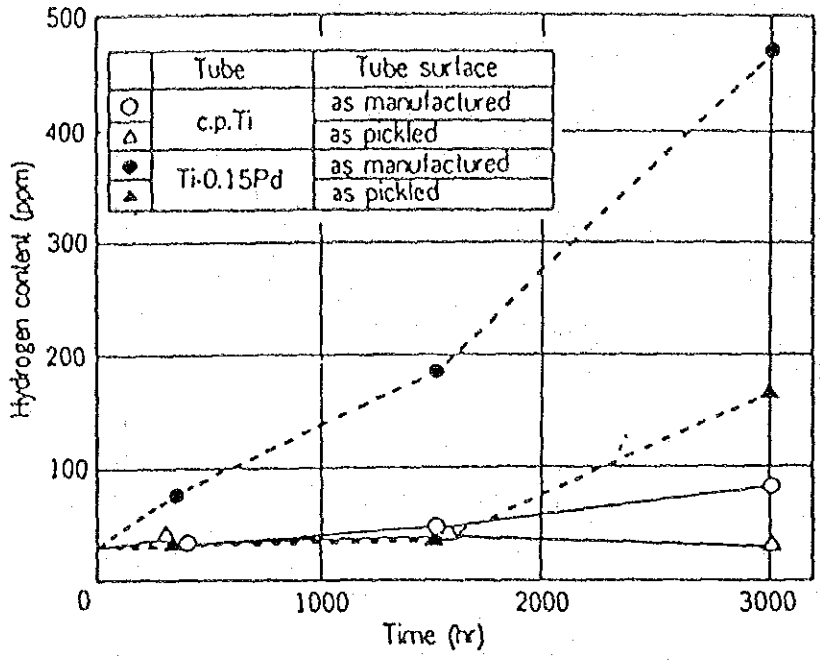

Fig.3.1.35 Hydrogen absorption of Ti-0.15Pd alloy tube (1M $Fe(OH)_3$, 120°C).[26]

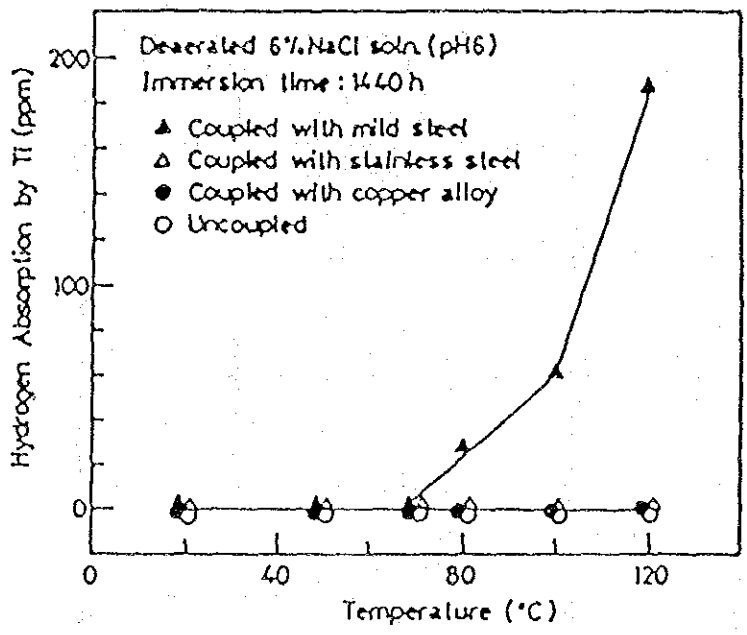

Fig.3.1.36 Effect of temperature on hydrogen absorption by titanium coupled with dissimilar metals.[27]

Table 3.1.39 Hydrogen absorption of titanium under the condition of deaerated flowing sea water at 120℃. [9]

Specimens	Duration (h)	Potentiial (V vs SCE)	Current density ($\mu A/cm^2$)	Content of hydrogen (ppm)	Hydride formation
As received	——	——	——	15~25	None
As immersion	624	−0.2~−0.72	——	21~25	None
−750mV impressed	1,500	−0.75	10~150	43	Yes
−1000mV impressed	720	−1.0	250~650	50	Yes

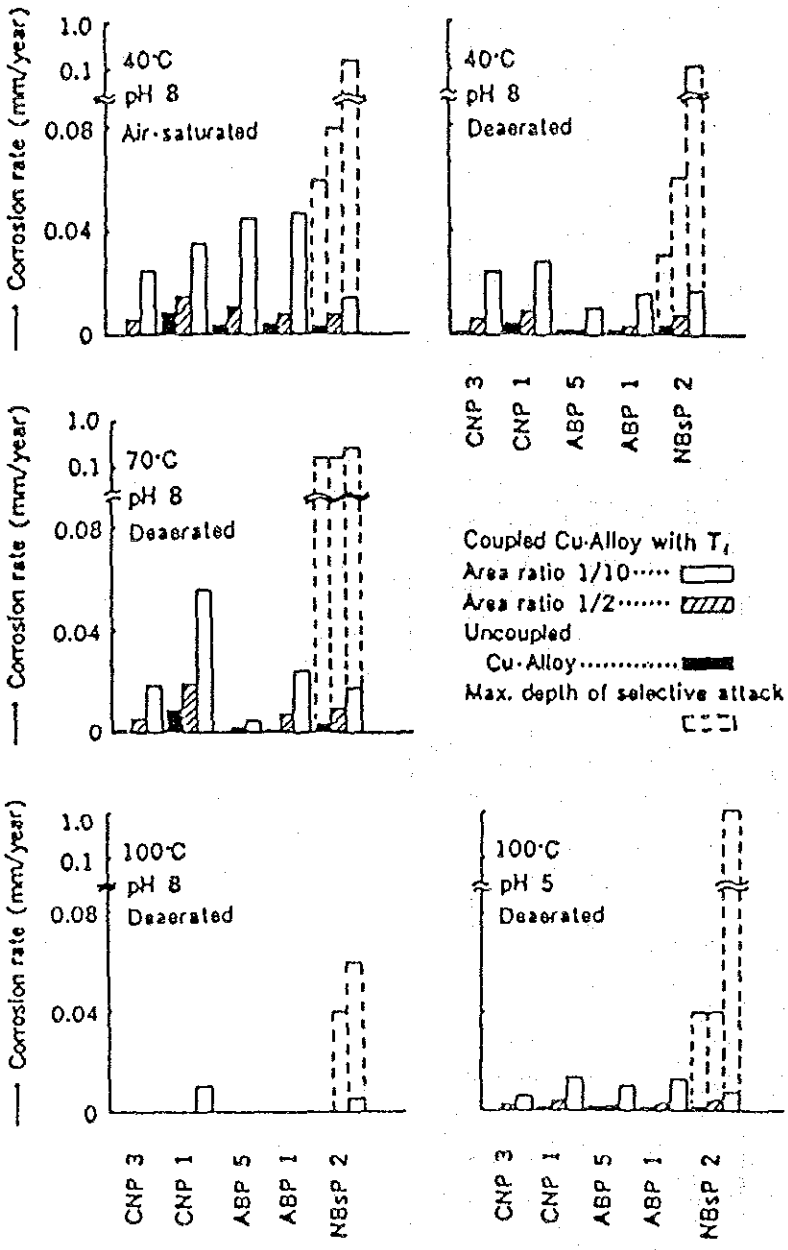

Fig.3.1.37 Effect of Cu alloys/Ti area ratio of titanium-copper alloys couple on corrosion rate of copper alloys after imersion in artificial sea water for one month [28]

Figure 3.1.38 shows corrosion rates of brass when a titanium and brass couple in seawater is cathodic polarized to −0.6V, indicating that polarization to −0.5V or lower achieves nearly complete corrosion protection. Figure 3.1.39 shows the hydrogen absorption rates when titanium in seawater is cathodic polarized to −1.0V, and from this figure, holding titanium more noble than −0.65V can prevent hydrogen absorption. To summarize these experimental results, a proper range of protection potential for titanium coupled with copper alloy is obtained as shown in Figure 3.1.40. Therefore, as sacrificial iron anodes, materials whose anodic polarization potential acts in this potential range, such as Fe−9Ni, are suited for this purpose. Table 3.1.40 shows experimental results which confirm the effects.

c) Development of New Alloy Resistant to Crevice Corrosion

Ti−0.15Pd exhibits excellent resistance to crevice corrosion as described above, but the costs of using noble metal Pd are considerably high, preventing popularization of this metal. Consequently, investigation has been made on materials which provide equivalent corrosion resistance but cost less than this alloy.

TICOREX[29], developed by Nippon Mining Co., Ltd. to satisfy these requirements, possesses a composition of Ti−0.05Ru−0.5Ni and is described as reducing costs from those of Ti−0.15Pd. Figure 3.1.41 shows the equi−corrosion rate curves of various metals plotted against a hydrochloric acid solution with varying concentration and temperature, and each curve shows the critical line of penetration of 0.1 mm/y (outside is greater than 0.1). As is clear from the figure, the uniform corrosion of TICOREX corresponds to that of Ti−0.15Pd. Table 3.1.41 shows the results of a crevice corrosion test in a boiling 15 % NaCl solution , and TICOREX shows considerably better results than Ti−0.15 Pd. Sumitomo Metal Industries, Ltd. investigated inexpensive Ti−based material equivalent to Ti−0.15Pd, reducing the content of costly Pd as much as possible and adding further a small amount of another metal to the condition. Figure 3.1.42 shows the test results indicating the relationship between Pd content in Ti and resistance to hydrochloric acid. These results indicate that even a Pd content of 0.05% contributes to improvement in resistance to hydrochloric acid. Table 3.1.42 shows test results of the crevice corrosion of eight types of Ti−based materials at 4.3 M/L of NaCl and under air saturated conditions. In Ti alloys containing more than 0.02% Pd, all the specimens exhibit complete resistance to corrosion. In this way, Ti−0.05Pd nearly corresponds to Ti − 0.15Pd, but by adding traces of Co to Ti−0.05Pd, further improvement in resistance to acid and crevice corrosion was attempted. Figure 3.1.43 shows the results of a crevice corrosion test carried out on five types of Ti−based materials including Ti−0.05Pd−0.3Co and Ti−0.05Pd in the same NaCl solution. In this figure,three kinds of Ti−Pd type show the complete resistance to crevice corrosion. Table 3.1.43 shows some

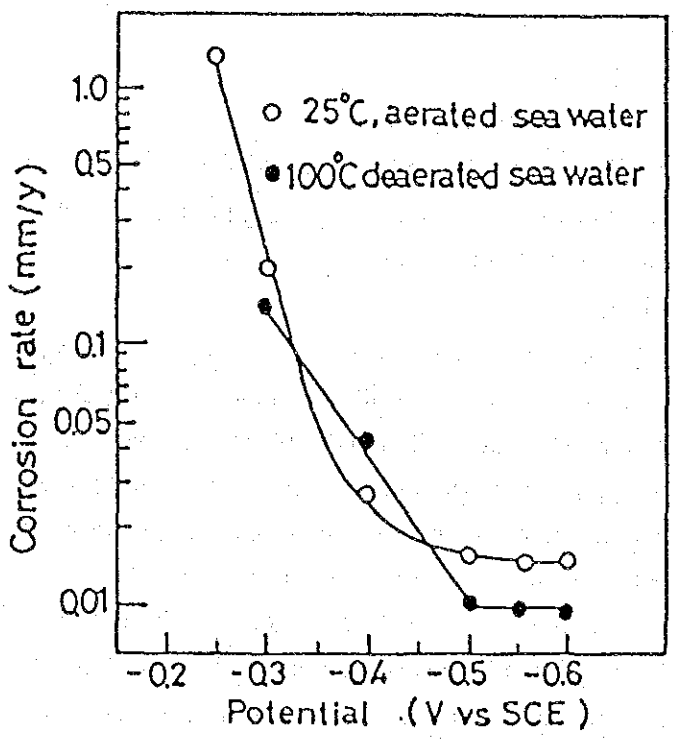

Fig.3.1.38 : Relationship between galvanic corrosion rate of naval brass coupled with titanium (area ratio 1/10) and the applied potential in sea water.[27]

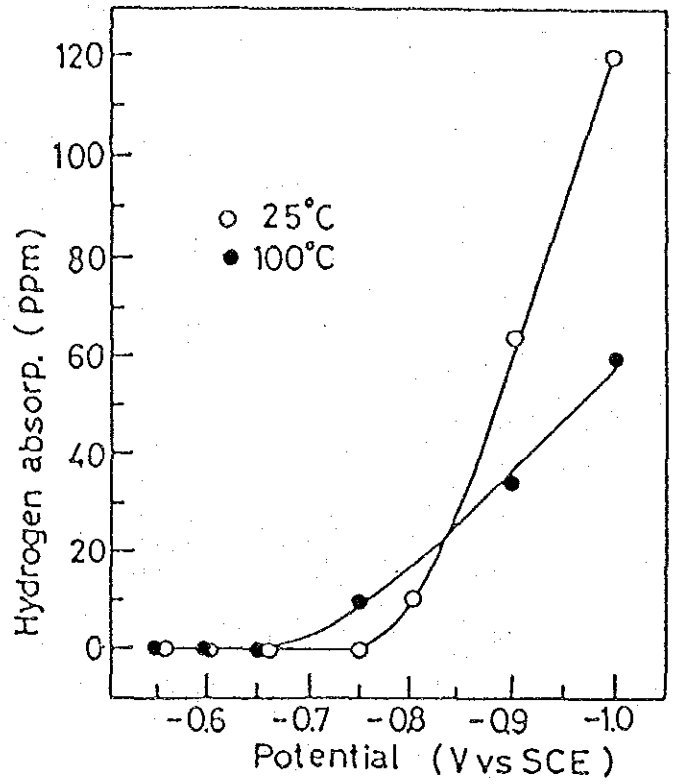

Fig.3.1.39 : Relationship between hydrogen absorption of titanium (thickness: 0.5mm) and the applied potential in sea water (test time is: 3 months at 25°C and 2 months at 100°C)[27]

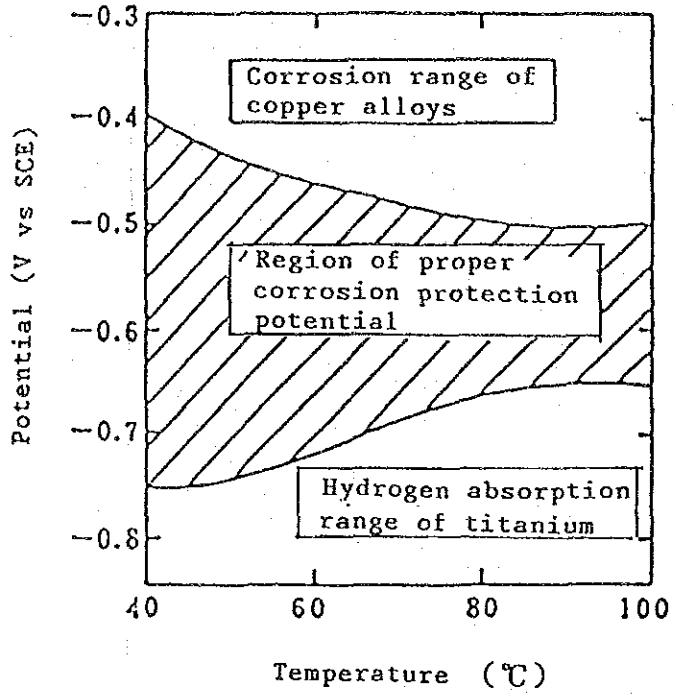

Fig.3.1.40 Region of proper corrosion protection potential of copper alloy/titanium couples[24] Deaerated 6%NaCl, pH 6, 30-day test

Table 3.1.40 Corrosion rate of copper alloy and hydrogen absorption of commercially pure titanium in copper alloy/commercially pure titanium couples with or without sacrificial anode (Deaerated 6% NaCl solution (pH8), 100°C, 40 days' test) [23]

Specimens	Corrosion Rate of Cu Alloy mm/y		Hydrogen Abs. of Ti ppm
	Al Bronze	Naval Brass	
Cu Alloy/Ti	0.03	0.05	0
Fe-9Ni/Cu Alloy/Ti	<0.005	<0.005	0
Fe/Cu Alloy/Ti	<0.005	<0.005	19

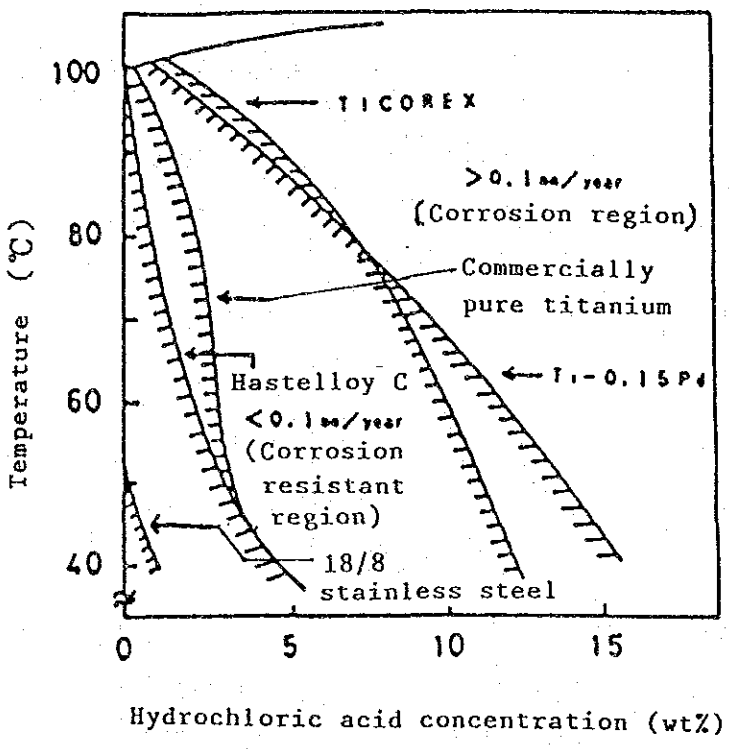

Fig.3.1.41 General corrosion test results of various titanium materials in hydrochloric acid solution [29]

Table 3.1.41 Crevice corrosion test results[29]

15% NaCl, boiling solution, pH: 6.1

Alloy name \ Time (h)	3	6	10	24	60	Remarks
TICOREX (Ti-0.5Ni-0.05Ru)	○	○	○	△	×	TICOREX
Titanium-palladium alloy (Ti-0.15Pd)	○	○	○	×	×	equivalent to ASTM G7
G12 alloy (Ti-0.8Ni-0.3Mo)	○	○	△	×	×	equivalent to ASTM G12
Commercially pure titanium JIS 2 type	○	×	×	×	×	JIS 2 type equivalent to ASTM G12

○: No generation of crevice corrosion recognized
△: Crevice corrosion occurred in less than 50% of the specimens.
×: Crevice corrosion occurred in 50% and more of the specimens.

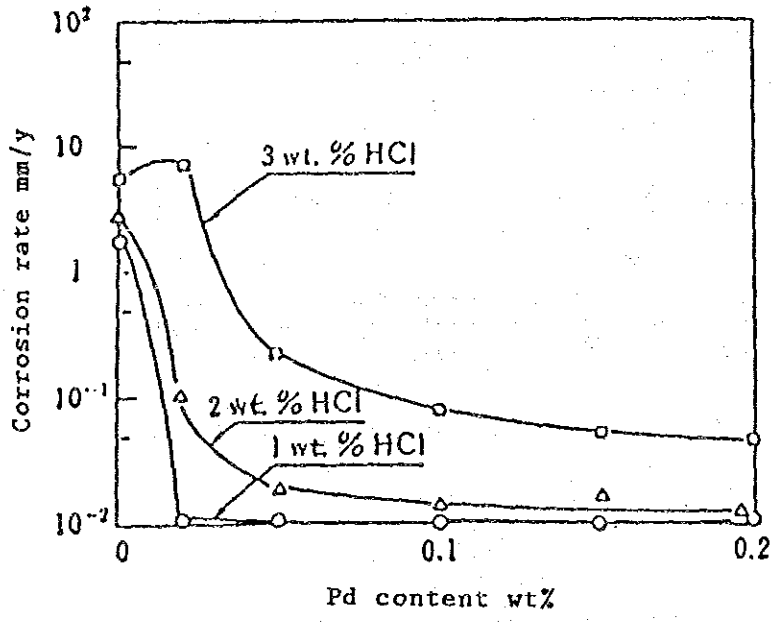

Fig.3.1.42 Effects of Pd additions on corrosion resistance in hydrochloric acid resistance (boiling for 20 h)[30]

Table 3.1.42 Crevice corrosion resistance under various environments [30] (NaCl 4.3 M/L, air saturated)

Test conditions	150℃				200℃			
	pH=2		pH=6		pH=2		pH=6	
Test time	500 h	1 000 h	500 h	1 000 h	500 h	1 000 h	500 h	1 000 h
CP-Ti	4/4	4/4	4/4	4/4	4/4	—	4/4	—
Ti-0.02 Pd	1/4	2/4	2/4	3/4	1/4	4/8	2/4	3/8
Ti-0.05 Pd	0/4	0/4	0/4	0/4	0/4	0/8	0/4	0/8
Ti-0.10 Pd	0/4	0/4	0/4	0/4	0/4	0/8	0/4	0/8
Ti-0.14 Pd	0/4	0/4	0/4	0/4	0/4	0/8	0/4	0/8
Ti-1 Ni	4/4	—	2/4	—	4/4	—	2/4	—
Ti-1 Mo	4/4	—	4/4	—	4/4	—	4/4	—
ASTM Gr. 12	4/4	—	4/4	—	4/4	—	4/4	—

Note) No. of surfaces with crevice corrosion/No. of test surfaces

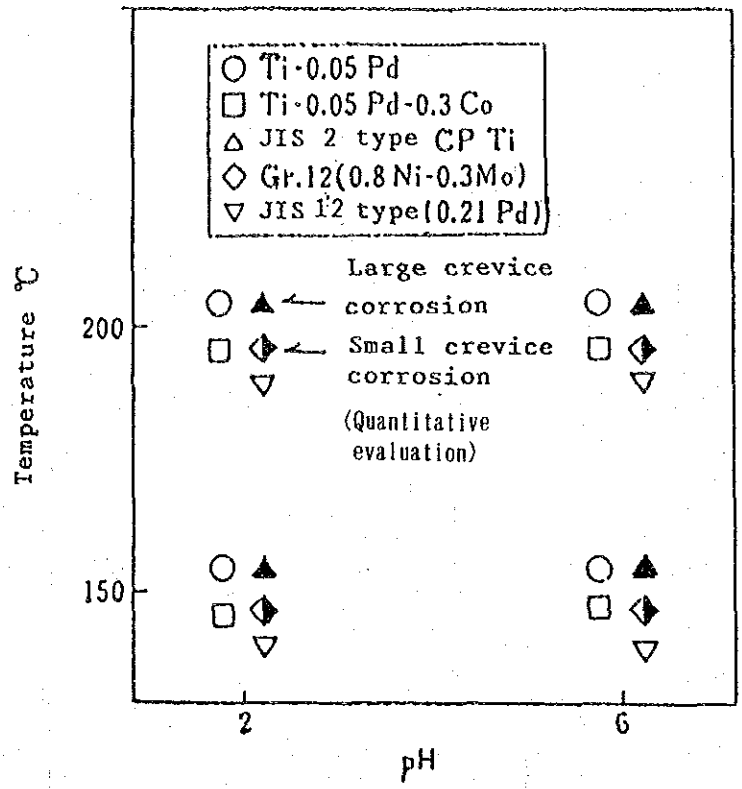

Fig.3.1.43 Crevice corrosion resistance of Ti0.05Pd and Ti0.05Pd 0.3Co (in NaCl 4.3 M/L, air-saturated) [30]

Table 3.1.43

Acid resistance of titanium alloys resistant to crevice-corrosion, mm/y [30] (boiling for 20 h)

Materials	Hydrochloric acid concentration, wt%		
	1	3	5
Ti-0.05 Pd	0.05	0.24	0.65
Ti-0.05 Pd-0.3 Co	0.04	0.16	0.41
JIS 2 type	1.61	11.0	28.2
JIS 12 type(0.2 Pd)	0.07	0.13	0.18
ASTM Gr. 12	0.05	10.5	37.0

comparisons of the resistance to hydrochloric acid and three kinds of Ti–Pd type are similarly superior (to others).After all, Sumitomo Metal Industries, ltd. prepares two kinds of materials, Ti–0.05Pd and Ti–0.05Pd–0.3Co as an alternative of Ti–0.15Pd.

(3) Aluminum Alloys

a) General Evaluation Related to Pitting of Aluminum Alloys

Table 3.1.44 shows the percentage of various heat transfer tube materials which accounted for the 86 desalting plants with evaporation processes in 1968, 1971, and 1980. Aluminum heat transfer tubes made their first appearance in 1980 , but accounted for only 0.5% of the total number of heat transfer tubes in service. Thus, the actual application of aluminum heat transfer tubes is extremely rare in desalting plants. This might be attributed to the poor reliability of aluminum as heat transfer tubes because of its pitting characteristics in saline water. For example, among aluminum alloys, resistance to seawater of the 3000 to 5000 series is believed to be relatively good, but determining the maximum pit depth of both alloy series in seawater from five data and plotting the results on log–log graph paper results in marked variations as shown in Figure 3.1.44. That is, the pitting characteristics of both alloy series exhibit a great difference by slight variation in measuring conditions. Evaluation of the pitting characteristics of both alloys by various researchers is diverse, and the results from ten data are summarized in Table 3.1.45, in which some researchers recommend the 5000 series, others the 3000 series, and still another both the 5000 and 3000 series. In the end, the reliability of each data is seriously impaired.

b) Pitting Data of Aluminum Alloys

Figure 3.1.45 is published as a pitting map of aluminum alloys. These results were achieved at a temperature of 240°F and a flow rate in tubes of 5 ft/s. At an oxygen concentration below 50 ppb, outstanding resistance to pitting is achieved at pH 5–7, but satisfactory results are achieved even at oxygen concentrations over 50 ppb, and less sensitivity of pitting resistance to oxygen concentration in this way might be an asset of aluminum alloy. Figure 3.1.46 plots the relationship between corrosion rates and the potential of 6063 alloy in the seawater temperature range of 25–130°C. It also indicates the domain of pitting occurrence with the boundary formed by a dotted line. That is, bringing the potential to be less noble than this dotted line can prevent pitting. In the corrosion of heat transfer tubes, pitting is the most fatal, and the description in this section places greater stress on data related to pitting. Examples of compiled data include reports on a desalting project of MITI and on aluminum heat transfer tubes of the Japan Light Metal Association, in which the portions related to pitting are introduced. As data pertaining to

Table 3.1.44

A comparison of the Percentage distribution of tube alloys as obtained from the surveys conducted in AIS in 1968,1971,1980.[31]

Alloys	*Total in 1968*	*Total in 1971*	*Total in 1980*
Aluminium Brass	74	53	56
90/10 Cu-Ni	9	33	35
70/30 Cu-Ni	15	1.8	.5
70/30 Cu-Ni		11.4	4
Titanium	2.	.8	4.
Aluminium	0	0	.5

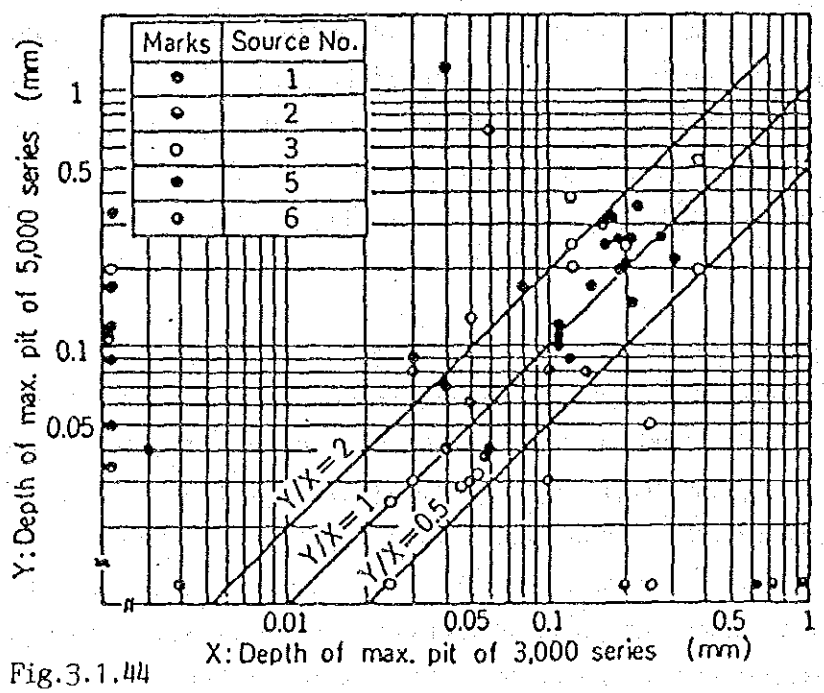

Fig.3.1.44

Comparison of max. pit depth of 3,000 series with that of 5,000 series in desalting environments, based on the data obtained from 5 sources.[9]

Table 3.1.45 Evaluation of aluminum alloys by pitting corrosion. [32]

Ref. No.	Test alloys	Most suitable	Unsuitable
2)	3005, 5052, 6061, Alclad 3003, Al clad 3004	5052 (2.5 Mg)	6061
3)	1200, 3004, 5050, 6063	3004 (1.2 Mn–1.0 Mg) 5050 (1.4 Mg)	—
12)	Mg (0.35–5.8) Mn (0.4–1.6) 6 alloys	AMCM (0.35 Mg–1.2 Mn)	—
13)	1100, 3003, Al–Mg (1.8–3.8)–Mn (0.2–0.8)	Artr3 (3.5 Mg–0.55 Mn–0.65 Si)	—
14)	1100, 3003, 5005, 5052, 5454, 6061 (T6), 6063 (T5) 6061 clad	3003 (1.25 Mn) 5454 (2.7 Mg–0.75 Mn)	1100, 6061
15)	1100, 3003, 5052, 5454, 6061	5052 (2.5 Mg), 3003 (1.2 Mn)	1100, 5454
18)	1100, 3003, 3004, 4042, 5050, 5052, 5154, 5454, 6061, 6351 (0.7 Mg–0.5 Mn–1.0 Si), ×8001	5454 (2.7 Mg–0.75 Mn)	6061
19)	1100, 1235, 3003, 3004, 5005, 5050, 5052, 6061 (T6)	Mg <0.9 or (Mg+Mn) alloy	5050, 5052, 6061
20)	1100, 3003, 3004, 5050, 5052, 6063	—	5050, 6063
21)	2024, 3003, 5454, 6061	5454 (2.7 Mg–0.75 Mn)	—
This work	loop test, 26 alloys	3105 (0.6 Mn–0.5 Mg), 5052, 6162, 5050, 1100	6063
	field test, 1100, 3003, 5050, 5052, 6063, clad (3003/7072)	3003, 5052	1100, 5050
JLMA	plant test, 3004, 5050, 5052, 6063, clad (3003/7072)	3004	5050

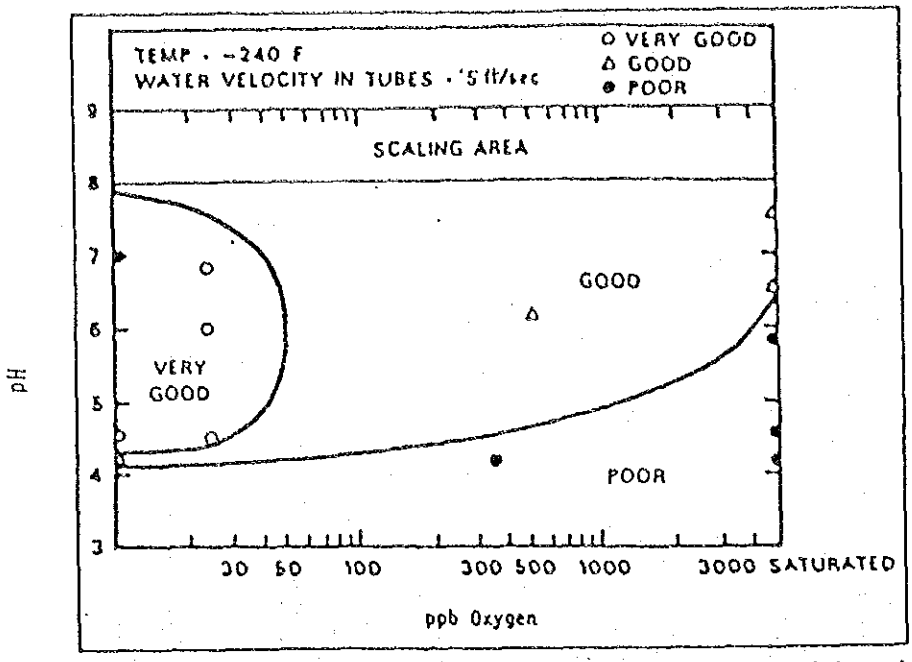

Fig.3.1.45 Effect of pH and oxygen content of sea water on pitting of aluminium alloy tubes from Freeport plant environmental side unit. [25] [31]

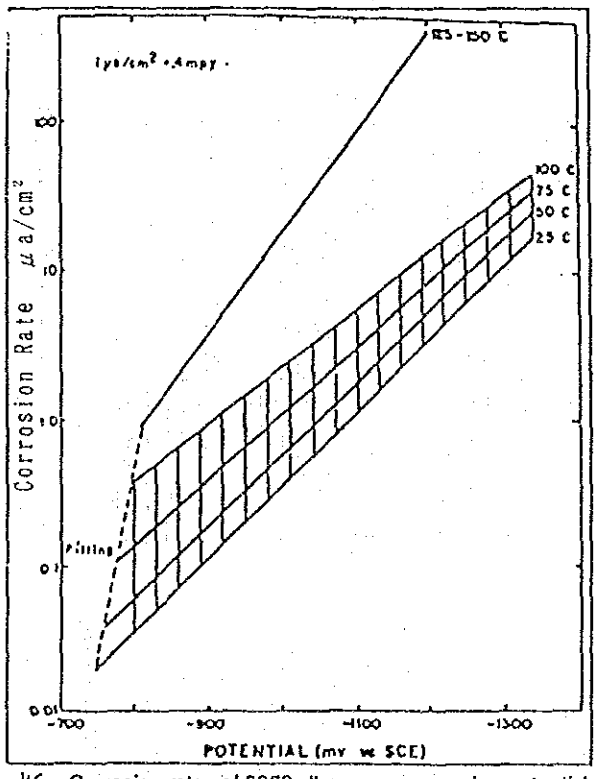

Fig.3.1.46 Corrosion rates of 6063 alloy versus corrosion potential at pH 7 to 8. [25] [31]

the desalting project, Table 3.1.46 shows the maximum pit depth and general corrosion rates of aluminum specimens in the loop test. This test did not show any significant difference based on the kinds of alloys. Summarizing this data and plotting the effects of temperature, dissolved oxygen, and flow rate on corrosion resistance to seawater of aluminum alloys produces Figure 3.1.47, indicating that when the temperature is low (70°C), the oxygen amount is large, and when the flow rate is fast, the pit depth increases. Table 3.1.47 shows the date of tubing for field tests using a test plant. The surface roughness on the inner surface of the tube at the C_3 stage (75–65°C) of the heat recovery section is large and penetration has occurred, exhibiting the same tendency as that of the loop test results. Table 3.1.48 shows the maximum pit depth and mean corrosion rates of aluminum alloy tubes at a MSF plant made of aluminum by the of Japan Light Metal Association, in which the pit depth of the 5000 series is excessive. Figure 3.1.48 summarizes various types of alloys and plots the change of pit depth with time according to stage. Large variation at the brine heater and large pit depth at the low temperature stage C_4 of the heat recovery are conspicuous. In these experiments, the phenomenon of pitting inactivation with time was not recognized. Bonewitz et al.[33] reported the results of the continuous operation over 3 years of a desalting test plant made of aluminum by the Aluminum association at Freeport. The portion related to pitting is shown as follows. Table 3.1.49 shows the pitting data for heat rejection (43°C) . Comparing raw sea water with treated sea water (organisms and solid substances are removed pH: 6.8; oxygen: 26 ppb), the latter generates excessive pitting. The report explains that as the raw seawater has a slightly higher pH, the capacity of heavy metal ions to be collected by aluminum decreases as compared to treated seawater. However, even in treated seawater, pit depth does not increase after 26 months and it is assumed that pitting has been inactivated. Table 3.1.50 shows the pitting data in the first pass for heat rejection, and in this case pitting tends to self–stop after 30 months. Because the tubes used in this case come in first contact with the inflow of treated seawater, it is possible for them to collect heavy metal ions, and in fact, deposits near pitting include more copper and iron than substrate. Table 3.1.51 shows pitting data at the 2nd, 3rd, and 4th passes. Pit depth gradually decreases because the data were recorded after heavy metal ions were collected. As a result, there is no significant difference in the pitting resistance of these aluminum heat transfer tubes at this plant. The maximum pit depth, 21 mil, at the 1st pass of heat recovery, and the mean pit depth, 10 mil, also at the 1st pass, are respectively the maximum values for each kind of pit depth, and the pitting is considered inactivated after about 3 years. Bonewitz et al. recognizes the suitability of aluminum alloys for desalting plants on the basis of these performance results, but these good results seem to be more related to seawater characteristics and its treatment process at Freeport.

c) Development of New Pitting–Resistant Aluminum Alloys

Table 3.1.46 Corrosion rate and maximum penetration depth of aluminum alloys in loop test (1,000 hr). [32]

Alloy series	Corrosion rate × 10^{-3} g/m²h		Depth of max. penetration mm	
	Mean	Range	Mean	Range
1,000	17.8 (0.055 mm/yr)	17.3–18.0	0.083	0.07–0.10
3,000	23.1 (0.072 〃)	15.9–35.8	0.091	0.04–0.18
5,000	20.2 (0.062 〃)	15.8–29.0	0.082	0.05–0.11
6,000	21.9 (0.068 〃)	15.2–35.6	0.091	0.05–0.18

Table 3.1.47 Roughness of aluminum alloys in field test (2,000 hr). [32]

Stage / Brine temp.(°C) / Alloys	Heater H (high temp.) 118–95	Heater H (low temp.)	Heat recovery C1 95–85	C2 85–75	C3 75–65	C4 65–55	H. reject, C5 —	Original tube
1100	120		130	740	760	80	40	20
Roughness of inner surface 3003	40		30	50	40	40	0	0
5050	50		120	220	perfo-ration	70	0	0
μ 5052	0		90	60	perfo-ration	70	0	0
6063	80		70	40	160	110	0	0

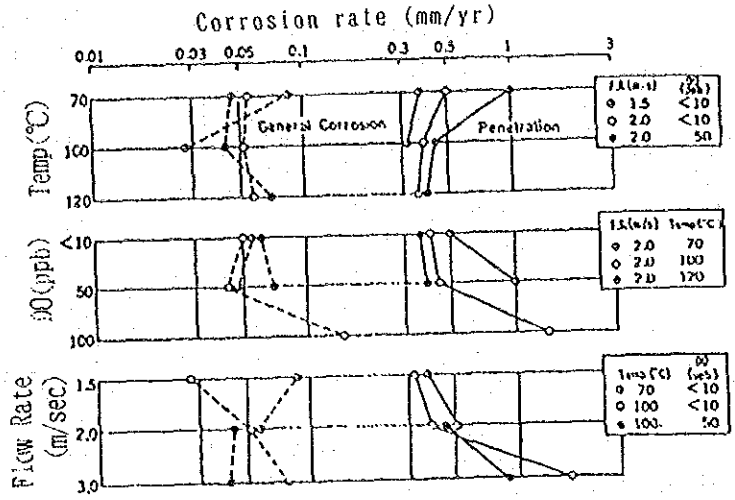

Fig.3.1.47 Effect of corrosion condition on the corrosion rate and penetration of aluminum alloys in loop test (1,000 hr). [32]

Table 3.1.48 Corrosion rate, maximum penetration depth aluminum alloys in Japan Light Metal Association test plant (5,008 hr). [32]

	Alloys	Brine heater		Heat recovery stage				H. rejection stage		Mean
		H1	H2	C1	C2	C3	C4	C5	C6	
Corrosion rate mm/yr	3004	0.031	0.065	0.013	0.012	0.022	0.018	0.020	0.020	0.025
	5050	0.023	0.054	0.015	0.010	0.014	0.012	0.017	0.025	0.022
	5052	0.041	0.087	0.019	0.011	0.020	0.017	0.021	0.049	0.033
	6063	0.046	0.071	0.028	0.028	0.035	0.024	0.023	0.037	0.037
	Clad	—	—	—	—	—	—	0.021	0.028	0.025
	Mean	0.042	0.069	0.019	0.015	0.023	0.018	0.021	0.031	—
Depth of max. penetration mm	3004	0.18	0.18	0.31	0.15	0.20	0.22	0.27	0.08	0.18
	5050	>1.2[1]	0.93	0.32	0.21	0.27	0.30	0.25	0.18	0.35[1]
	5052	0.20	0.28	0.22	0.17	0.21	0.36	0.27	0.17	0.24
	6063	0.34	0.21	0.23	0.21	0.26	0.33	0.23	0.16	0.25
	Clad	—	—	—	—	—	—	0.32	0.18	0.25
	Mean	0.24[1]	0.40	0.27	0.19	0.25	0.30	0.27	0.15	—

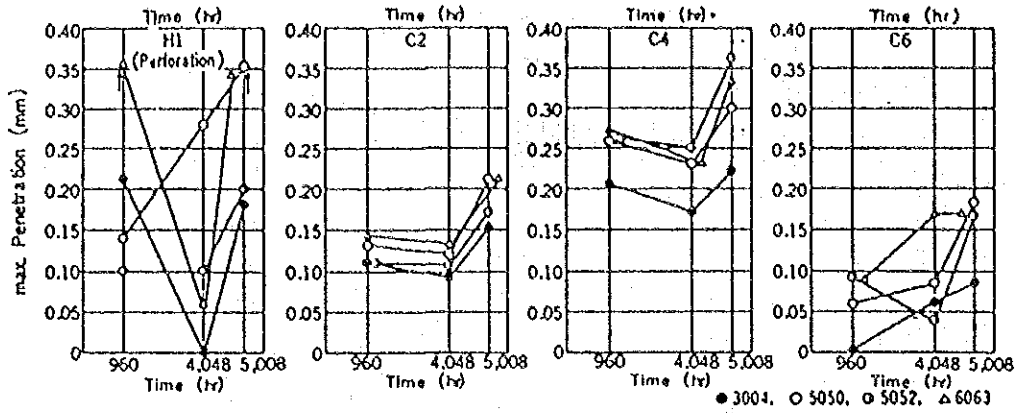

Fig.3.1.48 Variation of the maximum penetration of aluminum alloys in Japan Light Metal Association aluminum test plant. [32]

Table 3.1.49 Evaluation of Tubes from the Heat Reject Exchanger E-21 [33]

Alloy	Time (Months)	Max. Pit Depth (mils)	Avg. Pit Depth (mils)	Pits/Sq Inch[2]
		Treated Sea Water		
Alclad 3003	13	0[1]	0	0
	26	0	0	0
3003	13	< 0.5	--	1
	26	5	1	< 1
5052	13	15	7	1
	26	15	5	< 1
6063	13	7	5	< 1
	26	10	5	3
		Raw Sea Water		
3003	6	0	0	0
5052	6	8	2	1
6063	6	1	0	0
5050	6	0	0	0

[1] Depth of penetration into core, cladding entirely removed.
[2] 1 in^2 = 6.45 cm^2.

Table 3.1.50 Evaluation of Tubes from Heat Recovery Exchanger E-22 1st Pass 125 F [33]

Alloy	Time (Months)	Max. Pit Depth (mils)	Avg. Pit Depth (mils)	Pits/Sq Inch[2]
Alclad 3003	6	0[1]	0	0
	13	0	0	0
3003	6	5	3	.05
	13	15	10	2
	24	5	3	<1
	32	10	2	1
	38	15	5	1
5052	6	8	2	.01
	13	21	–	1 Pit
	24	10	3	<1
	32	0	0	0
	38	8	5	<.01
6063	6	8	2	.5
	13	10	5	1
	24	5	3	<1
	32	8	2	1
	38	6	3	<1
1200	6	0	0	0
	13	0	0	0

[1] Depth of penetration into core, cladding entirely removed.
[2] 1 in^2 = 6.45 cm^2.

Table 3.1.51 Evaluation of Tubes from Heat Recovery Exchanger E-22 [33]

Alloy	Time (Months)	Max. Pit Depth (mils)	Avg. Pit Depth (mils)	Pits/Sq Inch[1]
		Second Pass 165 F		
3003	13	0	0	0
	38	10	2	1
5052	13	0	0	0
	38	2	1	<1
6063	13	0	0	0
	38	1	<1	0.1
		Third Pass 188 F		
3003	13	1	<0.1	<1
	38	0	0	0
5052	13	0	0	0
	38	0	0	0
6063	13	<0.5	<0.1	<1
	38	0	0	0
		Fourth Pass 210 F		
3003	13	0	0	0
	38	0	0	0
5052	13	0	0	0
	38	0	0	0
6063	13	0	0	0
	38	0	0	0
5050	6	0	0	0
	20	3	2	0.1

Encouraged by good performance at test plants made of aluminum, as described above, some researchers are carrying forward development of new aluminum alloys for heat transfer tubes. One case involves the improvement study on Al–Mg series. The initial program development began at GKSS in Germany and studies on the resistance to seawater of this alloy series are currently being continued at the University of Petroleum and Minerals in Saudi Arabia. The chemical compositions and the alloy numbers of part of this alloy series are shown in Table 3.1.52. Figure 3.1.49 shows the changes in corrosion rates for this alloy series over time against the seawater of the Arabian Gulf, exhibiting similar behavior to that of conventional seawater-resistant aluminum alloys. Table 3.1.53 shows the results using flowing seawater (Max. 3.2 m/s). This indicates that 2778–H provides the best resistance. Figure 3.1.50 shows those conditions in which the corrosion rates in deaerated flowing seawater are free from the effects of flow rates. Figure 3.1.51 shows pitting data, and the depths of all alloys do not increase after 8500 hours, indicating possible inactivation of pitting. The alloy with the shallowest pit depth is 2778–H. Faninger et al.[34] as well intend to develop aluminum alloys for desalting plants, and have found that when Al–6–8 Fe alloys with traces of Cr and Mn are rapidly cooled by the splat cooling process, the pitting potential in the seawater greatly increases as the mechanical strength increases (pitting becomes difficult to occur), advocating a promising future for this type of material. This paper only introduces two types of alloys, but it is interesting to note that Germany is involved with the same two alloys.

(4) Stainless Steel

a) Practical Application of Super Stainless Steel

Super stainless steel falls into two broad categories: austenitic and ferritic. Development begins from 316L for the former and from 420 steel for the latter. Both provide extraordinarily outstanding resistance to pitting and crevice corrosion, as shown in Tables 3.1.54 and 3.1.55 (from the top to the third are super stainless steels in both cases), under environments containing a large quantity of chloride such as seawater compared with conventional stainless steels. The advent of these super stainless steels is a result of a wide range of research and development including the revolutionary advancement in the steel making process which enabled the control of traces of impurities in molten steel such as S and N, electrochemical studies of passivation, and improvement of pitting characteristics and crevice corrosion properties. Figure 3.1.52 shows the relationship between PI (pitting index: equivalent to %Cr+3x%Mo+16x%N), which is used in improvement of pitting characteristics by change in stainless steel composition, and critical temperature for pitting generation in the 10%$FeCl_3$ solution. The pitting generating temperature increases linearly as PI increases. That is, added elements play important roles in the improvement of pitting resistance in the order of Cr<Mo<N. Determining the pitting potential with

Table 3.1.52 Nominal Composition of the Modified Experimental Alloys (weight percent). [31]

Alloys	Si	Fe	Cu	Mn	Mg	Cr	Zn	Ti	Pb	Al
2775	0.68	0.18	0.01	<0.01	<0.01	<0.01	<0.01	<0.02	–	Balance
2776	0.77	0.19	0.01	<0.01	2.56	<0.01	0.01	<0.02	0.02	"
2777	0.67	0.17	0.01	0.01	0.03	0.26	0.01	<0.02	–	"
2778	0.71	0.19	0.01	0.02	0.60	0.29	0.02	<0.02	–	"

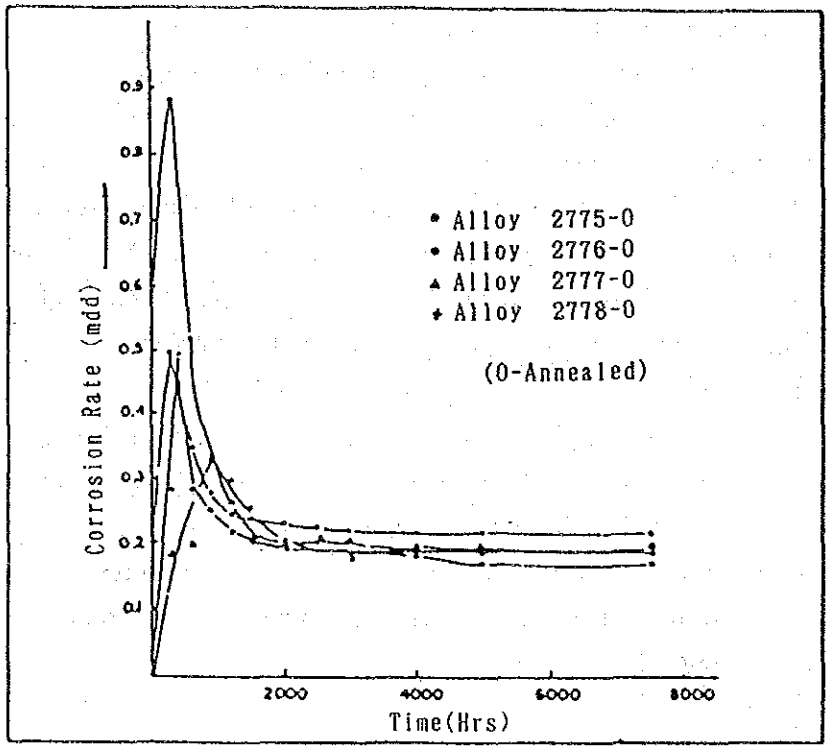

Fig.3.1.49 Variation of corrosion rate of aluminium alloys-O with time in Arabian Gulf water [31]

Table 3.1.53 Corrosion Rates of Modified Aluminium Alloys Under Dynamic Conditions [31]

Alloy	Corrosion Rate in Mdd*
2775–O	5.3
2775–H	10.8
2776–O	12.5
2776–H	20.5
2777–O	3.0
2777–H	2.4
2778–O	2.0
2778–H	1.9

At a variety of 1.9 m/s.

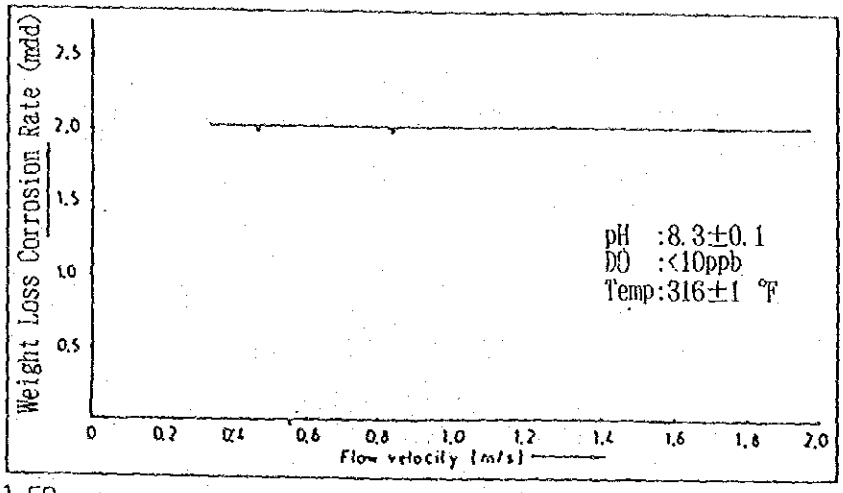

Fig.3.1.50 Variation of corrosion rate of cold rolled aluminium alloy 2778 with velocity of treated deaerated North Sea water [31]

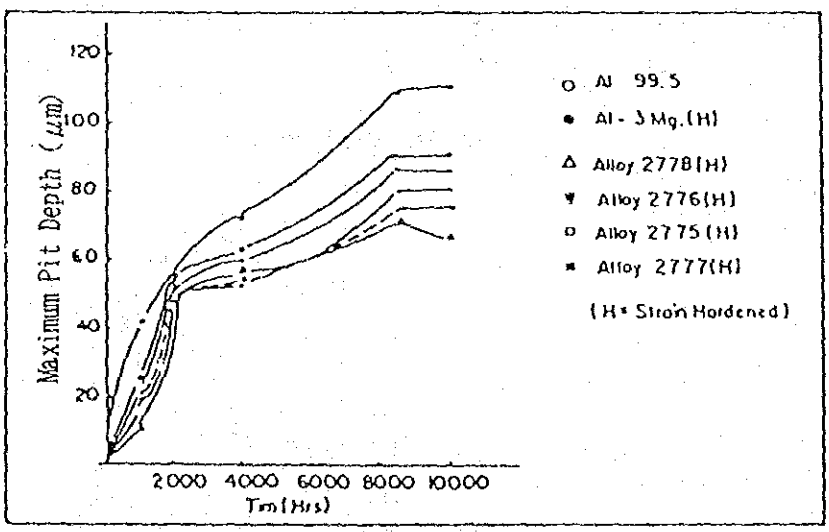

Fig.3.1.51 Variation of pitting depth of modified aluminium alloys-H with time [31]

Table 3.1.54 Potentiostatic Measurements.[35]

Alloy	Minimum Breakthrough Potential, volts vs. Standard Calomel Electrode
AL-6X	1.0+ (beyond range tested)
29-4	1.0+ (beyond range tested)
29-4-2	1.0+ (beyond range tested)
Hastelloy C	1.0+ (beyond range tested)
Titanium	1.0+ (beyond range tested)
26-1S	0.98
Type 216	0.95
20Cb3	0.55
18-2	0.40
Type 316	0.33
Type 439	0.30
Type 304	0.22
Type 430	0.05

Table 3.1.55 10% Ferric Chloride Rubber Band Test (ASTM G 48), 72 Hours, Room Temperature[35]

Alloy	Percent Weight Loss
AL-6X	0
29-4	0
29-4C	0
Hastelloy C	0
Titanium	0
E-Brite 26-1	0-0.1
Type 216	0.2-0.45
Type 317	0.8-1.1
Type 316	2.5-5.1
Type 304	2.5-5.1

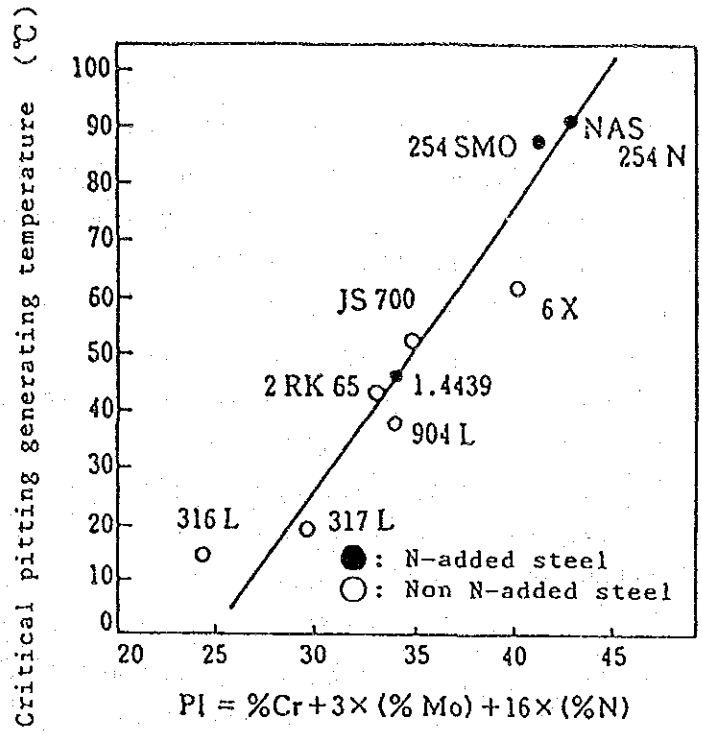

Fig.3.1.52

Effects of PI on critical pitting generating temperature in 10% $FeCl_3$ solution (Effects of Cr, Mo, N) [36]

PI=Cr+3Mo+10N of many kinds of stainless steel in deaerated artificial seawater at 80°C, the curve shown in Fig. 3.1.53 is produced. Different coefficient of N is used depending on the researchers,however,coefficient 16 is most commonly used.

b) Super Austenitic Stainless Steel

This stainless steel has an austenitic structure and contains Cr≥20%, Mo≥5%, and C≤0.03%, and generally N≥0.15%. Because many of them contain 6% Mo, they are sometimes called 6Mo stainless steels. For some of these steel grades, the steel grade symbols and chemical composition are shown in Tables 3.1.56 and 3.1.57. The latter table contains Japanese steel grades. Table 3.1.58 shows ASTM standards and ASME codes. The corrosion characteristics of these steels are described using charts. Table 3.1.59 shows the results of comparing critical pitting temperature (CPT) and other factors with those of ordinary stainless steels, exhibiting the superlative resistance to pitting of super stainless steels. Next, discussion is presented on the characteristics of austenitic super stainless steels with special emphasis on 254 SMO, the best-known steel grade. Figure 3.1.54 compares the pitting potential E C and repassivation potential EP of this steel in NaCl solution with that of 254 SLX (24Ni–20Cr–5Mo–1.5Cu). 254 SMO is located on the higher potential side, clearly exhibiting its superiority in resistance to pitting. Figure 3.1.55 compares temperature dependency of the pitting potential of NAS 254N (made by Nippon Yakin Kogyo) in 10% $FeCl_3$ solution with that of ordinary stainless steels; it also indicates the superiority of the pitting resistance of the 254 series. Table 3.1.60 shows the results of seawater immersion tests of welded specimens (crevice at welds) conducted in the LaQue Center, Wrightsville Beach. The 254 specimen was slightly corroded but the corrosion was extremely minor compared to other materials. Table 3.1.61 shows the results of a test conducted at a desalting plant in the Middle East. The 316 specimens for the liquid phase were washed away and only test results for the gas phase are shown, however, trouble was found in 254 and 904L specimens in the gas phase. Table 3.1.62 shows the crevice corrosion test results using seawater from the Atlantic Ocean, in which only one 254 SMO specimen was corroded (0.01 mm, depth), exhibiting superiority over 254 SLX. Table 3.1.63 shows the investigation results of pH which destroys passivation for 254 SMO and SLX. The 254 SMO stands to the lowest pH, indicating a strong resistance to crevice corrosion. Table 3.1.64 shows the results of three types of stress corrosion cracking tests conducted on three types of 6Mo stainless steel. It is not surprising that all steels cracked in 42%$MgCl_2$, but the 254 passed the other two tests. Table 3.1.65 shows stress corrosion cracking test results of NaS 254N in 20% NaCl+1%$Na_2Cr_2O_7$ solution, while Table 3.1.66 shows those of 254 SMO in 50%$CaCl_2$ solution, and neither of these generated any cracks. Next, discussion will concern the adoption of this type of stainless steel to special applications and development of special new stainless steels. In 316L of the air ejector in the MSF

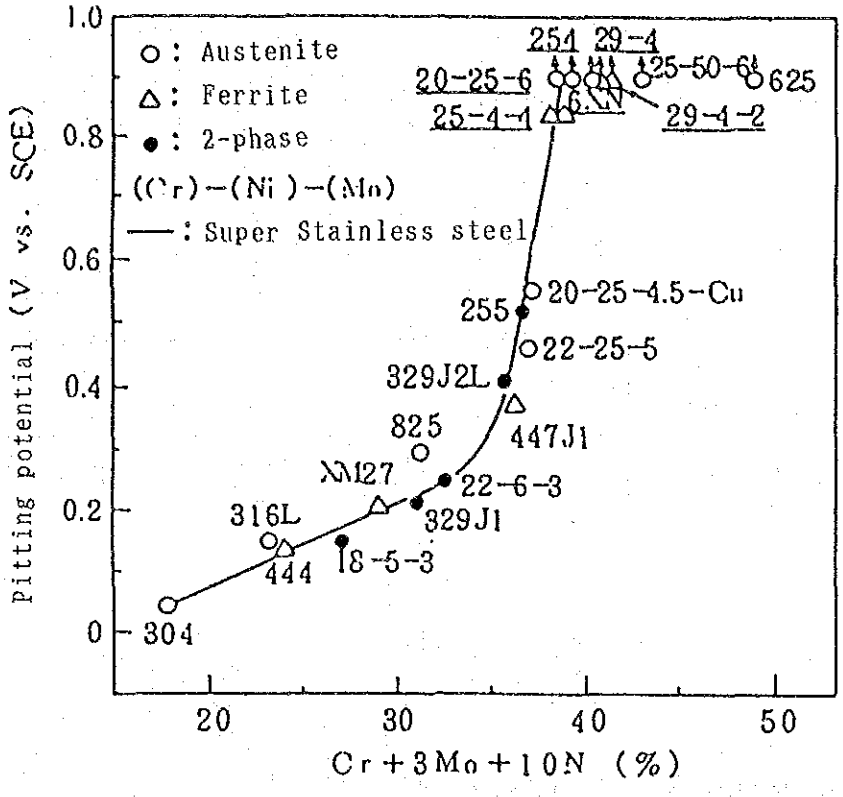

Fig.3.1.53 Pitting potential of various stainless steel and high alloys [37]
(Synthetic seawater: ASTM-D-1141
Deaeration : 30℃, 20 mV/min)

Table 3.1.56 Chemical composition of super austenitic stainless steel (example of commercially available steel grade)(%) [36]

Name of steel grade	C	Si	Ni	Cr	Mo	N	Others
NAS 254 N	0.008	0.4	25	23	5.5	0.20	S≤0.001
NTK M 6	0.03	0.4	25	20	6	0.2	—
HR 8 N	0.01	0.4	25	20	6	0.15	—
KES 825 MI	0.05	<0.1	22	20	5	0.2	1.5 Cu
Avesta 254 SMO	0.02	0.4	18	20	6	0.2	0.7 Cu
U・H・B 904 LN	0.02	0.4	25	20	5	0.15	1.5 Cu
AL 6 XN	0.05	0.4	24	20	6	0.2	—
UNS S3 1254	≤0.020	≤0.8	17.50 ~18.50	19.50 ~20.50	6.00 ~6.50	0.18 ~0.22	0.50~1.00 Cu

Table 3.1.57 6 Mo Austenitic Stainless Steels and Other Austenitic Grades [38]

UNS Number	Common Name	Producers	Chemical Composition (wt%)* Cr	Ni	Mo	Cu	N	C
S31254	254 SMO[1]	Avesta	19.50-20.50	17.50-18.50	6.00-6.50	0.50-1.00	0.18-0.22	0.020 max
J93254	Cast 254 SMO[1] CK-3MCuN	Various licencees	19.50-20.50	17.50-18.50	6.00-6.50	0.50-1.00	0.18-0.22	0.020 max
N08366	AL-6X[2]	Allegheny Ludlum	20.00-22.00	23.50-25.50	6.00-7.00	—	—	0.035 max
N08367	AL-6XN[2]	Allegheny Ludlum	20.00-22.00	23.50-25.50	6.00-7.00	0.75 max	0.18-.025	0.030 max
N08925	1925 hMo 25-6MO	VDM Technologies Inco Alloys International	19.00-21.00	24.00-26.00	6.0-7.0	0.8-1.5	0.10-0.20	0.020 max
N08026	20Mo-6[3]	Carpenter Technology	22.00-26.00	33.00-37.20	5.00-6.70	2.00-4.00	—	0.03 max

Table 3.1.58

6 Mo Austenitics Meet a Variety of
ASTM Specifications and ASME Codes [38]

UNS Number	Grade	ASTM	ASME Section VIII, Division 1	ASME Section III, Division 1
S31254	254 SMO	A167, A182, A240, A249, A267, A269, A312, A358, A409, A473, A479, A193,[1] A194,[1] A403[1]	Table UHA-23	Code Case N-439, N-441
J93254	Cast 254 SMO CK-3MCuN	A351, A743, A744	Code Case 2036	Code Case N-440
N08366	AL-6X	B675, B676, B688, B690, B691	Table UNF-23.3	Code Case N-304
N08367	AL-6XN	B366, B462, B472, B564, B675 B676, B688, B690, B691	Table UNF-23.3	Code Case N-438
N08925	1925 hMo 25-6MO	B625, B649, B673, B704, B677	Table UNF-23.3[1]	Code Case N-453, N-454, N-455
N08026	20Mo-6	B463, B464, B468, B474	Table UNF-23.3	No

[1] Pending

Table 3.1.59

Critical Pitting and Crevice Corrosion Temperatures for different stainless steels and nickel base alloys in 10 % $FeCl_3$ acc. to Garner [39]

Grade	CPT (°C)	CCT (°C)
Hastelloy C-276	n.t.	60
Inconel 625	n.t.	50
254 SMO	88	45
AL 6X	70	35
1925 HMO	60	38
Hastelloy G	n.t.	20
JS-700	53	20
Alloy 904L	40	8
Incoloy 825	n.t.	<-2
AISI 317 L	20	<-2
AISI 316 L	15	<-2

n.t. = not tested

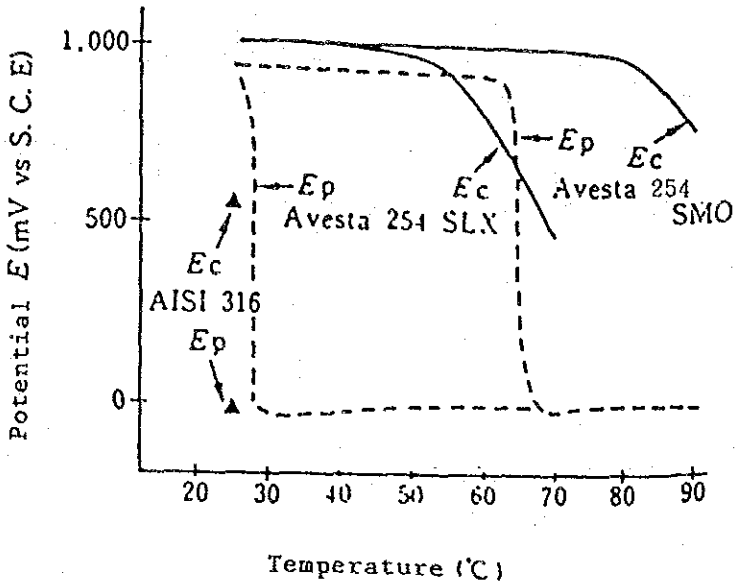

Fig.3.1.54

Temperature dependency of pitting potential (Ec) and repassivation potential (Ep) of super stainless steel AVESTA 254 SMO (18Ni-20Cr-6.2Mo-0.2N-0.7Cu) in 3.56% NaCl solution, sweep rate: 20 mV/min, reverse sweeping when it reaches 5 mA/cm^2 [36]

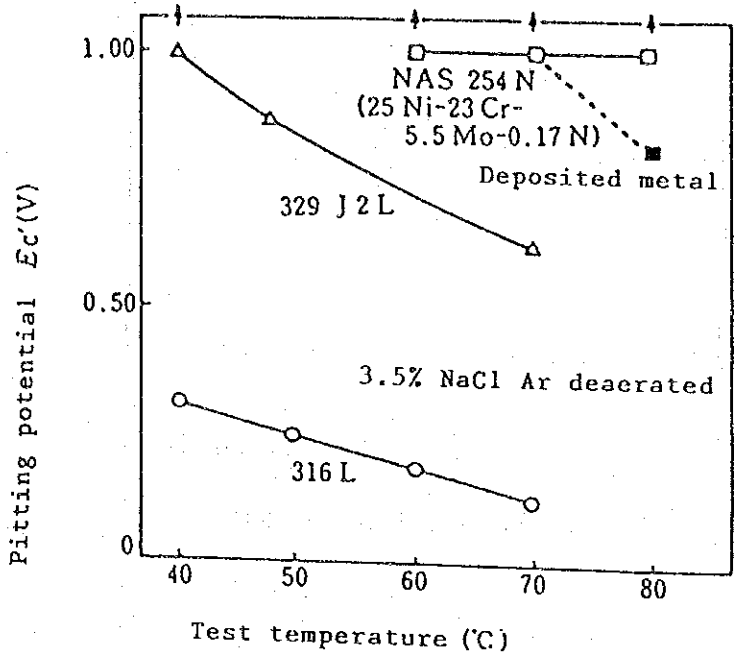

Fig.3.1.55

Temperature dependency of pitting potential of super stainless steel NAS 254 N in 3.5% NaCl solution [36]

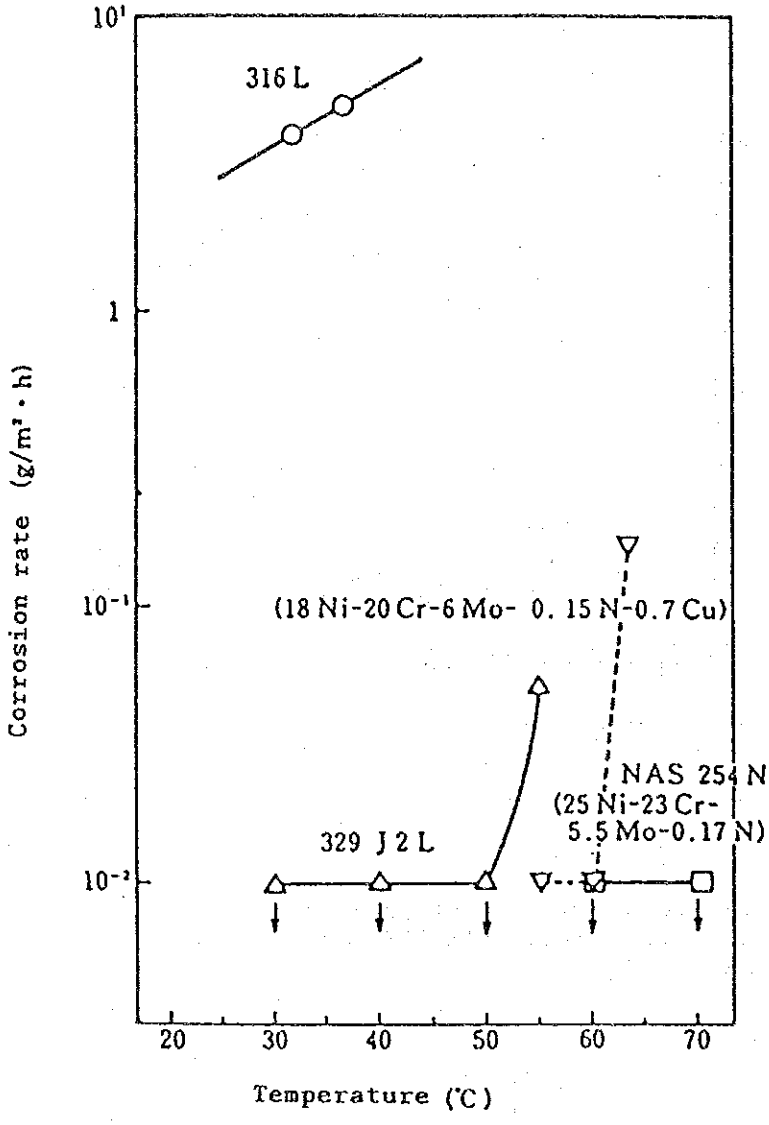

Fig.3.1.56

Temperature dependency of pitting resistance of super stainless steel[36]
(10% $FeCl_3 \cdot 6H_2O$ + 1/16 N HCl, 24 hours)

Table 3.1.60

Crevice corrosion tests in natural seawater [39]

Grade	Thickness (mm)	Exposure time (months)	Number of attacked crevice sites	Max depth (mm)
254 SMO	3	40	1 out of 12	0.04
	15	40	2 out of 12	0.18
	3	18	0 out of 12	-
	15	18	2 out of 12	0.09
Alloy 904L	3	18	6 out of 6	1.1 1)
AISI 316	3	18	6 out of 6	3.0 1)

1) Fouling sites attacked

Table 3.1.61

Crevice corrosion test results for stainless steels after 10 months exposure in a Middle East MSF desalination plant. [39]

Grade	Number of attacked crevice sites
254 SMO	0 out of 80 (liquid phase)
Alloy 904L	10 out of 80 (liquid phase)
316	80 out of 160 (gas phase)

Table 3.1.62 Immersion test results in the Atlantic Ocean (with crevice corrosion specimen)[36]

Specimen				Conditions			Results	
Name of steel grade	Plate thickness (mm)	Welding conditions: Welding method	Welding conditions: Deposited metal	Temperature (°C)	Flow rate (m/sec)	Test period (month)	Penetration depth (mm)	No. of corroded specimens *2
AISI Type 316	2	—	—	22	0.5	1	1.1	3/3
Avesta 254 SLX	2	—	—				0.2	2/3
Avesta 254 SMO	2	—	—				Not corroded	0/3
AISI Type 316	2	—	—	52	0.06	1	0.1	2/3
Avesta 254 SLX	2	—	—				Not corroded	0/3
Avesta 254 SMO	2	—	—				Not corroded	0/3
AISI Type 316	3	MMA	AISI 316	25	0.05	3	1.1	3/3
Avesta 254 SLX	3	MMA	254 SLX				1.5	3/3
Avesta 254 SMO	0.8	TIG	—				Not corroded	0/3
Avesta 254 SMO	3	MIG	P 12				Not corroded	0/3
Avesta 254 SMO	3	MMA	P 12				Not corroded	0/3
Avesta 254 SMO	15	MIG	P 12				Not corroded	0/3
Avesta 254 SMO	15	MMA	P 12				Not corroded	0/3
AISI type 316	3	MMA	AISI 316	70	0.05	6	0.08	3/3
Avesta 254 SLX	3	MMA	254 SLX				0.03	3/3
Avesta 254 SMO	0.8	TIG	—				0.01	1/3
Avesta 254 SMO	3	MIG	P 12				Not corroded	0/3
Avesta 254 SMO	3	MMA	P 12				Not corroded	0/3
Avesta 254 SMO	15	MIG	P 12				Not corroded	0/3
Avesta 254 SMO	15	MMA	P 12				Not corroded	0/3

*1 MMA= manual metal arc welding *2 No. of corroded speccimens/total specimens
(Seawater conditions) Cl^-: 18.1~19.8 g/l, O_2: 5.0~9.3 mg/l, pH: 7.8~8.1

Table 3.1.63 Depassivation pH [36]

Name of steel grade	depassivation pH*
AISI 316	2.5
24 Ni-20 Cr-5 Mo-1.5 Cu -Fe (Avesta 254 SLX)	1.6
18 Ni-20 Cr-6 Mo-0.7 Cu -0.2 N-Fe (Avesta 254 SMO)	0.6

Excellent crevice corrosion resistance

* Critical pH value when pH in the crevice lowers and the potential becomes less noble and the passivity cannot be held and corrosion develops.

Table 3.1.64

Chloride Stress Corrosion Cracking Resistance of the 6 Mo Austenitics and Common Stainless Steels [38]
(P = Pass, F = Fail)

UNS Number	Grade	Boiling 42% $MgCl_2$	Wick Test	Boiling 25% NaCl
S31254	254 SMO	F	P	P
N08366	AL-6X	F	P	P
N08026	20Mo-6	F	P	P
S30403	Type 304L	F	F	F
S31603	Type 316L	F	F	F
N08904	Alloy 904L	F	P or F	P or F[p:-4q

(Specimen shape and dimensions are not given in the text)

Table 3.1.65 Stress corrosion cracking test results in 20% NaCl + 1% $Na_2Cr_2O_7 \cdot 2\ H_2O$ (2 mmt, U-bend specimen)[36]

Steel grade	Test conditions	Cracking
316L	Boiling for 300 hours	Cracked
329J2L	"	Cracked
NAS 254 N (25 Ni-23 Cr-5.5 Mo-0.17 N)	"	No cracking

Table 3.1.66 Stress corrosion cracking test results in 50% $CaCl_2$ solution at 100 ℃ (stress=2/3 x proof strength, direct loading system)[36]

Steel grade	Time to failure (hour)
AISI 316	450
Avesta 254 SMO (18 Ni-20 Cr-6 Mo-0.2 N-0.7 Cu)	Not cracked in 3,000 hours

plant, violent stress corrosion cracking was generated and the cause was identified as Br. 904L (20Cr–25Ni–4.5Mo–Cu) was then selected after the material selection tests. The ejector system manufactured with this material continues to operate satisfactorily to date.S. Nordin[40], who reported the failure mentioned above, published the results of crevice corrosion tests using seawater from the Arabian Gulf in the same report as shown in Table 3.1.67, and has proposed the use of crevice numbers (CN) and crevice ranking numbers (CRN) as a method to express the degree of crevice corrosion. CN is expressed by the following equation and in the parentheses of the equation, the crevice corrosion numbers shown in Columns 1, 2, 3, and 4 of Table 3.1.67 shall be inserted:

CN = 1/100( ) + 30/100( ) + 70/100( ) + 95/100( )

This method is designed to specify the product of CN by the Max. depth to CRN in order to enable further consideration of Max. depth. The evaluation results obtained by this method are shown in Table 3.1.68, which are in good agreement with the observation results of specimens. Next, a report on the development of super stainless steels for thick plates or cladding is introduced. Figure 3.1.57 shows the interrelation between the results of an immersion test in the Seto Inland Sea for 1 year and critical pitting temperature (CPT) determined by the $FeCl_3$ test. It has been determined that a CPT higher than 60°C is required for seawater–resistant stainless steel. Figure 3.1.58 determines CPT when PRI (pitting resistance index) was kept constant while the Mo amount was varied. At PRI=41 and Mo greater than 4.5%, CPT is 70 and does not show any variation. If Mo% is increased excessively, sensitization during hot rolling is anticipated, and the Mo content was, therefore, determined to be 4.5% according to the results of Fig. 3.1.58. The material developed in this way is 310 Mo shown in Table 3.1.69 and B was added to improve hot workability.These steels contain less than 6% Mo and are not classified as 6Mo stainless steels, but they are all high–alloyed austenitic stainless steel with excellent seawater resistance, and are introduced as a material with properties conforming to 6Mo stainless steel.

c) Super Ferritic Stainless Steel

Recent innovations in the steelmaking process have enabled mass–production of extra low C, N ferritic stainless steel and have led to the development of super ferrite stainless steels. These are steels with ferrite structures containing Mo at Cr contents greater than 25%. Table 3.1.70 shows chemical compositions of some of the commercially available steel grades. Figure 3.1.59 shows pitting test results of several steel grades in 10%$FeCl_3$ solution, while Table 3.1.71 shows the pitting potential in 3.5% NaCl solution. In these data, SR–4 is superior. Table 3.1.72 shows stress corrosion test results using U–bend specimens, indicating that an increase of Ni in ferritic stainless steel increases susceptibility to stress
corrosion cracking.

Table 3.1.67

Summary of crevice corrosion test evaluations [40]

Grade	Number of crevice attacks (out of 40) 1x)	2x)	3x)	4x)	Total number (out of 40)	Max depth, mm Base metal	Weld
NU Stainless 53	5	0	0	9	14	> 2.7xx)	> 2.7xx)
NU Stainless 54	15	13	5	0	33	0.15	0.10
NU Stainless 44LN	14	9	1	0	24	0.042	0.040
NU Stainless 904L	12	7	0	0	19	0.038	0.030
NU MONIT	0	0	0	0	0	0	0

x) 1: 0-10% of creviced area attacked

2:10-50% of creviced area attacked

3:50-90% of creviced area attacked

4:90-100% of creviced area attacked

xx) Sample penetrated

Table 3.1.68

Results of crevice corrosion tests [40]

Grade	CN	CRN	cf Figure
NU Stainless 53	8.55	26	3
NU Stainless 54	8.15	1.2	4
NU Stainless 44LN	4.1	0.17	5
NU Stainless 904L	2.7	0.10	6
NU MONIT	0	0	7

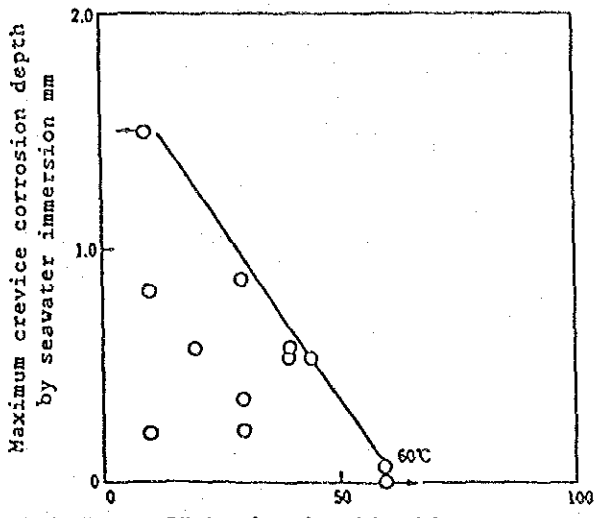

Fig.3.1.57 CPT by ferric chloride immersion test ℃

Interrelation between maximum crevice corrosion depth by seawater immersion test and ferric chloride test (JIS G 0578) [41]

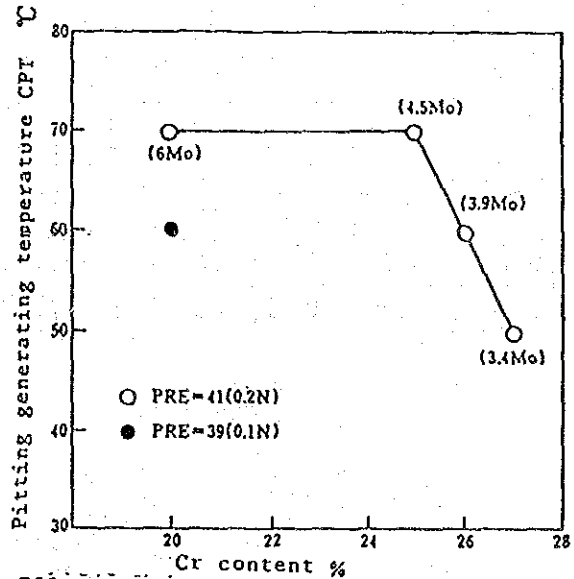

Effects of Cr, Mo and N contents on pitting resistance [41]

Fig.3.1.58

Table 3.1.69 Chemical composition of seawater-resistant stainless steel (wt·%)[41]

Steel grade	C	Si	Mn	Cr	Ni	Mo	Cu	B	N
310Mo	0.005	0.24	1.51	24.5	22.1	4.5	—	0.0027	0.229
254	0.007	0.25	0.63	19.8	18.1	6.2	0.61	—	0.225

Table 3.1.70 Chemical composition of super ferritic stainless steel (Example of commercially available steel grade)(%)[36]

Steel grade and standard name	C	Si	Ni	Cr	Mo	N	Others
SUS 447 J1	0.010	≦0.4	—	30	2	<0.015	—
SUS XM 27	0.010	<0.4	—	26	1	<0.015	
SEA-CURE	0.025	0.3	1.2	27	3.5	—	Ti 0.5
AL29-4 C	0.025	0.02	—	29	4	—	Ti 0.5
MOXIT	0.025	—	4	25	4	—	Ti 0.5
SR*26-4	0.010	<0.4	—	26	4	—	Nb
SR 26-1	0.002	0.34	0.17	26	1.3	0.005	Nb0.15
SHOMAC 30-2	0.003	0.15	0.18	30	2.0	0.007	Nb0.15

*SHOMAC-RIVER

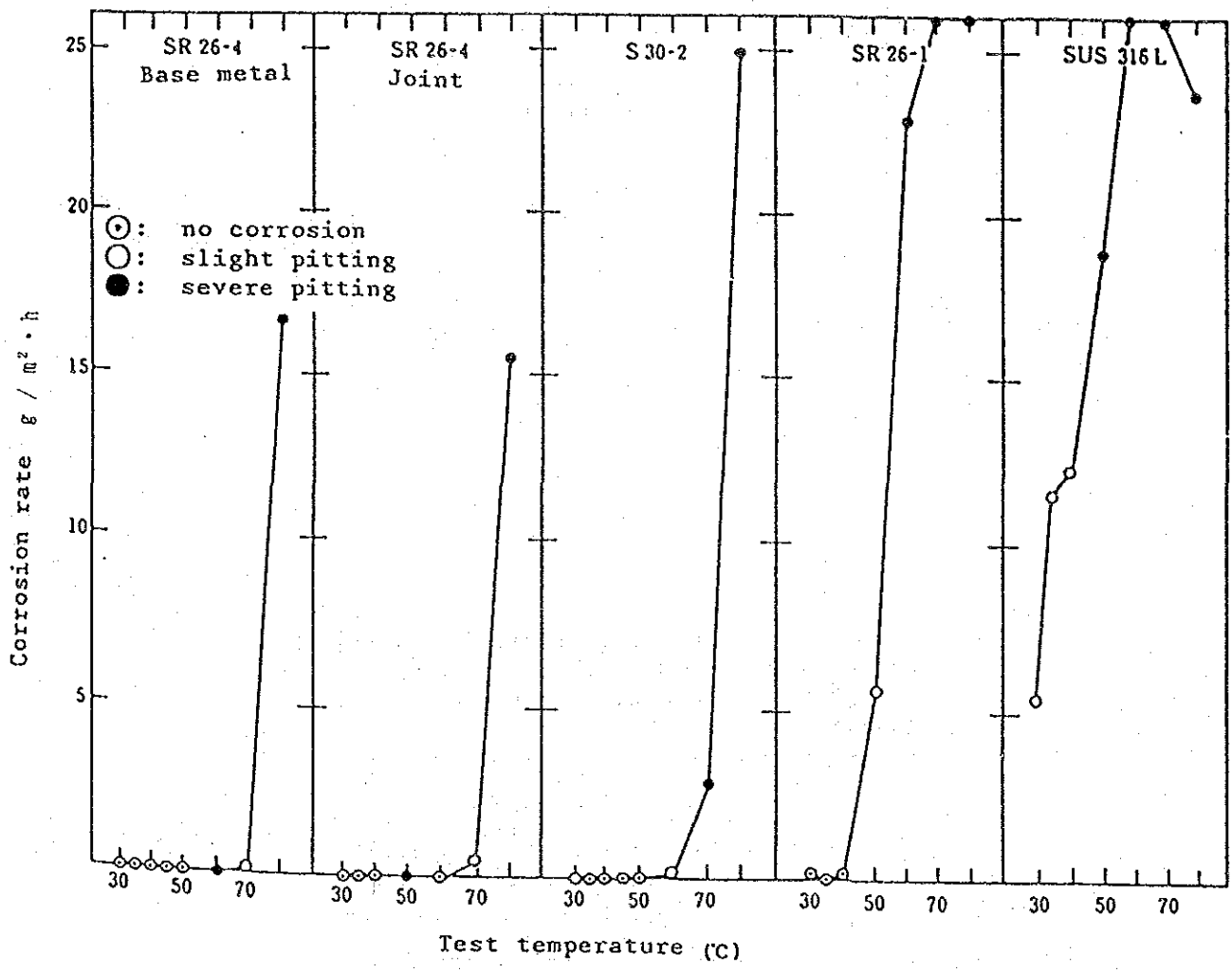

Fig.3.1.59 Pitting test results of super ferritic stainless steel (26Cr-4Mo, 30Cr-2Mo, 26Cr-1Mo) in 10%$FeCl_3 \cdot 6H_2O$ solution (48-hour test)[36]

Table 3.1.71

Pitting potential in 3.5%NaCl solution (mV vs SCE) [36]

Steel grade	Temperature (℃)		
	80	70	60
SR 26-1	271	304	452
S 30-2	413	621	○
SR 26-4	547	716	○
SUS 316 L	96	—	174

○: Pitting potential unable to observe.

Table 3.1.72 Stress corrosion cracking test results (U-bend test) of 29Cr-2Mo steel in boiling 42%$MgCl_2$ and 20%NaCl+1%$Na_2Cr_2O_7 \cdot 2H_2O$ solutions [36]

Steel grade	Boiling 42%$MgCl_2$ solution	Boiling 20%NaCl+ 1%$Na_2Cr_2O_7 \cdot 2H_2O$ solution
29 Cr-2 Mo	Not cracked	Not cracked
29 Cr-2 Mo-0.5 Ni	Cracked	Not cracked
29 Cr-2 Mo-1 Ni	Cracked	Not cracked
29 Cr-2 Mo-2 Ni	Cracked	Cracked

Table 3.1.73 Chemical composition of tube, tubesheet and seal-welding material[37]

	Steel grade	Chemical composition (wt%)			
		Cr	Ni	Mo	Others
Super stainless steel tube	29－4－2	29	2	4	low C,N
	254	20	18	6	0.2N,0.7Cu
Stainless steel tubesheet	254	20	18	6	0.2N,0.7Cu
	904L equivalent	20	25	4.5	1.5Cu
	316L	17	13	2	
Welding material (TIG φ)	625	22	62	9	3.5Nb
	25M	20	25	4.5	1.2Cu
	825	23	43	3	1.7Cu,1Ti
	316L	19	13	2.5	

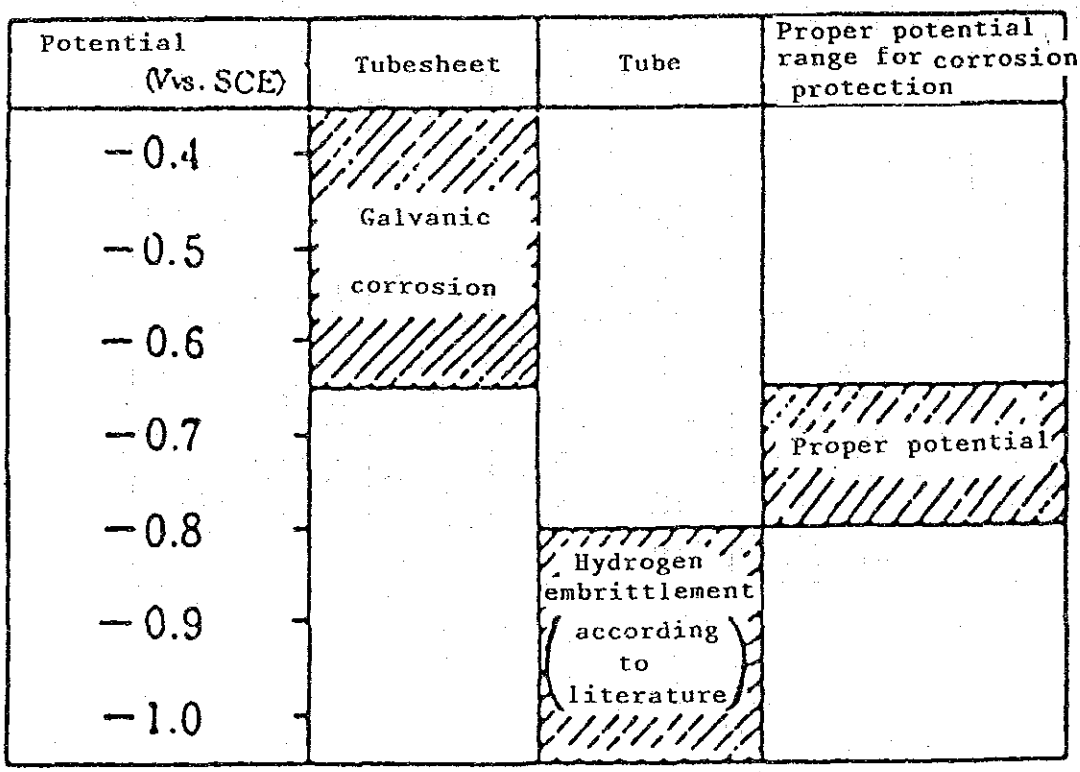

Fig.3.1.60 Proper corrosion protectin potential region (29-4-2 tube/naval brass tubesheet)[37]

Table 3.1.74

Seawater immersion test results of seal-welded simulating tubesheet specimen [37]

Tube	Tube-sheet	Seal welding material (TIG)	Corrosion resistance		
			Tube	Tube-sheet	Seal welded material
29-4-2	316L	None	○	× (P)	× (P)
		316L	○	× (P)	△ (P)
		625	○	× (P)	○
	904L Equivalent	None	○	△ (P)	× (P)
		625	○	△ (P)	○
	254	None	○	○	× (P)
		625	○	○	○
254	316L	None	○	× (P)	× (P)
		316L	○	× (P)	△ (P)
		825	○	× (P)	HAZ △ (P)
		25M	○	× (P)	HAZ △ (P)
		625	○	× (P)	HAZ △ (P)
	904L Equivalent	None	○	△ (P)	× (P)
		25M	○	△ (P)	○
		625	C	△ (P)	○
	254	None	○	○	△ (P)
		625	○	○	○

○: No corrosion △: Mild corrosion ×: Severe corrosion
(P): Pitting corrosion

Fig.3.1.61 Polarisation curves for low-oxygen seawater at 16-18 C [42]

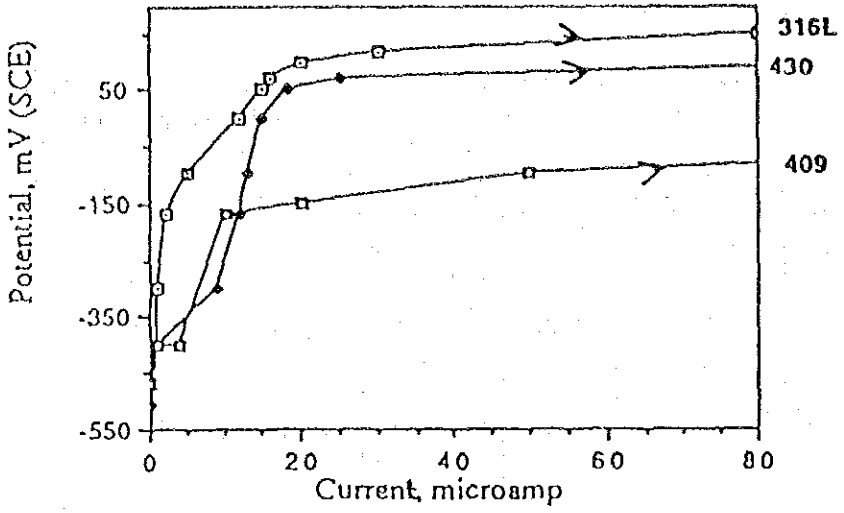

Fig.3.1.62 Scatter bands in breakdown potentials for seawater at 60°C [42]

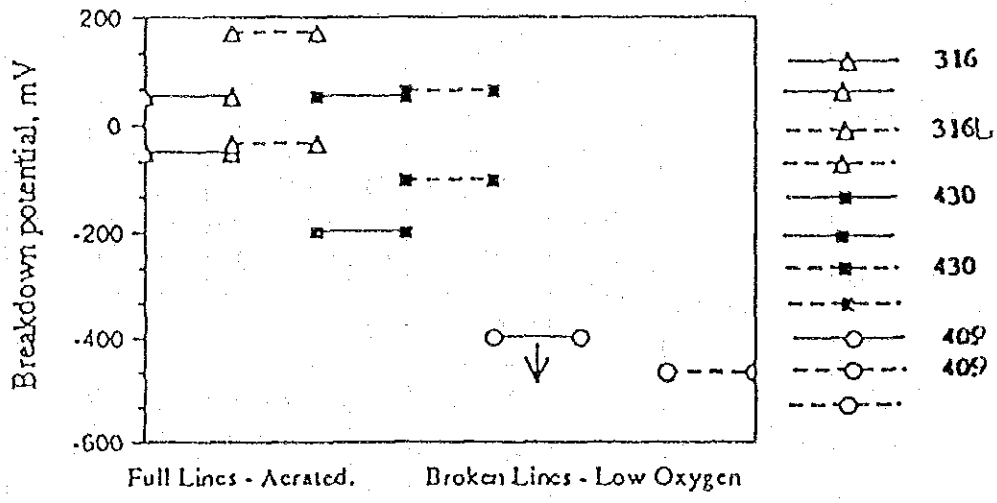

transfer tube materials, but it can more easily be attributed to insufficient basic data related to corrosion resistance and workability in utilizing nonmetallic materials and to a lack of reliability due to the absence of these data. When conventional nonmetallic materials have been used, improper selection of materials or improper working has caused accidents, frequently impairing the reliability of nonmetallic materials themselves .

However, in general, many nonmetallic materials provide excellent corrosion resistance to seawater and are insensitive to pH, oxygen, carbon dioxide and hydrogen sulfide, which constitute problems in the case of metallic materials, and have an advantage of lower installation costs than those of metal. Consequently, except for the case in which no other material than metal can be used, such as for heat transfer tubes, more nonmetallic materials should be used for other components, and for this purpose, data must be collected to put nonmetallic materials into practical use and experimental equipment should be completed to systematically acquire these data. It is also essential to collect the details of application examples available to date in the form of data bases and establish guidelines for the selection of correct materials, the selection of correct applications, and correct working."

The essential points of the four sources of data are described as follows:

(1) U.S. Dow Chemical data: "Performance and Utilization of Nonmetal under Seawater Desalting Environment" [43]

This data was compiled from the research defined in the title which the OSW (Office of Saline Water) of the U.S. Department of State carried out at the Materials Test Center. This is the only available comprehensive evaluation report published to date concerning nonmetallic materials investigated as materials for seawater desalting plants, and compiles evaluation results on 5 types of corrosion resistant cement, 75 types of paint, 19 types of FRP, and 13 types of thermoplastic resin.

The evaluation method of nonmetallic materials used in the OSW report is to first heat pretreated (deaerated, decarbonated, pH adjusted) seawater to a specified temperature, introduce this into a cell inserted with panels formed with various materials to be evaluated and allow it to pass, and then compare the degree of deterioration of these materials. The pipes are made from FRP and six test temperatures are selected; namely, four for water: 110, 160, 210, and 250°F, 215°F for condensed steam, and 215°F for brine phase. Test results will be discussed in detail in the subsequent section and thereafter, but the general conclusion is summarized as follows:

All the nonmetals are likely to be adopted to desalting plants because of their low cost, easy working, and excellent corrosion resistance. However, they have the disadvantage of susceptibility to breakage, as experienced with metals.

In actual application, first select the correct materials , establish applications properly,

and select excellent manufacturers to work the materials. Technical service and assistance from material manufacturers and design companies are essential for selection of the correct materials and the correct construction of plants."

(2) Data of Japanese Society for Materials (Corrosion Committee): "Extended Life and Corrosion Protection Measures of Seawater Desalting Plant-1976"

This data is furnished by Sasakura Engineering Co., Ltd., and provides information on corrosion-resistant materials for MSF seawater desalting plants in terms of applied sections. According to this data, for low-temperature evaporators for the water chamber, resin coating is used in Hong Kong, resin coating or rubber lining is used in Kuwait. In Saudi Arabia and Kuwait resin coating is used for low-temperature evaporators for the evaporation chamber as well as for barrel portions of the circulating pumps, resin coating, rubber coating and FRP for raw seawater as a distributing pipe, and rubber lining and FRP for make-up seawater. In general, for the evaporator proper, the data reveals that it is effective to provide resin coating in the range of permissible temperature conditions (lower than about 90°C) to restrict the general corrosion of steel plates.

(3) Data of Cocan/Tenperley and Associate, Saudi Arabia: "Material Specification and the availability and life of desalination equipment in Saudi Arabia and Arabian Gulf"[44]

This data recommends desirable materials in accord with each member on the basis of abundant operating experience concerning MSF plants comprising various structural materials with respect to two cases: one in which polyphosphoric acid treatment is carried out at relatively low temperatures and the other in which acid treatment is performed at high temperatures. What should be noted is that the data recommends metallic materials for almost all members and nonmetallic materials for only a small number of limited portions. That is , for places in which nonmetal is applicable, carbon steel coated with tar epoxy or GFRP is recommended for the suction thimble material in the seawater and evaporator system, and the possibility of building brine gates with FRP is pointed out as components inside the evaporator.

The data also pointed out that the selection of equipment materials for seawater desalting plants has tended to be erroneous and enumerated the following reasons for this. At the time of bidding for plant construction, inexpensive materials are likely to be used unless otherwise specified in the customer's order sheet, in order that the lowest possible estimates can be made. For example, when pitting is not entirely understood, stainless steels and carbon steels are proposed by contractors because they can pass the specifications in accordance with the data on general corrosion. In some cases, where these applied, the generated pitting penetrated plates and resulted in serious accidents. In this sense, the data correctly points out the necessity of strictly

specifying the material specifications for future designs.

4) Data of Japan Society of Corrosion Engineers: "MSF Desalting Plant" General Report on National Project (Research on Heat Transfer Tube Material for Multistage Seawater Desalting Plants) [45]

Description concerning nonmetallic materials is shown as follows:

a) Resin Coating

Investigation was made on resin coating for heat transfer tubes. Paints blended with epoxy-based and phenol-based resins were applied to the steel surface in a thickness of 220 to 390μ and loop and field tests were carried out. Satisfactory results were obtained at heaters and heat recovery sections up to 2,000 hours. However, it indicated the excessively low thermal conductivity and the difficulty in removal of sludge.

b) FRP

No special comment is given.

c) Concrete

Investigation was made to change the structural material of the evaporation chamber from iron to concrete and reduce construction costs, but the importance of solving problems of air tightness, corrosion, and thermal stress was stressed.

In short, the data accepts primarily metallic materials to be used for the corrosion-resistant materials of Japan's National Projects and investigates nonmetallic materials for possible application only.

The application conditions and problems of nonmetallic materials are described as follows depending on the type of the material.

3.2.2 Concrete

The most highly anticipated application of concrete at seawater desalting plants is for the shell, and various reports have been published by Kajima Corp., Japan, with their essential points given as follows:

1) Requirements for Concrete Shell

a) Corrosion Resistance

The inner surface of the shell wall comes into constant contact with condensed seawater

at temperatures of 40–120°C and a flow rate of 1.0–1.5 M/sec. Concrete must provide corrosion resistance that can stand this condition as well as resistance to distilled water which is formed by steam condensation. Kajima Corp. immersed specimens of ordinary Portland cement, fly ash cement, moderate-heat cement, ASTM V type cement, and expansive cement with varying water-cement ratios into 120°C seawater and investigated the reduction ratio of compressive strength in order to identify corrosion resistance to high-temperature condensed seawater. The results indicated that the resistance of concrete to hot brine depends more on water-cement ratio than on the cement types, and when this ratio is 45% or lower, the strength tends to increase after immersion, and at 55% or higher anhydrous gypsum precipitates in the matrix, giving rise to decay. Apart from this experiment, the results of operation of demonstration plants using concrete shells carried out by the Agency of Industrial Science and Technology of MITI (operated for 270 days at 100°C or lower) indicated that concrete is negligibly attacked by high-temperature condensed seawater. Based on these results, high-quality concrete with proper blending has sufficient corrosion resistance to high-temperature seawater . With respect to corrosion resistance to high-temperature distilled water, the amount of substance dissolved from concrete is extremely small. In the operation results of the above demonstration plants, the concrete surface where distilled water condenses on the concrete shell surface becomes slightly rough, indicating no significant change which might affect durability.

b) Mechanical Properties

The shell inside is held to a high temperature to achieve its functions, producing a significant temperature difference between the shell inside and outside. In particular, the thermal stress due to nonsteady temperature distribution is quite large when the system is started and stopped. On the other hand, concrete reduces both strength and elastic modulus and increases creep under high-temperature conditions.

Consequently, it is necessary to design the shell to satisfy the required conditions using the property values concerning these characteristic changes. Investigation results, however, have identified that the thermal stress acting on the shell can be accurately estimated by providing the temperature conditions acting on the shell as critical conditions. The above demonstration plants were designed by this technique and satisfactory results have been obtained.

c) Air Tightness

Air permeability of concrete proper is closely connected with water permeability, and the air permeability coefficient is said to be 1,000–10,000 times that of water permeability. Due to structural factors, air tightness of the overall shell is affected by shell joints as well as by the interconnections of the through pipe and concrete, from which air tends to leak. Experimental

results have indicated that leakage from the interconnection between the steel around the through-hole and the concrete is the greatest and complete air tightening treatment for the portion causing leakage is required when constructing a shell.

Discussion has been made on the various problems concerning the shell where a large amount of concrete is expected to be used in seawater desalting plants. Based on data from the U.S. OSW, results of comparison evaluation tests carried out by OSW on various cement materials are summarized.

OSW selected five types of corrosion-resistant cement and using the above test plants, tests were carried out for 12 months. For the evaluation method, the physical testing method of ASTM was employed and the results were compared with the conditions before testing. The greater part of the five types were so severely damaged that there was no need for comparison, but of the five aluminum silicate cement provided good results. This cement was then actually applied to the steam wall of the OSW test bed plant, which has been operating free of damage for 4 years. This result provided the chance for the cement to be popularly used in steam walls in desalting plants at various places. The recommendation of the OSW related to the problem of employing concrete for seawater desalting plants was to "select proper cement materials and ask a reliable construction company with abundant experience to work with the cement on the proper places. Then, the cement will have a high possibility for practical application."

3.2.3 FRP

FRP is an acronym for fiber reinforced plastics and is a resin material with increased strength due to various types of reinforcement fibers such as glass, carbon, and boron fibers. Of these, the one best suited for use in seawater desalting plants, from the viewpoint of economy, is primarily GFRP only (glass fiber reinforced plastics), which is reinforced with glass fiber. This section describes GFRP.

The superior features of GFRP as a material are listed as follows:

(1) Good corrosion resistance. It is strong against strong corrosive soils and can be used without surface coating.
(2) Low specific gravity. Less than 1/10 that of concrete, thus providing easy erection.
(3) Smooth surface. Good liquid flow with minimal encrustation adherence.
(4) Can be supplied in various sizes. In the case of pipes, diameters which can be supplied range from 50 mm to 4 meters.
(5) Easy connection with pipes. However, instructions require professionals for connection works.
(6) Easy fabrication. Can be fabricated in optional shapes.

Next, actual examples of GFRP applied to seawater desalting plants are described. This information has been compiled from data released by Dow Chemical in 1983. According to this data, in the Arabian Peninsula, GFRP has attracted keen attention as a material for seawater desalting plant equipment, and details are shown below.

Jeddah No. 1 of Saudi Arabia was constructed without using corrosion-resistant materials. For 10 years thereafter, the plant suffered from serious corrosion, particularly in pumps, intake valves, and vents. As a result, in the plants built thereafter stainless steels such as AISI 3O4 and 316 as well as Hastelloy C were employed. In the recent Yanbu Al-Sinaiya case, however, leakage occurred in stainless steel intake valves 6 months after construction, and for corrective actions, this portion was replaced with GFRP and remarkably good results have been achieved. Based on these actual results, the popularity of GFRP has increased and it has since been adopted in many places including Al Khobar, Al Jubail, and Al Kafji, with its employment currently is being investigated in UAE.

Actual application examples of GFRP have been discussed, and this section describes the essentials of comparison tests carried out at the U.S. OSW, referring to their data to elucidate the problems of what kinds of methods are available for evaluating GFRP performance. In the OSW, immersion tests were carried out on GFRP using 19 types of thermoplastic resin and the surface conditions were observed by four examiners and ranked by the 5-step ranking method from 0 to 5. For the evaluation of polymer deterioration caused by changes of appearance and physical properties, the ASTM process was applied and flexural strength, flexural rigidity, tensile strength, tensile rigidity, and changes in hardness and weight were measured. These data were arranged by temperature and time, and it has been clarified that physical properties of FRP deteriorate more quickly with time than those of metallic materials.

What is important for evaluation is to determine what percentage of tensile strength and rigidity attained before exposure are maintained after exposure, and it is considered desirable to maintain 50-60% of the tensile strength and rigidity after 12 months in the case of FRP. What matters next is how long the decrease in strength and rigidity with time would continue or whether the initial decrease is great but no significant change occurs thereafter. For example, it is common to accept cases in which strength and rigidity are reduced by 25-40% in the first few months and thereafter hardly change.

Only a few specimens exhibited satisfactory results even at 250°F, and the best example was high-grade Bisphenol A epoxy. At 210°F or lower, Bisphenol A epoxy may be acceptable, but in view of economy, vinylester or Bisphenol A polyester are recommended. At 110°F or lower, a considerably large number of FRPs exhibit good results, but still, in this range, iso or ortho polyester are unsatisfactory.

The above are some of the essential points of the GFRP evaluation report from the U.S.

OSW. In addition to this, the same data provides the following comments on actual application examples of GFRP pipes.

It is said that there are many failure accidents involving FRP pipes used in desalting plants. These accidents occur at the connections between pipes and flanges but breakage of the pipes themselves is extremely rare. The pipe proper has a different resin–glass ratio between the outer and inner layers. The outer layer consists of 70% glass and 30% resin, which provides less corrosion resistance but sufficient strength. On the other hand, the inner layer consists of 80% resin and 20% glass, providing sufficient corrosion resistance. The flange is made from GFRP but is connected with the pipe by a joint system, resulting in failure due to stress applied to the connections from overtightening of the flange bolts or defective alignment of both flanges. OSW carried out 15–month immersion tests using 15 types of commercially avail able GFRP. As a result, only one case generated breakage, which occurred at the connections between pipes and flanges. The recommended resins are high grade Bisphenol A epoxy for temperatures exceeding 250°F, and vinylester or Bisphenol A polyester for temperatures below 210°F.

3.2.4 Resin Coating and Rubber Lining

Resin coating is defined as the coating of surfaces of metal–built equipment and concrete structures with resin to isolate and to protect them from corrosive environments. Resin painting and resin lining are expressions analogous to resin coating and there is no strict distinction among these expressions, but in view of the coating film thickness and the applicable temperature environment, these processes are called lining, coating, and painting in that order in accord with the film thickness or applicability to high temperature. For construction, in the case of lining, resin film sheet is fitted and fixed with screws and adhesives, while in the case of coating and painting, coating is applied with trowel, brush, or spray. Of these, resin coating is popularly used in desalting plants, and is described in further detail below.

For actual examples of the application of resin coating, that portion describing resin coating is taken from data compiled on the rehabilitation work of two MSF plants (11,500 m^3/day each) at the Bahrain Sitra Power Plant which Sasakura Engineering Company of Japan took charge of.

These MSF plants were constructed by an Italian company and operation was commenced in 1976 but troubles occurred one after another from the initial stages of operation. In 1986, Sasakura Engineering took charge of the rehabilitation work and after reoperation in 1987 the plants have been operating smoothly. Causes of trouble included air leakage to evaporators, the existence of carbon dioxide, low venting rate in cascades, and carry–over of splashing brine, and rehabilitation work was carried out to improve these structural defects. From the viewpoint of corrosion prevention, problems of resin coating were investigated.

Because 10 years have passed since the plants were constructed, the container (flash chamber) inner surface of each MSF stage was covered with corrosion products and investigation was made on what type of pretreatment was suited for applying resin coating on these surfaces and how often coating should be repeated. Prior to the main rehabilitation work, the following test conditions were prepared and the plants were operated for 10 months. Based on the results, the work procedure was selected. That is, a polyamide epoxy resin system, brand name "Ankinol" (Astral, France), was selected for the paint, and investigation was made on the following:

(1) When the surface is cleaned and Ankinol is coated.
(2) In view of the limitations to cleaning the surface, completely new carbon steel specimens are prepared separately, to which Ankinol oating is applied.
(3) When coating was not performed and corrosion products formed previously are removed by sand-blasting.

As a result, it has been confirmed that certain effects are achieved by only sand-blasting but that further applying Ankinol on the surface will achieve further better effects, producing a nearly similar effect as when it is applied to completely new carbon steel. It was confirmed, however, that coating must be carried out once every 2-3 years. Therefore, based on these test results, Sasakura Engineering undertook the main rehabilitation work and attained satisfactory results. In the ma in work, removal of corrosion products prior to coating was extremely difficult. Using primarily an air chisel and a needle wire vibrator as well as the proper sand-blasting, the removal of corrosion products was attempted, but it took 3 weeks to treat one unit of an MSF plant. For the application of Ankinol coating and monitoring of the process, the prior approval of Astral of France, the manufacturer, was obtained . Prior to coating, a large number of cavities were observed on the surface, but no welding repair was carried out and blast cleaning was repeated twice. For abrasives, copper slag was used for the first time and a mixture of copper slag and alumina was used for the second time. Coating was performed just after blasting and once every day for four days to produce a 350-550μ thickness. One month was required for curing after completion of coating, during which care was taken to prevent adherence of moisture or dew on the coated surface. In concluding the main rehabilitation work, thorough surface cleaning carried out in advance will result in practical and effective coating treatment, and annual repairing thereafter requires only partial repairing with paint, possibly shortening the work period. The plant life may be potentially extended to 5-6 years.

The foregoing describes one example of resin coating operation in a seawater desalting plant. Next, the data of the U.S. OSW is referred to again for discussion of the evaluation re-

sults of various types of paint for resin coating carried out by OSW.

OSW carried out comparison evaluation tests on 75 types of paints recommended by leading paint manufacturers. For evaluation, these paints were applied to panels, which were arranged on racks, placed in the above-mentioned test containers and tested under six temperature conditions. Then, four examiners judged the results in accordance with ten levels of criteria. In judging, blisters, spalling, rust, chalk, and loss of luster were taken into account. These judgment results were arranged as a function of time and temperature a nd processed by computer. The results are shown as follows. Resins which exhibit satisfactory results at temperatures up to 250°F include baked phenolic, epoxy-phenolics (note: according to manufacturers, coal tarepoxy cannot be used at temperatures exceeding 160°F.

On the other hand, almost all paints were impossible to use at 160°F, but up to 110°F, 60 out of 75 types can be used as desalting plant material. Specimens in which some of the coal tar epoxy was applied on zinc rich primer produced spalling caused by blisters at high temperatures, but zinc itself served to provide cathodic corrosion protection to steel. Specimens in which coal tar epoxy was applied directly without applying zinc rich primer produced no blisters and provided satisfactory results up to 250°F. This temperature exceeded the recommended temperature of the manufacturer by 90°F. Epoxy mixed with stainless steel flakes was out of service after six months. The corrosion resistance of this paint against the desalting environment is good unless it is immersed in seawater.

It was concluded that "the correct use of paints is much more important than selecting the correct paints." That is, the observance of various requirements, such as thorough surface cleaning before coating to proper thickness for correct application, and thorough inspection after application, will produce good results. It is also essential to carry out periodic inspection and early repair during service and to prevent development of corrosion areas before it is too late.

Lastly, discussion is made on the problem of rubber lining. Rubber lining is generally defined as coating the metal or concrete surface with rubber to provide corrosion and wear resistance. In the beginning, the type of rubber primarily used was natural rubber, but more recently various synthetic rubbers such as chloroprene rubber, nitrile rubber, butyl rubber, and chlorostyrenated polyethylene has been developed, and suitable materials can be properly used in accord with application conditions as the processing technique advances. The application process is to first apply adhesives after the surface is sand blasted for metal, on which an uncured rubber sheet is placed and fixed, and then to cure the rubber sheet as a rubber lining.

As an actual example of rubber lining in a seawater desalting plant, the MSF plant delivered by Sumitomo Heavy Industries of Japan for a power plant in Dubai, the United Arab Emirates, is described. Rubber lining is used only for piping materials. That is, when rubber lining was applied to seawater lines and product water lines, it exhibited corrosion resistance capabili-